

## INFORMATION TO USERS

This manuscript has been reproduced from the microfilm master. UMI films the text directly from the original or copy submitted. Thus, some thesis and dissertation copies are in typewriter face, while others may be from any type of computer printer.

**The quality of this reproduction is dependent upon the quality of the copy submitted.** Broken or indistinct print, colored or poor quality illustrations and photographs, print bleedthrough, substandard margins, and improper alignment can adversely affect reproduction.

In the unlikely event that the author did not send UMI a complete manuscript and there are missing pages, these will be noted. Also, if unauthorized copyright material had to be removed, a note will indicate the deletion.

Oversize materials (e.g., maps, drawings, charts) are reproduced by sectioning the original, beginning at the upper left-hand corner and continuing from left to right in equal sections with small overlaps. Each original is also photographed in one exposure and is included in reduced form at the back of the book.

Photographs included in the original manuscript have been reproduced xerographically in this copy. Higher quality 6" x 9" black and white photographic prints are available for any photographs or illustrations appearing in this copy for an additional charge. Contact UMI directly to order.

# UMI

A Bell & Howell Information Company  
300 North Zeeb Road, Ann Arbor, MI 48106-1346 USA  
313/761-4700 800/521-0600



**Order Number 9520429**

**An experimental investigation of the effect of oil on convective  
heat transfer and pressure drop of a HFC-32/HFC-125 mixture**

**McJimsey, Bert Ashford, Ph.D.**

**Texas A&M University, 1994**

**U·M·I**  
300 N. Zeeb Rd.  
Ann Arbor, MI 48106



**AN EXPERIMENTAL INVESTIGATION OF THE EFFECT OF  
OIL ON CONVECTIVE HEAT TRANSFER AND PRESSURE  
DROP OF A HFC-32/HFC-125 MIXTURE**

A Dissertation

by

**BERT ASHFORD MCJIMSEY**

Submitted to the Office of Graduate Studies of  
Texas A&M University  
in partial fulfillment of the requirements for the degree of

**DOCTOR OF PHILOSOPHY**

December 1994

Major Subject: Mechanical Engineering

**AN EXPERIMENTAL INVESTIGATION OF THE EFFECT OF  
OIL ON CONVECTIVE HEAT TRANSFER AND PRESSURE  
DROP OF A HFC-32/HFC-125 MIXTURE**

A Dissertation

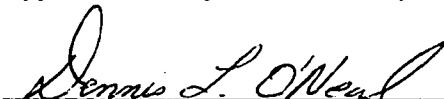
by

**BERT ASHFORD MCJIMSEY**

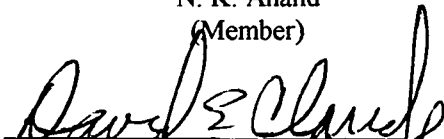
Submitted to Texas A&M University  
in partial fulfillment of the requirements  
for the degree of

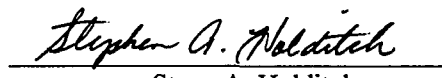
**DOCTOR OF PHILOSOPHY**


Approved as to style and content by:

  
Dennis L. O'Neal  
(Chair of Committee)

  
N. K. Anand  
(Member)

  
Dave E. Claridge  
(Member)

  
Steve A. Holditch  
(Member)

  
G. P. Peterson  
(Head of Department)

December 1994

Major Subject: Mechanical Engineering

**ABSTRACT**

An Experimental Investigation of the Effect of Oil on Convective

Heat Transfer and Pressure Drop of a HFC-32/HFC-125

Mixture. (December 1994)

Bert Ashford McJimsey, B.S., Texas A&M University;

M.S., Texas A&M University

Chair of Advisory Committee: Dr. Dennis O'Neal

The heat transfer coefficients and pressure drops of HCFC-22 and a 50% mass mixture of HFC-32/HFC-125 were experimentally measured under flow boiling conditions in a smooth tube. The refrigerants were flowed through an 8 mm diameter smooth tube at mass fluxes of 277, 434, 520 and 700 kg/m<sup>2</sup>s. Heat fluxes were applied at values of 5100, 7100 and 11000 W/m<sup>2</sup>. The heat transfer coefficients and pressure drops were measured at refrigerant qualities of 10, 15, 20, 25, 30, 40 and 60 percent. The refrigerants were examined at temperatures near 4°C. Oil was added to the HFC-32/HFC-125 mixture in concentrations of 2.6% and 5.4%. Experiments were repeated with the oil laden refrigerant.

The heat transfer coefficients for HCFC-22 increased with quality, mass flux and heat flux. The heat transfer coefficients for HFC-32/HFC-125 often decreased at low qualities and increased with quality at high qualities.

The pressure drop increased with quality and mass flux for both refrigerants. The heat transfer had a minimal effect upon pressure drop. HFC-32/HFC-125 had a lower pressure drop than HCFC-22 for all conditions. The addition of oil increased the pressure drop.

A pressure drop correlation and heat transfer correlation were developed for HFC-32/HFC-125.



## ACKNOWLEDGMENTS

I would like to thank my advisor and committee chairman, Dr. Dennis O'Neal for his guidance during this research.

I thank Dr. N. K. Anand, Dr. Dave E. Claridge and Dr. Steve A. Holditch for serving as committee members of my advisory committee. I thank Dr. Jack Bryant for serving as my graduate council representative. A special thanks to Frank Scott who helped me with many of the practical problems I encountered. I acknowledge the financial support provided by the Texas Advanced Technology Program. I acknowledge DuPont for providing some of the refrigerant used in this research.

I thank my wife Karen for her support, encouragement and love that enabled me to persevere. I thank my children, Trey and Mason, for providing joy when there were times of trial. I thank my father and mother for believing in me in everything I do.

**DEDICATION**

**TO MY FAMILY  
KAREN, TREY AND MASON**

## TABLE OF CONTENTS

CHAPTER	Page
I INTRODUCTION.....	1
II REVIEW OF LITERATURE .....	14
Pressure Drop Prediction Methods.....	14
Convective Heat Transfer Coefficient Prediction Methods .....	22
Experimental Techniques and Results .....	29
The Effect of Oil on Pressure Drop and Heat Transfer ....	32
Summary of Literature Review .....	32
III EXPERIMENTAL APPARATUS AND PROCEDURE .....	35
Experimental Setup.....	35
Oil Injection and Sampling.....	41
Instrumentation .....	43
Data Acquisition.....	45
Experimental Conditions.....	46
Testing Procedure.....	47
IV EXPERIMENTAL RESULTS FOR HCFC-22 .....	51
Results of Single Phase Experiments.....	51
Results of Two-phase Experiments.....	52
V EXPERIMENTAL RESULTS FOR HFC-32/HFC-125 50/50 MASS MIXTURE .....	84
HFC-32/HFC-125 Mixture .....	85
Flow Pattern Prediction .....	85
The Effect of Mass Flux on Pressure Drop.....	91
The Effect of Heat Flux on Pressure Drop .....	92
Pressure Drop Correlations.....	96
The Effect of Mass Flux on Heat Transfer Coefficient.....	100
The Effect of Heat Flux on Heat Transfer Coefficient ....	108
Summary .....	119

**TABLE OF CONTENTS (Continued)**

CHAPTER	Page
VI	<b>DEVELOPMENT OF A HEAT TRANSFER CORRELATION FOR HFC-32/HFC-125</b> ..... 121 Summary of Correlation Development ..... 136
VII	<b>EXPERIMENTAL RESULTS FOR HFC-32/HFC-125 50/50 MASS MIXTURE WITH A POLYOL ESTER (POE)</b> ..... 139 The Effect of Oil Properties Upon Mixture Properties..... 140 The Effect of Oil on Pressure Drop..... 142 The Effect of Mass Flux on Heat Transfer..... 149 The Effect of Heat Flux on Heat Transfer ..... 152 The Effect of Oil on Heat Transfer..... 154 Summary of Experimental Results..... 163
VIII	<b>COMPARISON OF HFC-32/HFC-125 EXPERIMENTAL RESULTS WITH HCFC-22 EXPERIMENTAL RESULTS</b> .... 164
IX	<b>CONCLUSIONS AND RECOMMENDATIONS</b> ..... 174 Conclusions ..... 174 Recommendations ..... 177
REFERENCES	..... 179
APPENDIX A	..... 184
APPENDIX B	..... 199
VITA	..... 201

**LIST OF TABLES**

<b>Table</b>		<b>Page</b>
1.1	Degenerative Properties of Some Common Refrigerants.....	8
3.1	Description of Data Acquisition Sensor Channels.....	46
3.2	Test Conditions for Two-phase Experiments.....	48
6.1	Error Comparison of Heat Transfer Correlations.....	130
7.1	Properties of HFC-32/HFC-125 and a POE Oil.....	140
8.1	Fluid Properties of HCFC-22 and HFC-32/HFC-125 at 4.5 °C (40°F).....	165

## LIST OF FIGURES

FIGURE		Page
1.1	Possible Refrigerant Combinations Based upon Methane and Ethane .....	4
1.2	A Summary of Refrigerant Properties Based upon Composition .....	5
1.3	The Ozone Depleting Process .....	7
1.4	Air-conditioner Schematic and Vapor Compression T-s Diagram....	10
1.5	Flow Patterns in Horizontal Flow .....	11
1.6	Regions of Evaporative Heat Transfer . .....	12
2.1	The Effect of Mass Flux Upon Pressure Drop Correlations .....	21
2.2	The Overall Nucleate Boiling Contribution .....	25
3.1	Schematic Diagram of Experimental Setup .....	36
3.2	Cut Away View of the Test Section .....	38
3.3	Oil Sampling Device .....	42
3.4	Measurement of Bulk Temperature .....	44
4.1	Comparison Between Measured Convective Coefficients and Previously Published Convective Coefficients for the same Flow Conditions .....	54
4.2	Evaporative Heat Transfer Coefficients at Various Mass Velocities and Heat Fluxes Using Test Section Inlet Qualities .....	55
4.3	Evaporative Heat Transfer Coefficients at Various Mass Velocities and Heat Fluxes Using Average Test Section Qualities ..	58
4.4	A Comparison of Evaporation Heat Transfer Data with Prediction Correlations Using Test Section Inlet Qualities .....	59

**LIST OF FIGURES (Continued)**

FIGURE		Page
4.5	A Comparison of Evaporation Heat Transfer Data with Prediction Correlations Using Average Test Section qualities .....	60
4.6	A Comparison of Evaporation Data and Prediction Correlations for a Heat Flux of $11000 \text{ W/m}^2$ and a Mass Flux of $520 \text{ kg/m}^2\text{s}$ ....	62
4.7	A Comparison of Evaporation Data and Prediction Correlations for a Heat Flux of $11000 \text{ W/m}^2$ and a Mass Flux of $430 \text{ kg/m}^2\text{s}$ ....	64
4.8	A Comparison of Evaporation Data and Prediction Correlations for a Heat Flux of $7100 \text{ W/m}^2$ and a Mass Flux of $434 \text{ kg/m}^2\text{s}$ .....	65
4.9	A Comparison of Evaporation Data and Prediction Correlations for a Heat Flux of $7100 \text{ W/m}^2$ and a Mass Flux of $280 \text{ kg/m}^2\text{s}$ ....	66
4.10	A Comparison of Evaporation Data and Prediction Correlations for a Heat Flux of $5100 \text{ W/m}^2$ and a Mass Flux of $280 \text{ kg/m}^2\text{s}$ .....	67
4.11	Evaporative Heat Transfer Coefficients as a Function of the Liquid Convective Coefficient .....	70
4.12	Evaporative Heat Transfer Coefficients as a Function of Pool Boiling Convective Coefficient as Calculated from Cooper .....	72
4.13	Evaporative Heat Transfer as a Function of Martinelli Parameter ...	73
4.14	The Ratio of Two-phase to Predicted Single Phase Convective Heat Transfer Coefficient .....	74
4.15	Flow Pattern Map .....	75
4.16	Flow Pattern Map .....	78
4.17	Pressure Drop for Various Mass Velocities and Heat Fluxes .....	79
4.18	A Comparison of Pressure Drop with Predicted Pressure Drops .....	81
5.1	Flow Pattern Map for HFC-32/HFC-125 .....	87

**LIST OF FIGURES (Continued)**

FIGURE	Page
5.2	Flow Pattern Map for HFC-32/HFC-125 with Constant Quality..... 89
5.3	Flow Pattern Map for an HFC-32/HFC-125 Mixture ..... 90
5.4	Pressure Drop Per Unit Length for Various Mass Fluxes at a Heat Flux of 5100 W/m <sup>2</sup> ..... 93
5.5	Pressure Drop Per Unit Length for Various Mass Fluxes at a Heat Flux of 11000 W/m <sup>2</sup> ..... 94
5.6	Pressure Drop Per Unit Length for Various Heat Fluxes at a Mass Flux of 520 kg/m <sup>2</sup> -s ..... 95
5.7	The Ratio of Two-Phase Pressure Drop to Single-Phase Pressure Drop ..... 98
5.8	A Comparison of Experimental Pressure Drop with Predicted Pressure Drop ..... 99
5.9	The Ratio of Two-phase Pressure Drop to the Predicted Single-phase Pressure Drop Flowing at the Same Mass Rate as the Two-phase mixture ..... 101
5.10	Regions of Evaporative Heat Transfer ..... 104
5.11	The Effect of Mass Flux upon Heat Transfer Coefficient of HFC-32/HFC-125 at a Heat Flux of 5100 W/m <sup>2</sup> ..... 105
5.12	The Effect of Mass Flux upon Heat Transfer Coefficient of HFC-32/HFC-125 at a Heat Flux of 7100 W/m <sup>2</sup> ..... 109
5.13	The Effect of Mass Flux upon Heat Transfer Coefficient of HFC-32/HFC-125 at a Heat Flux of 11000 W/m <sup>2</sup> ..... 110
5.14	The Effect of Heat Flux upon Heat Transfer Coefficient of HFC-32/HFC-125 at a Mass Flux of 277 kg/m <sup>2</sup> -s ..... 113



**LIST OF FIGURES (Continued)**

FIGURE	Page
5.15 The Effect of Heat Flux upon Heat Transfer Coefficient of HFC-32/HFC-125 at a Mass Flux of 434 kg/m <sup>2</sup> ·s .....	114
5.16 The Effect of Heat Flux upon Heat Transfer Coefficient of HFC-32/HFC-125 at a Mass Flux of 520 kg/m <sup>2</sup> ·s .....	115
5.17 The Effect of Heat Flux upon Heat Transfer Coefficient of HFC-32/HFC-125 at a Mass Flux of 700 kg/m <sup>2</sup> ·s .....	117
6.1 The Effect of Nucleate Boiling and Convective Forces on Heat Transfer Coefficient.....	126
6.2 The Effect of Mass Flux and Heat Flux on the Nucleate Contribution to Heat Transfer.....	128
6.3 The Effect of Mass Flux and Heat Flux on the Convective Contribution to Heat Transfer.....	129
6.4 A Comparison of Evaporation Heat Transfer Data with Prediction Correlations for a Heat Flux of 5100 W/m <sup>2</sup> and a Mass Flux of 277 kg/m <sup>2</sup> ·s .....	131
6.5 A Comparison of Evaporation Heat Transfer Data with Prediction Correlations for a Heat Flux of 11000 W/m <sup>2</sup> and a Mass Flux of 277 kg/m <sup>2</sup> ·s .....	134
6.6 A Comparison of Evaporation Heat Transfer Data with Prediction Correlations for a Heat Flux of 11000 W/m <sup>2</sup> and a Mass Flux of 434 kg/m <sup>2</sup> ·s .....	135
6.7 A Comparison of Evaporation Heat Transfer Data with Prediction Correlations for a Heat Flux of 5100 W/m <sup>2</sup> and a Mass Flux of 700 kg/m <sup>2</sup> ·s .....	137
7.1 Flow Pattern Map for HFC-32/HFC-125 with 2.5 Percent POE Oil.....	143
7.2 The Effect of Oil Concentration on Pressure Drop Per Unit Length for a Heat Flux of 5100 W/m <sup>2</sup> and a Mass Flux of 277 kg/m <sup>2</sup> ·s ..	144

**LIST OF FIGURES (Continued)**

FIGURE		Page
7.3	The Ratio of Pressure Drop for Heat Flux of 5100 W/m <sup>2</sup> and a Mass Flux of 277 kg/m <sup>2</sup> ·s .....	146
7.4	The Effect of Oil Concentration on Pressure Drop Per Unit Length for a Heat Flux of 11000 W/m <sup>2</sup> and a Mass Flux of 520 kg/m <sup>2</sup> ·s .....	147
7.5	The Ratio of Pressure Drop for Heat Flux of 11000 W/m <sup>2</sup> and a Mass Flux of 520 kg/m <sup>2</sup> ·s .....	148
7.6	The Effect of Mass Flux upon Heat Transfer Coefficient of HFC-32/HFC-125 Containing a 2.6 Percent Oil Concentration at a Heat Flux of 5100 W/m <sup>2</sup> .....	150
7.7	The Effect of Mass Flux upon Heat Transfer Coefficient of HFC-32/HFC-125 Containing a 2.6 Percent Oil Concentration at a Heat Flux of 11000 W/m <sup>2</sup> .....	151
7.8	The Effect of Heat Flux upon Heat Transfer Coefficient of HFC-32/HFC-125 Containing a 2.6 Percent Oil Concentration at a Mass Flux of 277 kg/m <sup>2</sup> ·s .....	153
7.9	The Effect of Heat Flux upon Heat Transfer Coefficient of HFC-32/HFC-125 Containing a 2.6 Percent Oil Concentration at a Mass Flux of 520 kg/m <sup>2</sup> ·s .....	155
7.10	The Effect of Heat Flux upon Heat Transfer Coefficient of HFC-32/HFC-125 Containing a 2.6 Percent Oil Concentration at a Mass Flux of 700 kg/m <sup>2</sup> ·s .....	156
7.11	The Effect of Oil Concentration upon Heat Transfer Coefficient for a Heat Flux of 7100 W/m <sup>2</sup> and a Mass Flux of 277 kg/m <sup>2</sup> ·s .....	158
7.12	The Effect of Oil Concentration upon Heat Transfer Coefficient for a Heat Flux of 11000 W/m <sup>2</sup> and a Mass Flux of 277 kg/m <sup>2</sup> ·s .....	159

**LIST OF FIGURES (Continued)**

<b>FIGURE</b>		<b>Page</b>
7.13	The Effect of Oil Concentration upon Heat Transfer Coefficient for a Heat Flux of $5100 \text{ W/m}^2$ and a Mass Flux of $520 \text{ kg/m}^2\cdot\text{s}$ .....	161
7.14	The Effect of Oil Concentration upon Heat Transfer Coefficient for a Heat Flux of $11000 \text{ W/m}^2$ and a Mass Flux of $520 \text{ kg/m}^2\cdot\text{s}$ .....	162
8.1	The Ratio of HFC-32/HFC-125 and HCFC-22 Two-phase Heat Transfer Coefficients .....	168
8.2	The Ratio of HFC-32/HFC-125 and HCFC-22 Two-phase Pressure Drops .....	171
8.3	T-s Diagram of a Vapor Compression Cycle for HCFC-22 and HFC-32/HFC-125 .....	172
8.4	Pressure-Enthalpy Diagram of a Vapor Compression Cycle for HCFC-22 and HFC-32/HFC-125 .....	173

**NOMENCLATURE**

A	area, m <sup>2</sup>
Bo	boiling number
cp	specific heat, kJ/kg°C
Co	convection number
D	diameter, mm
E	enhancement factor
f	friction factor
Fr	Froude number
G	mass flux, kg/m <sup>2</sup> s
g	gravitational acceleration, 9.815 m/s <sup>2</sup>
h	convective coefficient, W/m <sup>2</sup> °C
i <sub>fg</sub>	enthalpy of vaporization, kJ/kg
k	thermal conductivity, W/m°C
<i>m</i>	mass flow rate, kg/s
M	molecular weight
P	pressure, kPa
Pr	Prandtl number
q	heat flux, w/m <sup>2</sup>
<i>Q</i>	power, watt
Re	Reynolds number
S	suppression factor
T	Temperature, °C
W	weight percent of oil
x	quality
z	distance, meter

**NOMENCLATURE (Continued)****Greek Symbols**

$\alpha$	void fraction
$\chi$	Martinelli parameter
$\phi$	two-phase multiplier
$\mu$	viscosity
$\rho$	density
$\sigma$	surface tension
$\Omega$	angle with the horizontal

**Subscripts**

conv	convection
fr	friction
l	liquid
le	liquid equivalent
lo	liquid flowing at the mass rate of the two-phase refrigerant
mic	microscopic
pool	pool boiling
r	reduced
sat	saturated
tp	two phase
tt	turbulent-turbulent
v	vapor

## CHAPTER I

### INTRODUCTION

Chlorofluorocarbons, or CFCs, are currently used for four major purposes: aerosol propellants, blowing agents for manufacturing foam, industrial solvents and refrigerants in various types of air-conditioning, heat pump and refrigeration applications. Because of their known degenerative effect upon ozone in the earth's atmosphere, the production of CFCs will be reduced considerably in the next decade and ecologically acceptable refrigerants will be used instead.

The United States consumes 40 percent of the world's production of CFCs with one third of that amount used for refrigeration. [Braswell, 1988] While Refrigerant 22 (R-22) used in residential air-conditioners is at this time exempt from production or usage quotas, the production of R-22 will be curtailed in the year 2010 along with CFCs. [Hearn, 1990] R-22 is also being hailed as an interim replacement for CFCs in many moderate temperature refrigeration applications and in lower temperature refrigeration applications as a primary component of R-502. R-502 is more efficient than R-22 when used in low temperature applications. [Reitz, 1990] The properties of R-22 are such that its detrimental effects upon the atmosphere are much less than that of CFCs. The chemical industry is capable of producing adequate supplies of R-22 and equipment manufacturing companies are familiar with the properties and capabilities of R-22. Manufacturing companies require long lead times to develop new equipment capable of meeting energy efficiency standards even when using a familiar refrigerant in a new application. Banning R-22 without a suitable replacement would be devastating to all who depend upon air-conditioning and refrigeration\* .

---

\* The format of this proposal follows that of the *Transactions of the American Society of Heating, Refrigerating and Air-Conditioning Engineers*.

Chlorofluorocarbons or CFCs are distinguished as carbon chains with only chlorine and fluorine atoms attached to the chain. CFC-12 is a methane molecule with all of the hydrogen atoms replaced with chlorine and fluorine. A molecule like CFC-12, which contains only a carbon and halogens, is a fully halogenated molecule. Other refrigerant variations of interest are hydrofluorocarbons, HCFCs, and hydrofluorocarbons, HFCs. HCFCs and HFCs such as R-22 and R-134a respectively, are often considered as interim and long term replacements for CFCs. HCFCs have fluorine and chlorine atoms as well as a hydrogen atom attached to the carbon chain. HFCs have only hydrogen and fluorine attached to the carbon chain. One final refrigerant chemical group of interest is the hydrocarbons. Methane, ethane and propane are familiar hydrocarbons. Hydrocarbons have only hydrogen atoms attached on the carbon chain and are referenced by the letters HC, such as HC-290 for propane.

The very earliest refrigerants such as propane and ammonia were often toxic and/or flammable. In 1928, Thomas Midgley, a research engineer with a General Motors subsidiary attempted the task of developing a non-toxic, non-flammable refrigerant. Dr. Midgley used the periodic chart, arranging the elements according to the number of vacancies in the outer shell of electrons. The number of potential refrigerants was reduced by eliminating the inert elements because they would not bond well with any other elements and their boiling points were much too low. The inert elements are in the right most column of the chart. Secondly, the metals were eliminated as the bonds with other atoms often tend to be non-volatile or combinations with other molecules form solids. Several of the other elements were eliminated because they tended to form toxic compounds. This left eight elements: hydrogen, carbon, nitrogen, oxygen, fluorine, sulfur, chlorine and bromine. Recent database searches of chemical compound properties using criteria such as freezing temperature, critical temperature, vapor pressure at 80 degrees Celsius and latent heat of

vaporization and then eliminating known toxic or flammable compounds have turned up replacement refrigerants that are comprised of elements from this original list of elements determined by Dr. Midgley [McClinden and Didion, 1987]. The most promising replacements are expected to come from a rather limited group of compounds built upon either the methane or ethane carbon chain. The element list can be further shortened to seven by eliminating bromine which is even more harmful to the atmosphere than chlorine. Sulfur and nitrogen tend to form toxic and chemically reactive compounds. Compounds formed with oxygen tend to have boiling points that are not compatible with traditional refrigeration equipment. The chemicals that remain are carbon, hydrogen, chlorine and fluorine. All of the possible compounds that can be formulated on the methane and ethane carbon chain can be easily shown in Figure 1.1.

Once potential chemical replacements are identified, then the process of choosing the best and most appropriate replacement refrigerant still remains. The refrigerant should be nonflammable, non toxic and should not cause further degradation of the atmosphere. It must also be stable and possess proper thermal characteristics such as boiling point and critical point within the right range of temperatures. The oil solubility, metal compatibility and cost are significant considerations. Some properties of refrigerants formed on the methane and ethane carbon chain may be generalized as shown in Figure 1.2. The molecules having the most hydrogen atoms are more flammable. The molecules containing the most chlorine are usually more toxic. Toxicity is how a chemical reacts with a living organism. The molecules with only fluorine and chlorine attached are fully halogenated with long atmospheric life. The boiling point temperature increases as the chlorine content increases. The obvious place to start searching for a replacement is in the non-shaded region in Figure 1.2. The mixing or blending of refrigerants is a very real possibility. The positive aspect of one may overshadow the degrading aspect of another.



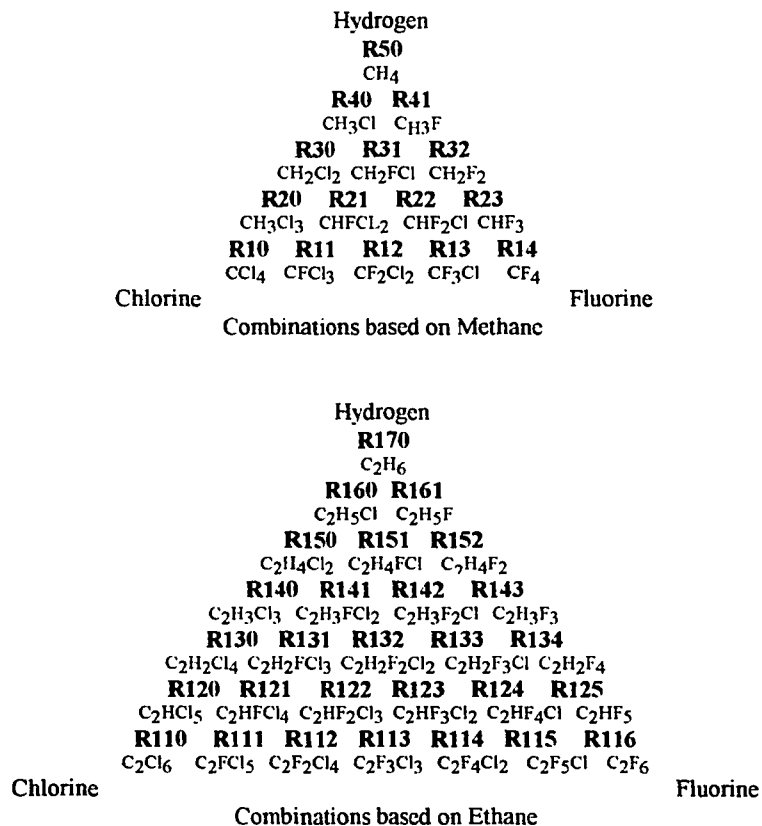


Figure 1.1 Possible refrigerant combinations based upon Methane and Ethane.

In 1974, forty four years after Dr. Midgley introduced R-12, to the American Chemical Society, Professor Sherwood Rowland and Dr. Mario Malina proposed the theory that chlorofluoromethane compounds might adversely affect the earth's ozone. The "ozone layer" consists of ozone, O<sub>3</sub>, formed in the stratosphere. The stratosphere is the layer in the earth's atmosphere that lies between 7 and 28 miles in height. Ozone is formed from oxygen (O<sub>2</sub>) and UV radiation emitted by the sun. The ozone absorbs UV radiation during formation and continues to absorb it after its formation [Beardsley, 1990]. The destruction of the ozone layer allows harmful UV radiation to

reach the earth's surface. The long term effects include increased incidence of skin cancer, global climate changes, destruction of crops and disruption of the marine food chain.

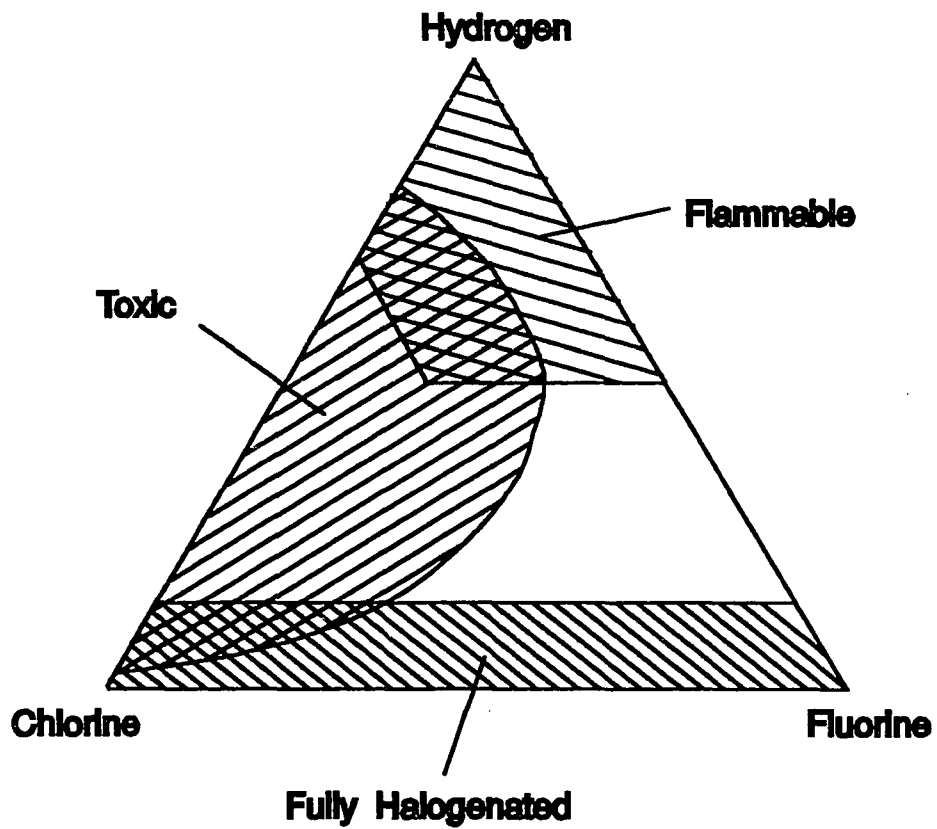


Figure 1.2 A Summary of Refrigerant Properties Based upon Composition.

For CFCs to harm the ozone layer, the molecule must be stable enough to survive until it reaches the stratosphere. The process that destroys the ozone starts when UV radiation emitted by the sun reacts with CFCs, causing the release of chlorine atoms as shown in Figure 1.3. The chlorine atom then reacts with one of the three oxygen atoms contained by ozone forming a chlorine oxygen molecule. When the chlorine oxygen molecule comes into contact with a free oxygen atom, the chlorine releases the oxygen atom leaving a free chlorine atom and a molecule of oxygen. The free chlorine is then able to react with another oxygen atom from ozone. HCFCs go through the same steps but the presence of a hydrogen atom makes the molecule less stable allowing it to break down in the lower atmosphere or troposphere where it is washed out by rain.

The amount of ozone depletion potential is referenced to the ozone depletion potential of CFC-11. The ODPs of some common refrigerants are listed in Table 1.1. Along with the ozone depleting properties, refrigerants also contribute to the greenhouse effect. The greenhouse effect is caused by chemical compounds in the earth's atmosphere that transmit UV radiation emitted by the sun and absorb UV radiation emitted by the earth, thus heating the atmosphere and causing global warming in much the same manner as a greenhouse. The global warming potential, or GWP rating, is referenced to the GWP of CFC-11 and is listed in Table 1.1 along with the atmospheric life of some common refrigerants. carbon dioxide is the biggest contributor to global warming but it is generally accepted that the greenhouse effect should be addressed immediately after ozone destruction is brought to acceptable limits.

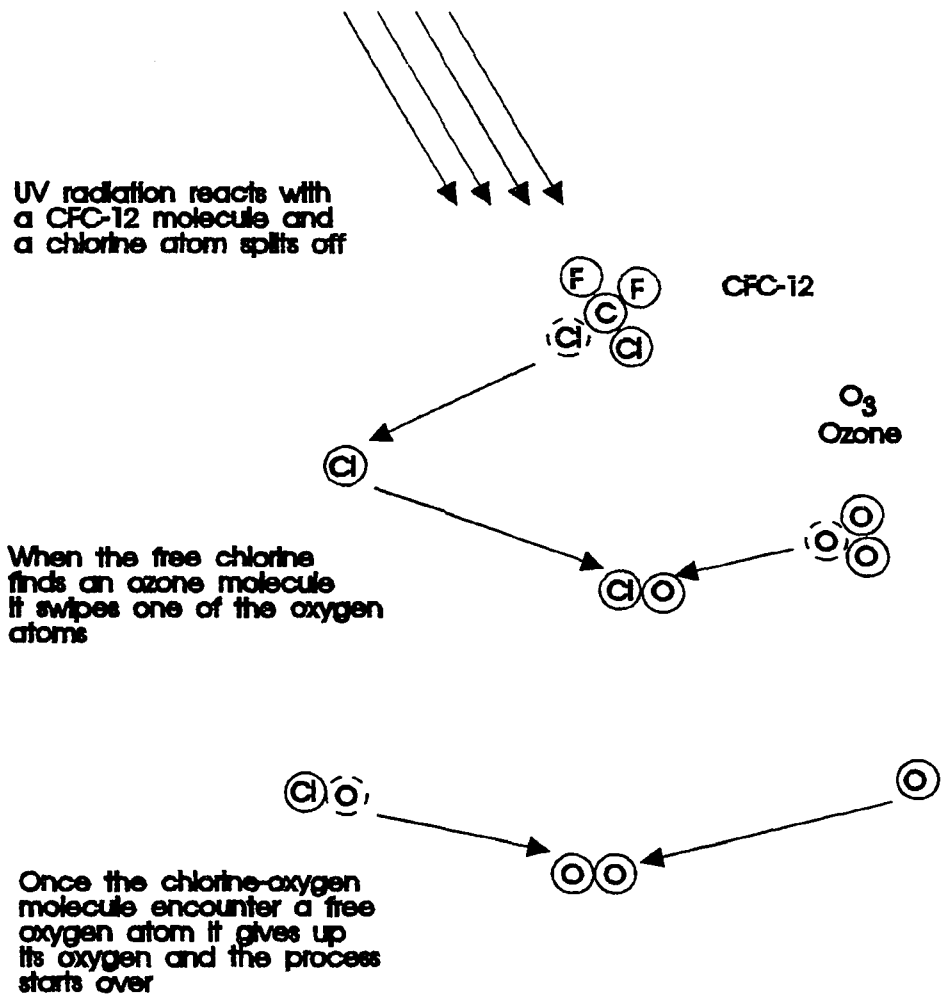


Figure 1.3 The Ozone Depleting Process.

Table 1.1 Degenerative Properties of Some Common Refrigerants

	ODP	GWP	ATMOSPHERIC LIFETIME (YEARS)
CFC-11	1.00	1.00	61
CFC-12	1.00	3.10	121
CFC-113	0.80	1.35	102
CFC-114	1.00	3.90	268
CFC-115	0.60	7.50	493
CFC-13	0.50	-	-
CFC-502	0.30	5.35	493
HCFC-22	0.05	0.34	15
HFC-134a	0.00	0.27	10
HFC-125	0.00	0.58	22

The push to reduce and eventually eliminate CFCs began once the first indication of the ozone problem became evident. The earliest step to phase out and eventually ban CFCs in this country was in the banning of fully halogenated CFCs for non-essential aerosol propellants. The concern over ozone depletion waned until a link was established between CFCs and the green house effect and the ozone hole above Antarctica. The concern for world health and the global nature of the Greenhouse affect and the ozone problem was followed by the Montreal protocol [Anderson, 1987]. In September of 1987, thirty one nations signed the Montreal protocol which established future restrictions on fully halogenated chlorofluorocarbons (CFCs). HCFCs, such as R-22 were excluded. The Montreal protocol limited CFC 11,12, 113, 114 and 115 to 1986 levels [Likes, 1988]. Since R-115 was a component of R-502, R-502 is also limited. The quantities were further reduced by 20% in 1993 and 50 % in 1998.

A residential air conditioner uses the refrigerant as the working fluid in a vapor compression cycle to produce a cooling effect. The evaporator is an integral part of

the vapor compression cycle. During evaporation, or boiling of the working fluid, heat is absorbed. The heat absorption corresponds to heat removal from the air in a refrigerator or residence. The heat removal is synonymous with the cooling effect that takes place. Refrigerant performance data during evaporation must be gathered before efficient air conditioners can be designed.

The purpose of the evaporator in a refrigerator or air-conditioner is to absorb heat from the air. This heat is rejected at the condenser which is physically located outside the refrigerated or air-conditioned area. The vapor compression air-conditioning cycle along with an air conditioner schematic is shown in Figure 1.4. The refrigerant flows into the compressor as a low pressure vapor and flows out as a high pressure gas, then into the condenser. The refrigerant condenses along path 2-3 where heat is rejected. The refrigerant then flows as a saturated liquid through an expansion valve 3-4 and exits as a low pressure two phase mixture. The two phase mixture flows into the evaporator along path 4-1 where heat is absorbed. The refrigerant leaves the evaporator as a superheated vapor and enters the compressor. The refrigerant evaporates as it flows through a horizontal pipe or tube . All of the components are interdependent upon the other components. The evaporator should be sized consistent with the other components and the cooling load. To assist this design process, refrigerant thermal and transport characteristics must be available.

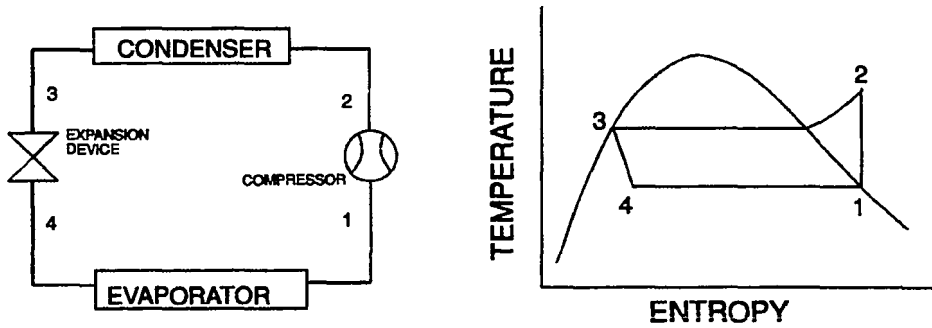


Figure 1.4 Air-conditioner Schematic and Vapor Compression T-s Diagram.

The evaporation of refrigerant flowing in a horizontal tube is a complicated process. The heat transfer mechanism of an evaporating refrigerant can best be described as three separate boiling regions (1) nucleate boiling, (2) two-phase convective boiling and (3) the liquid deficient region [Collier, 1982]. The refrigerant will proceed through different flow patterns for the nucleate boiling, convective boiling and liquid deficient regions. The different flow patterns for horizontal flow are shown in Figure 1.5. The flow pattern, flow region, convective heat transfer coefficient and the pressure drop are dependent on the heat flux, mass velocity, temperature, pressure and fluid type. Evaporation performance of the replacement refrigerants is a function of these independent variables.

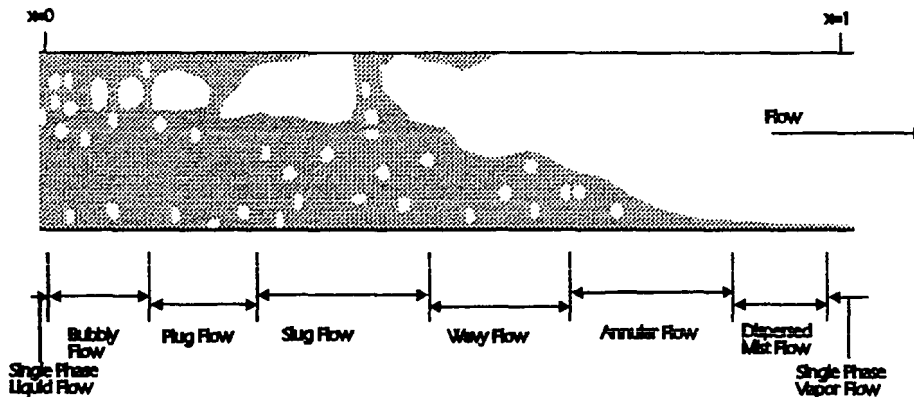


Figure 1.5 Flow Patterns in Horizontal Flow.

The saturated boiling heat transfer is dominated by three modes of heat transfer shown in Figure 1.6 [Collier, 1982]. Saturated nucleate boiling is dominant at low qualities. For this boiling region bubbles form at the wall and grow to the point of collapse or departure [Hsu and Graham, 1976; Zuber, 1961] from the wall. The bubble formation at the wall disrupts the velocity profile of the liquid. This impedes the convective heat transfer to the liquid. The flow patterns associated with this saturated nucleate boiling region are bubbly slug and plug.



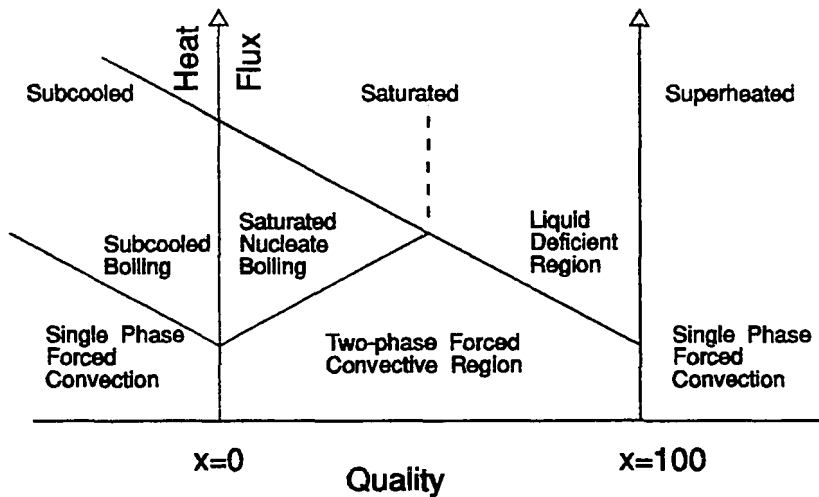


Figure 1.6 Regions of Evaporative Heat Transfer.  
[Collier, 1982] (Reprinted with permission)

Once the quality is sufficiently high, there is a thin layer of liquid flowing along the wall, the vapor bubble growth is stifled and the bubbles can no longer depart from the wall. In the two phase convective heat transfer region the convective heat transfer and conduction through the liquid at the wall are the primary modes of heat transfer. The flow patterns in this region are usually annular and annular with entrained liquid droplets. Saturated nucleate boiling and two phase convective heat transfer are not mutually exclusive. There is a region of transition from one to the other. There is also a region of transition from the convective region to liquid deficient region. The qualities are higher in the liquid deficient region and the liquid is completely entrained in the vapor. The flow pattern is mist-like. Heat is transferred from the wall to the refrigerant vapor by convection.

To gain a better understanding of refrigerant behavior during evaporation an experimental investigation has been initiated to define average heat transfer and frictional characteristics of a binary HFC-125/HFC-32 binary mixture. The primary focus of this work shall include studying the nucleate boiling/convective transition and

the effect of oil on this transition. The evaporation process will be studied for mass velocities and temperatures similar to those in residential air-conditioners.

## CHAPTER II

### REVIEW OF LITERATURE

The literature relevant to two-phase refrigerants flowing in a horizontal tube can be divided into four categories: (1) pressure drop models, (2) convective heat transfer prediction techniques, (3) experimental measurement of convective heat transfer and pressure drop of refrigerants flowing in a horizontal tube and (4) the effect of oil on convective heat transfer and pressure drop. These topics are discussed below:

#### PRESSURE DROP PREDICTION METHODS

Two basic flow models that have been used to predict pressure drop in two-phase fluids are the homogeneous model and the separate flow model. The homogeneous model is based on two phases flowing together as a single-phase and having mean properties determined from the vapor and liquid. The separate flow model is based upon the two phases flowing together at separate but not necessarily equal velocities. Both models start with an equation derived from conservation of mass and conservation of momentum for vapor and liquid flowing in a tube and is shown in Equation 2.1.

$$-\left(\frac{dP}{dz}\right) = \frac{P}{A} \left(\frac{dA}{dz}\right) - \left(\frac{dP}{dz}\right)_{fr} + [(1-\alpha)\rho_l + \alpha\rho_v] g \sin \Omega$$

$$+ \frac{1}{A} \frac{d}{dz} \left( \frac{G^2 x^2 A}{\alpha \rho_v} + \frac{G^2 (1-x)^2 A}{(1-\alpha)\rho_l} \right) \quad (2.1)$$

Four parts make up the total pressure drop per unit length. The first term on the right hand side of Equation 2.1 represents the pressure variation due to a change in flow area. The second term represents the pressure drop due to friction. The third term

accounts for the gravitational pressure drop and the last term represents acceleration or deceleration of the flow. The  $\alpha$  term represents void fraction and the  $\Omega$  term represents the angle the tube is inclined from the horizontal.

Several simplifications can be made to Equation 2.1 to address either the homogeneous or separate flow model. If a test section is formed out of rigid copper tubing, the internal diameter does not change. Thus, the first term that accounted for changing area can be set to zero. If the test section is horizontal, the term accounting for pressure drop due to gravity will also be zero. Equation 2.1 reduces to:

$$-\left(\frac{dP}{dz}\right) = -\left(\frac{dP}{dz}\right)_{fr} + \frac{1}{A} \frac{d}{dz} \left( \frac{G^2 x^2 A}{\alpha \rho_v} + \frac{G^2 (1-x)^2 A}{(1-\alpha) \rho_l} \right) \quad (2.2)$$

The simplifying assumptions regarding the homogeneous model and the separate flow model differ. The key assumptions for the homogeneous flow model include: 1) the vapor and liquid velocities are equal and 2) the two-phase flow behaves like a single-phase fluid. Once the assumption of equal velocities is made, the void fraction can be estimated. The void fraction for two-phases flowing together at equal velocities is shown in Equation 2.3.

$$\alpha = \left( \frac{(x / \rho_v)}{[(1-x) / \rho_l] + (x / \rho_v)} \right) \quad (2.3)$$

When the velocities are equal the void fraction is only a function of quality, liquid density and vapor density. The key to this method is predicting the two-phase equivalent viscosity and the two-phase equivalent density. Several methods have been used to predict the two-phase viscosity from the liquid and vapor properties. The most

commonly used method is that proposed by McAdams [1942] and shown in Equation 2.4. The two-phase density can be predicted similarly as shown in Equation 2.5.

$$\frac{1}{\mu_{tp}} = \frac{x}{\mu_v} + \frac{1-x}{\mu_l} \quad (2.4)$$

$$\frac{1}{\rho_{tp}} = \frac{x}{\rho_v} + \frac{1-x}{\rho_l} \quad (2.5)$$

The two-phase frictional pressure drop can be calculated using a single-phase approach. The two-phase Reynolds number is calculated using the two-phase viscosity shown in Equation 2.6. The Blasius correlation can be used to calculate the two-phase friction factor for turbulent flow in round tubes. This equation was developed for single-phase fluids and is given by Equation 2.7. Once the two-phase friction factor is calculated, the frictional pressure drop can be determined for the fluid in the same manner as it would be for a single-phase fluid. The frictional pressure drop is calculated using Equation 2.8. .

$$Re_{tp} = \frac{G D}{\mu_{tp}} \quad (2.6)$$

$$f_{tp} = 0.079 \cdot Re^{-0.25} \quad (2.7)$$

$$-\left(\frac{dP}{dz}\right)_{fr} = \frac{2 f_{tp} G^2}{\rho_l D} \quad (2.8)$$

Equation 2.2 still contains a void fraction term along with liquid and vapor density and quality. Equation 2.3 shows that the void fraction was a function of quality and vapor and liquid density. Substituting Equation 2.3 and the frictional pressure

drop, Equation 2.8, into Equation 2.2 gives an expression that does not contain void fraction, (Equation 2.9).

$$-\left(\frac{dP}{dz}\right) = \left( \left( \frac{2 f_p G^2}{\rho_l D} \right) + G^2 v_{lv} \frac{dx}{dz} \right) / \left( 1 + G^2 x \frac{dv_v}{dP} \right) \quad (2.9)$$

The denominator contains a term relating the change in vapor specific volume to the change in pressure. This term accounts for the compressibility of the vapor but is generally much smaller than unity for small changes in pressure. The final version of the homogeneous pressure drop per unit length is shown in Equation 2.10 where the vapor compressibility term is considered negligible and is removed. The change in quality per change in length,  $\frac{dx}{dz}$ , is constant for a constant heat flux.

$$-\left(\frac{dP}{dz}\right) = \left( \left( \frac{2 f_p G^2}{\rho_l D} \right) + G^2 v_{lv} \frac{dx}{dz} \right) \quad (2.10)$$

The separated flow model considered both the liquid and vapor to be flowing as separate streams within the tube. Both phases are assumed to flow at constant but not necessarily equal velocities. If both phases flow at constant velocity then there cannot be a quality gradient along the tube [Collier, 1982]. A finite difference technique must be used with the separated flow model when refrigerant evaporates in a tube and the quality changes along the length. The first literature on the separated flow model [Lockhart and Martinelli, 1949] showed a relationship between the vapor and liquid pressure drop as shown in Equation 2.11. This relationship between the pressure drop of the liquid and pressure drop of the vapor was developed based upon constant velocities of vapor and liquid, the area that each phase would occupy (void fraction) and mass rate of each phase. This ratio of two-phase pressure drop was

correlated to the vapor and liquid properties represented by the what was to become known as the Martinelli parameter  $\chi$  shown in Equation 2.12 and the four possible combinations of liquid and vapor, laminar or turbulent flow regimes.

$$\chi^2 = \left( \frac{\partial p}{\partial z} \right)_l / \left( \frac{\partial p}{\partial z} \right)_v \quad (2.11)$$

$$\chi = \left( \frac{1-x}{x} \right)^{0.9} \left( \frac{\rho_v}{\rho_l} \right)^{0.5} \left( \frac{\mu_l}{\mu_v} \right)^{0.1} \quad (2.12)$$

The pressure drop of the vapor or liquid phase alone needs to be connected to the two-phase pressure drop. Lockhart and Martinelli [1949] did this by developing two-phase multipliers shown in Equations 2.13, 2.14 and 2.15. The subscripts v, l and lo represented the vapor phase, liquid phase and the liquid phase flowing at the total mass velocity respectively. The fr subscript represents the two-phase frictional pressure drop.

$$\phi_v = \left( \frac{(dp/dz)_{fr}}{(dp/dz)_v} \right)^{1/2} \quad (2.13)$$

$$\phi_l = \left( \frac{(dp/dz)_{fr}}{(dp/dz)_l} \right)^{1/2} \quad (2.14)$$

$$\phi_{lo} = \left( \frac{(dp/dz)_{fr}}{(dp/dz)_{lo}} \right)^{1/2} \quad (2.15)$$

The parameters developed by Martinelli were curve fit [Chisholm, 1967] with the two-phase multiplier as a function of the Martinelli parameter and an empirically derived constant shown in Equation 2.16. The constant C took its value based upon the flow regimes present in the tube. There exists four possible combinations of vapor

and liquid flow regimes where each could either be turbulent or laminar. The equations were used to predict two-phase pressure drop by calculating the Martinelli parameter and the two-phase multiplier from Equation 2.16 and using a single-phase correlation to predict the single-phase pressure drop. The two-phase frictional pressure drop was calculated using an Equation like 2.17. The frictional pressure drop was only a part of the pressure drop in the tube. The complete equation used to calculate the two-phase pressure drop using the separate flow model as originally developed by Lockhart and Martinelli [1949] was shown in Equation 2.18.

$$\phi_1^2 = 1 + \frac{C}{\chi} + \frac{1}{\chi^2} \quad (2.16)$$

$$\left(\frac{\partial p}{\partial z}\right)_{tp} = \left(\frac{\partial p}{\partial z}\right)_{l0} \phi_{l0} \quad (2.17)$$

$$-\left(\frac{dP}{dz}\right) = \left(\frac{2 f_{l0} G^2}{\rho_l D}\right) \phi_{l0} + \frac{1}{A} \frac{d}{dz} \left( \frac{G^2 x^2 A}{\alpha \rho_v} + \frac{G^2 (1-x)^2 A}{(1-\alpha) \rho_l} \right) \quad (2.18)$$

A second technique for calculating the frictional pressure drop was presented by Friedel [1979]. This technique was stated to be the most accurate general pressure drop correlation for two-phase flow [Whalley, 1987]. The end result of this method was the determination of  $\phi_{l0}$ . Equation 2.18 was still used to calculate the overall pressure drop, only the technique used to calculate  $\phi_{l0}$  was different.

The calculation of frictional pressure drop by the method presented by Friedel [1979] is shown in Equations 2.19 through 2.25. These equations were not all dimensionless and the density was input in  $\text{kg/m}^3$ , the viscosity in  $\text{N s/m}^2$ , surface



tension in N/m and acceleration due to gravity in  $m/s^2$ . The friction factors for vapor and liquid phases can be calculated from Equation 2.7.

$$\rho_{tp} = \left( \frac{x}{\rho_v} + \frac{1-x}{\rho_l} \right)^{-1} \quad (2.19)$$

$$We = \frac{G^2 D}{\sigma \rho_{tp}} \quad (2.20)$$

$$Fr = \frac{G^2}{g D \rho_{tp}^2} \quad (2.21)$$

$$H = \left( \frac{\rho_l}{\rho_v} \right)^{0.91} \left( \frac{\mu_v}{\mu_l} \right)^{0.19} \left( 1 - \frac{\mu_v}{\mu_l} \right)^{0.7} \quad (2.22)$$

$$F = x^{0.78} (1-x)^{0.224} \quad (2.23)$$

$$E = (1-x)^2 + x^2 \frac{\rho_l f_{vo}}{\rho_v f_{lo}} \quad (2.24)$$

$$\phi_{lo}^2 = E + \frac{3.24 F H}{Fr^{0.045} We^{0.035}} \quad (2.25)$$

Because the frictional pressure drop was generally over 90 percent of the calculated total pressure drop and the two-phase multiplier was a function of the Martinelli parameter as shown in Equation 2.16, attempts were often made to correlate pressure drop to Martinelli parameter. In Equation 2.16 the middle term,  $\frac{C}{\chi}$ , was the dominant term in the equation. This brought about attempts to correlate the pressure drop to the inverse of the Martinelli parameter.

Figure 2.1 shows the pressure drop per unit length in Pascals per meter predicted by each prediction method for a 50 / 50 mixture of HFC-32/HFC-125 flowing at rates of  $700 \text{ kg/m}^2\text{s}$  and  $277 \text{ kg/m}^2\text{s}$  in an eight mm diameter tube.

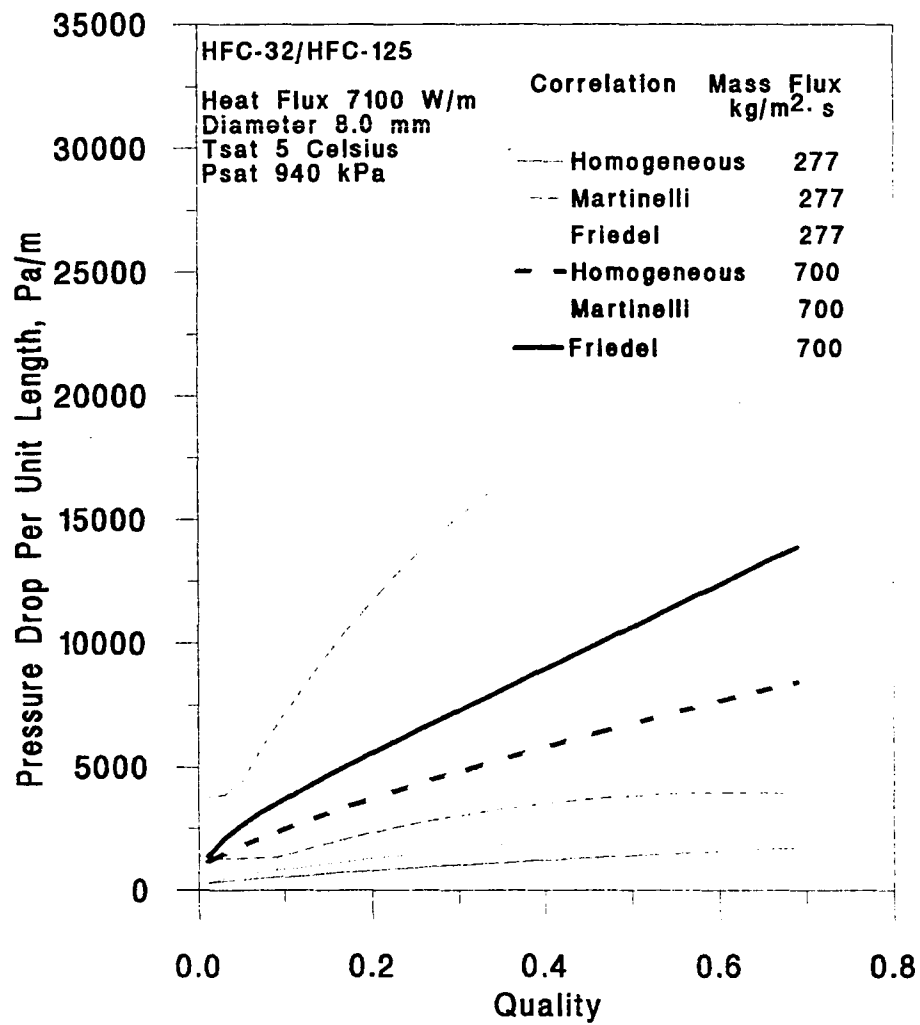


Figure 2.1 The Effect of Mass Flux Upon Pressure Drop Correlations.

These curves were generated for a heat flux of  $7100 \text{ W/m}^2$ , but calculated pressure drops for heat fluxes of  $5100 \text{ W/m}^2$  and  $7100 \text{ W/m}^2$  were equivalent. For the three methods (homogeneous, Martinelli and Friedel), the pressure drop per unit length was higher for the higher mass flux of  $700 \text{ kg/m}^2\text{s}$ . The homogeneous method predicted the lowest pressure drop per unit length of the three methods. The Martinelli method predicted the highest pressure drop per unit length. The Friedel method was developed through a series of empirical equations and the theoretical basis for comparing the results predicted by this method with other methods was impractical. The homogeneous technique is considered applicable at very low or very high qualities or very high flow rates where the refrigerant would behave similar to a single-phase. The conditions shown in Figure 2.1 were neither.

#### CONVECTION HEAT TRANSFER COEFFICIENT PREDICTION METHODS

The complexity of evaporation of refrigerants flowing in a horizontal tube virtually prohibits a general analytical solution. The current solutions are based on a combination of empirical and analytical results. The solution techniques commonly address the nucleate boiling phenomena, the convective heat transfer phenomena and are additionally applied to the liquid deficient region. The most recent methods [Gungor and Winterton, 1982; Kandlikar, 1988] tend to curve fit equations containing relevant dimensionless variables to large amounts of two-phase heat transfer data. The flow patterns contributed to the two-phase heat transfer mechanisms.

The nucleate and convective heat transfer have often been handled independently [Chen, 1966], and their effects added. The most common technique was to add the nucleate heat transfer and convective heat transfer contribution separately [Chen, 1966] as shown in Equation 2.26.

$$h_{tp} = h_{conv} + h_{nucleate} \quad (2.26)$$

The contribution of each heat transfer mechanism was tempered by factors, such as the nucleate term multiplied by a suppression factor and the convective term multiplied by an enhancement factor as shown in Equation 2.27.

$$h_{tp} = E \cdot h_{conv} + S \cdot h_{nucleate} \quad (2.27)$$

The suppression factor was used to account for nucleate boiling that was less than fully developed. The reduction in nucleate boiling was caused by: (1) having parts of the tube wall exposed to vapor where there was no liquid available to form bubbles, (2) having a thin liquid level that prevented bubble departure, or (3) having high velocity liquid flowing over the bubbles. The suppression of nucleate boiling was also attributed to heat fluxes that were not high enough to initiate nucleation.

The geometric distribution of vapor and liquid is influenced by the flow pattern and so is the local acceleration that takes place in slug or plug flow. The refrigerant proceeds through several flow patterns as the vapor quality goes from zero to one. The flow pattern is bubbly at low qualities where the tube is filled predominantly with liquid and just a few bubbles. It is during this flow pattern that the nucleate boiling is dominant. For a given mass flux, the overall liquid and vapor velocities are much lower at the lower qualities. The liquid wets the tube wall. Low velocities and liquid wetting the tube wall are conditions conducive to nucleate boiling. Chen [1966] proposed that the nucleate contribution is the microscopic contribution. Chen [1966] advocated using the Forster and Zuber [1955] equation to predict the nucleate boiling contribution and to correct for nucleate boiling that is less than full scale or full tube area. The Forster and Zuber relationship is given in Equation 2.28 and the suppression

factor is given in Equation 2.29. The microscopic heat transfer coefficient calculated with Equation 2.28 would be used as the nucleate boiling heat transfer coefficient in Equation 2.27.

$$h_{mic} = 0.00122 \left( \frac{k_l^{0.79} c_{pl}^{0.45} \rho_l^{0.49}}{\sigma^{0.5} \mu_l^{0.29} h_{lv}^{0.24} \rho_v^{0.24}} \right) \times (T_w - T_{sat}(P_l))^{0.24} (P_{sat}(T_w) - P_l)^{0.75} S \quad (2.28)$$

$$S(Re_{tp}) = (1 + 2.56 * 10^{-6} Re_{tp}^{1.17})^{-1} \quad (2.29)$$

The effect of mass flux and heat flux upon the nucleate boiling effect is shown in Figure 2.2. The product of the Forster and Zuber nucleate heat transfer coefficient and the suppression factor was graphed for a 50% / 50% mixture of HFC-32 / HFC-125 at a temperature of 5 °C, a saturation pressure of 940 kPa, mass fluxes of 277 kg/m<sup>2</sup>s and 520 kg/m<sup>2</sup>s with heat fluxes of 5100 W/m<sup>2</sup> and 11000 W/m<sup>2</sup>. The nucleate contribution is highest for low mass fluxes and high heat fluxes and consequently the nucleate heat transfer is lowest for high mass fluxes and low heat fluxes. The overall trend for all of the curves is decreasing nucleate boiling with increasing quality. At higher qualities, two things should occur to suppress nucleate boiling. First, the velocities are higher and there is less liquid wetting the wall. In addition, there should also be an annular flow pattern that would have imparted a thin liquid film over part of the tube wall and that suppressed nucleate boiling as well.

Several investigators [Dengler and Addoms, 1956; Guerrieri and Talty, 1956; Chaddock and Noerager, 1966] have proposed two-phase convective correlations for heat transfer absent of nucleate effects.

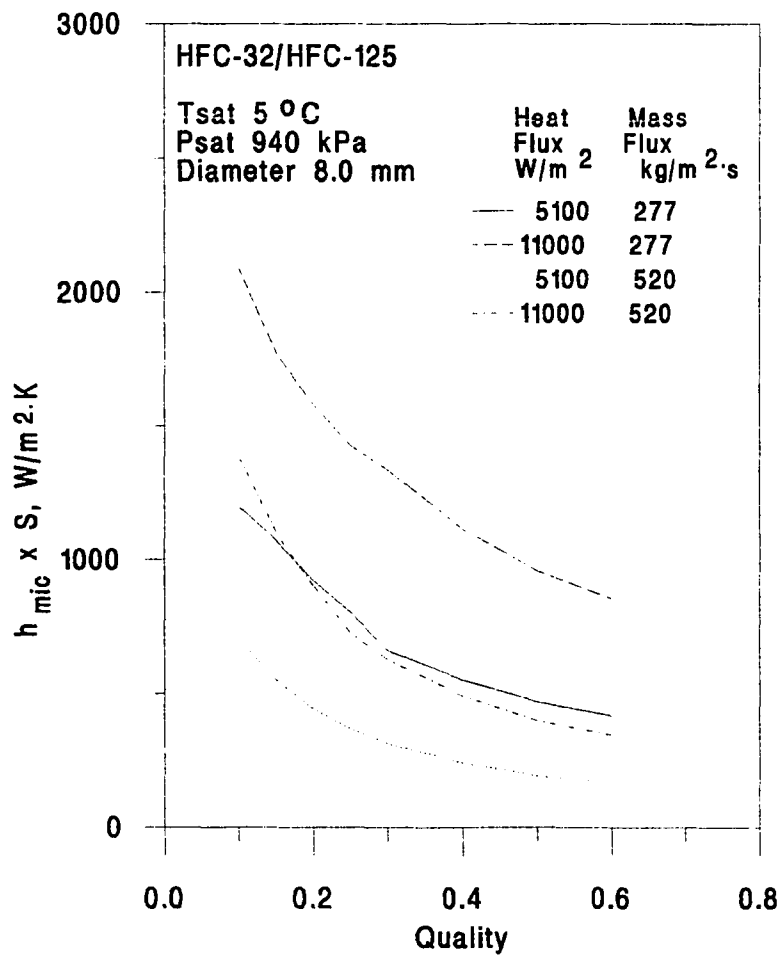


Figure 2.2 The Overall Nucleate Boiling Contribution.

The form followed the pressure drop correlations where the two-phase convective coefficient was a function of the single-phase convective coefficient predicted by the Dittus-Boelter equation and the inverse of the Martinelli parameter. The exponents of such equations were curve fit to experimental data. Two correlations of the same form are provided in Equations 2.30 and 2.31, by Dengler and Addoms [1955] and Guerrieri and Talty [1956], respectively.

$$\frac{h}{h_{1c}} = 3.5 \left( \frac{1}{X_{tt}} \right)^{0.5} \quad (2.30)$$

$$\frac{h}{h_{1c}} = 3.4 \left( \frac{1}{X_{tt}} \right)^{0.45} \quad (2.31)$$

A technique introduced by Shah [1982] correlated the two-phase heat transfer convection coefficient to four dimensionless variables. The four variables are listed in Equations 2.32 through 2.35.

$$\Psi = h_p / h_t \quad (2.32)$$

$$Co = \left( \frac{1}{x} - 1 \right)^{0.8} \left( \frac{\rho_v}{\rho_l} \right)^{0.5} \quad (2.33)$$

$$Bo = q / Gi_{fs} \quad (2.34)$$

$$Fr_l = G^2 / \rho_l^2 gD \quad (2.35)$$

The liquid convection coefficient can be calculated from the Dittus Boelter equation. The boiling phenomena was divided into four regions: (1) pure nucleate boiling, (2) bubble suppression (3) convective boiling with a partially dry surface and (4) post dry out region. The two-phase convective heat transfer was traditionally normalized to the liquid convection coefficient, as represented by the variable  $\Psi$  in equation 2.32. The convection number,  $Co$ , was used to distinguish between nucleate boiling dominated heat transfer and convection dominated heat transfer. The boiling number,  $Bo$ , was a normalized nondimensional heat flux. The liquid Froude number,  $Fr_l$ , was a ratio of the inertia to the gravitational forces. For horizontal flow, the Froude number along with the quality was an indication of the degree of wetting along the wall.

The two-phase convective coefficient was calculated from the boiling number and the liquid convection coefficient only for heat transfer dominated by nucleate boiling. Boiling was caused by bubble nucleation only. Nucleation and convective heat transfer are important in the bubble suppression region. Nucleation was suppressed with and without a completely wetted wall in the convective boiling region. Heat was transferred to the vapor at the wall in the post dryout region.

$\Psi$  was determined by either  $Fr$  and  $Co$  or  $Bo$  depending upon whether nucleation or convection was dominant in the bubble suppression region.  $\Psi$  was determined from only  $Co$  and  $Fr$  in the convective region. The equations for each region are empirical and curve fit to data over the smaller quality changes associated with each region.

A later method presented by Gungor and Winterton [1986] was based upon a combination of the convective heat transfer and nucleate boiling effects. The basic form of this method was represented in equation 2.36.



$$h_p = E h_i + S h_{pool} \quad (2.36)$$

The liquid convective heat transfer was determined from the Dittus-Boelter equation and  $h_{pool}$  was determined from an empirical relation shown in equation 2.37. The E and S factors are enhancement of liquid only convective heat transfer and suppression of pool boiling respectively. The value E, equation 2.38, was determined from the boiling number, Bo, and the Martinelli parameter,  $\chi$ . S was determined from E and  $Re_i$  in Equation 2.39. The constants and exponents for the variables E and S were determined from a curve fit to empirical data [Gungor and Winterton, 1986].

$$h_{pool} = 55 P_r^{0.12} (-\log P_r)^{-0.55} M^{-0.5} q^{0.67} \quad (2.37)$$

$$E = 1 + 24000 Bo^{1.16} + 1.37(1 / \chi_n)^{0.86} \quad (2.38)$$

$$S = \frac{1}{1 + 1.15 * 10^6 E^2 Re_i^{1.17}} \quad (2.39)$$

A method presented by Kandlikar was based on an additive model with fluid dependent constants as shown in Equation 2.40.

$$h_p / h_i = D_1 (Co)^{D_2} (25Fr_i)^{D_5} + D_3 (Bo)^{D_4} (25Fr_i)^{D_6} F_f \quad (2.40)$$

The convective heat transfer and nucleate boiling dominated region was divided at  $Co = 0.65$ . The values of  $D_1$ ,  $D_2$ ,  $D_3$ ,  $D_4$ ,  $D_5$  and  $D_6$  are constant, but different if the value of the convection number was greater or less than 0.65. The heat transfer was considered convective heat transfer dominated when the convection number was less

than 0.65 and nucleate boiling was dominant when the convection number was greater than 0.65. The term  $F_{fl}$  was fluid type dependent. This correlation was compared to over 5000 data points. Most correlations correctly predict a decreasing nucleate contribution with increasing quality and an increasing convective contribution with increasing quality. There was some discrepancy over the sum effect of nucleate and convective effects together. The Gungor and Winterton method predicts an increasing overall heat transfer coefficient over the entire range of qualities. The Kandlikar technique predicts a decreasing overall heat transfer coefficient at low qualities and an increasing heat transfer coefficient at higher qualities. The decreasing then increasing heat transfer predicted by Kandlikar was consistent with data by Ross et al [1986], Bryan and Quaint [1955] and Chaddock [1986].

Chen [1966] proposed a correlation of two-phase convective heat transfer dependent upon the Martinelli parameter, the boiling number, Nusselt number and Reynolds number. This was one of the first recognized approaches for treating the convective and nucleate boiling heat transfer mechanisms separately and adding both coefficients to obtain a two-phase coefficient. This correlation also incorporated critical bubble radius and boiling number. A correlation to the Martinelli parameter, film thickness and critical bubble thickness was used by Guerrieri and Talty [1956] and Dengler and Addoms [1956]. Techniques have been proposed to solve for the two-phase convective coefficient by correlating the convective and nucleate boiling effects to the Martinelli parameter, film thickness, critical bubble radius and the superposition of heat flux as shown by Bjorge [1982]

## EXPERIMENTAL TECHNIQUES AND RESULTS

Previous researchers [Hambraeus, 1991; Dengler and Addoms, 1956; Riedle and Purcupile, 1973; Chaddock and Noerager, 1966; Lavin and Young, 1965;

Guerrieri and Talty, 1956] have typically performed experiments for a given range of independent values and compared the pressure drop and convective heat transfer to proposed or existing correlations. The experimental facilities were designed so that the refrigerant inlet temperature, pressure and quality were measured. The flow rate and heat flux in the test section were determined. Other independent variables were test section diameter and length. Pressure drop was determined using pressure gages and transducers. The refrigerant temperature was often inferred from the pressure. Wall temperature was measured so that the convection heat transfer could be calculated. A considerable amount of experimental data was for water and traditional refrigerants (CFC-12 and HCFC-22).

Lavin and Young [1965] ran evaporation experiments on CFC-12 and HCFC-22 for both smooth and internally augmented tubes. They addressed the importance of obtaining local convective coefficients opposed to average values. Vapor and liquid streams were combined upstream of the test section to achieve the desired quality. The convective heat transfer for nucleate boiling, annular flow and mist flow were each treated separately. The nucleate boiling dominated region was stated as taking place only during sub cooled boiling. Additionally, a transition region from annular flow to mist flow was studied.

Anderson, Rich and Geary [1966] performed a series of tests on HCFC-22 at 5°C (40 °F). The same test section was used for all experiments. The mass velocity, inlet quality, exit quality and heat flux were varied and convective coefficient was determined. The convection coefficient increased with mass velocity. The data were compared to several correlations and the correlation of Dengler and Addoms [1956] was stated to be the most accurate. The refrigerant was heated by hot water in a shell and the results for parallel flow and counterflow were both deemed viable.

Chaddock and Noerager [1966] performed experiments using CFC-12. They used thermocouples placed circumferentially at eight locations along the test section. The convective coefficient at each circumferential point was very close to an average value at those locations. The convective coefficient increased with flow rate and mass velocity. The convective coefficient was highest at the top of the tube for higher mass velocities where the bottom is continuously wetted and highest at the top for lower mass velocities because the flow pattern is wavy or stratified. The reported convective coefficient differed by up to a factor of four between the bottom and top of the tube.

Riedle and Purcupile [1973] ran experiments on CFC-112 and CFC-113 for subcooled and nucleate boiling at low qualities but did not show the convective coefficient as a function of low qualities. El-Sallak, Morcos and Mobarak [1988] ran experiments using CFC-11 and R-21 and a condensing CFC-113 shell fluid to provide heat to the test section. Their results were similar to the theoretical results shown by Collier [1982]. The convective coefficient increased linearly as the subcooled liquid approaches a quality of zero. The two-phase convective coefficient decreased slightly until dryout occurred. Chaddock [1986] ran experiments with HCFC-22 with and without oil and the convective heat transfer decreased over low qualities from 0.0 to 0.15 and then increased until dryout. This is the same trend predicted by Kandlikar [1988]. Kubanek and Miletta [1979] performed experiments comparing the evaporation heat transfer of HCFC-22 with smooth and finned tubes. Primary results were the performance of the type of fin arrangement. Reid, Pate and Bergles [1988] studied the effect of using CFC-113 with internally augmented tubes. Chaddock [1986] studied the effect that oil had on the heat transfer of evaporating CFC-11 and CFC-12. Khanpara, Pate and Bergles [1986] studied the difference in using CFC-113 and HCFC-22 evaporating in internally augmented tubes. Wattelet et al [1991] studied CFC-12 and HFC-134a over a wide range of heat fluxes, mass fluxes and qualities.

The saturation pressures were similar to those found in automotive air conditioning evaporators.

#### THE EFFECT OF OIL ON PRESSURE DROP AND HEAT TRANSFER

Compressor lubricating oils were always present in air conditioning systems. The oil may hinder or enhance the performance of the air conditioner. The increased pressure drop and enhanced heat transfer was usually studied as a function of the mass percentage of oil in the system. The general trend was that heat transfer is increased for small concentrations to approximately three percent and decreased for higher concentrations.

Schlager et al [1987] summarized the published information on the effect of oil and augmentation on two-phase refrigerant heat transfer and pressure drop. Chaddock [1986] attempted to quantify the effect of oil on HCFC-22 during evaporation. Tichy et al [1985] performed experiments concerning the effect of oil on evaporation. The effect of oil on HFC-134a was carried out by Hambraeus [1991] and the results were compared to pure HFC-134a.

#### SUMMARY OF LITERATURE REVIEW

A variety of experimental techniques have been used to obtain heat transfer and flow characteristics of refrigerants flowing in a horizontal tube while evaporating. Much of this information is for HCFC-22, CFC-12 and CFC-113. There is little information available on the thermal and transport characteristics of the environmentally acceptable refrigerants. Several correlations exist for prediction of these characteristics. Because of the lack of experimental data, verifiable correlations for some proposed environmentally acceptable refrigerants could not be found. Also correlations of the flow pattern and local characteristics could not be correlated for the qualities ranging from 0 to 1. The experimental refrigerant cycle requirements were work input, condensation, pressure reduction and evaporation. Work may be input by

the use of a compressor or pump, which propels the refrigerant along the loop. The condenser is used to reject heat, either to the atmosphere or a separate chilling system. The pressure may be reduced by flashing to the atmosphere (refrigerant dependent) or flowing through a pressure reducing valve or choke. Lastly, heat is absorbed by the refrigerant in the evaporator. The test section must be instrumented so that heat flux, mass flow rate and temperature can be measured. The refrigerant inlet state must be recorded.

The evaporation region for qualities above  $x = 0$  and sub critical heat fluxes were divided into three regions. The regions were divided according to the heat transfer phenomena taking place in the evaporator. At low qualities, the heat transfer is primarily by bubble nucleation at the wall and is called the nucleate boiling. This nucleation of bubbles impedes the heat transfer. At higher qualities, the primary heat transfer is two-phase forced convective heat transfer, where convection and conduction through the sub layer were the primary heat transfer mechanism. The final region is the liquid deficient region where there is not enough liquid to sufficiently wet the wall. The heat is transferred primarily by convection to the vapor.

The pressure drop of flowing refrigerant can be estimated from any number of variations of two primary methods. These two common methods were the homogeneous flow model and the separated flow model. The separated flow model originally developed by Lockhart and Martinelli [1949] and simplified by Chisholm [1967] tends to produce more accurate results.

An experimental investigation was undertaken to gain insight into the evaporation characteristics of two proposed environmentally acceptable refrigerants flowing in a horizontal tube. This investigation utilized experimental data to validate existing prediction methods. The evaporation behavior of the environmentally

acceptable refrigerants was then be compared to refrigerants that were currently being used.

## CHAPTER III

### EXPERIMENTAL APPARATUS AND PROCEDURE

The experimental apparatus used in this study was capable of measuring the effect of variables such as heat flux, mass flux and quality on convective heat transfer and pressure drop of refrigerants flowing in a tube. The system was designed to allow control of each operating variable over a wide range of evaporating conditions. This chapter describes the test facility and the experimental procedures.

#### EXPERIMENTAL SETUP

A schematic of the entire experimental apparatus is shown in Figure 3.1. The apparatus consisted of three separate fluid loops. The refrigerant loop contained the refrigerant of interest. This part of the experimental apparatus was designed for the study of changes in mass flow rate, heat flux, inlet quality and refrigerant temperature. It also allowed one to vary the oil concentration in the system. Two auxiliary loops were used to remove heat from the refrigerant loop. These were a chilled water-glycol loop and a R-502 loop. The fluid did not mix between any of the three loops but interacted through respective heat exchangers.

The refrigerant loop consisted of a test section and support components. Nearly all of the pertinent information was obtained at the test section. The support components helped achieve proper inlet conditions for a given test. The measurements made in the test section were surface temperature, heat input, refrigerant temperature and corresponding pressure. The evaporation test section consisted of a 2.77 meter (109 inch) long 9.5 mm (3/8 inch) outside diameter (OD) copper tube wrapped with 2 electrical heating tapes. Both tapes contained NiCr strand elements with power ratings of 1000 watts. The power input to each tape was controlled individually by Staco 1050 variacs capable of 0 to 240 volt AC and 5 ampere output.



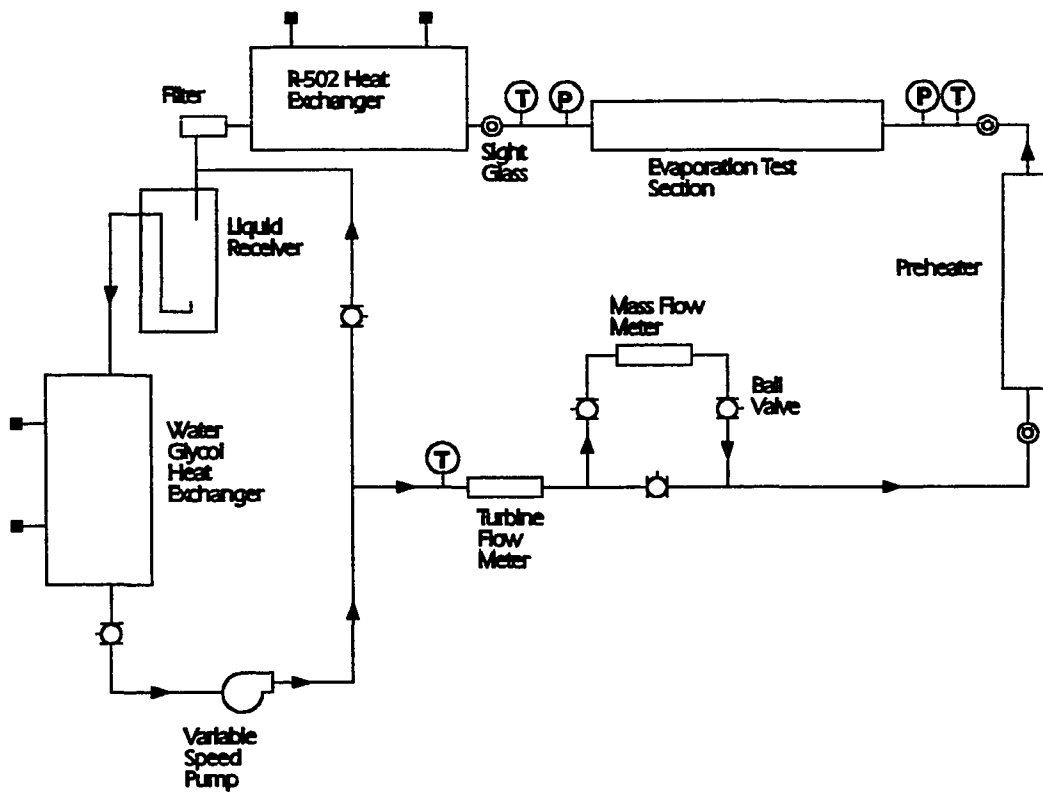


Figure 3.1 Schematic Diagram of Experimental Setup.

Thermocouples were placed on the top and bottom surface of the tube at 5 equally spaced locations along the length. The thermocouples were 30 gage copper-constantan type T and were mounted in a groove in the pipe. The remainder of the groove was filled with an Epoxy containing an Aluminum filler to promote a good thermal contact between the thermocouple and the tube wall. The entire tube and heating tapes were insulated with a 15.2 cm (6 inch) thick high temperature fiberglass batt insulation. This insulation was rated to 480 °C (900 °F). This large amount of insulation reinforced the assumption of an adiabatic boundary at the outer edge. A cut away of this arrangement is shown in Figure 3.2. Setra Model 207 pressure transducers with a 0 to 1720 kPa (0 to 250 psig) scale were located at the entrance and exit of the test section. Sight glasses were also placed at the entrance and exit of the test section so that the void fraction can qualitatively be determined.

A diaphragm pump with a variable speed DC motor was used to control the flow rate of the refrigerant. The pump was a Hydracell Model D with neoprene diaphragms. A diaphragm pump was chosen to reduce pulsation that is associated with piston type pumps. Neoprene diaphragms are compatible with most refrigerants and the low temperatures used in this study. The motor was a Baldor 90 vdc, 0.75 kW (1 hp) motor controlled with a Warner technologies Bronco II model 160 DC controller. The pump was placed at the lowest point in the system to insure liquid at the pump inlet during start up. A liquid receiver was placed just upstream of the second heat exchanger and the pump to stabilize the flow rate and to insure liquid phase at the pump entrance. This receiver acted as a reservoir and dampened out pressure pulses. It was not possible to completely control the flow by varying the pump speed because of the low mass flow rates used during some of the tests. Low mass rates affected the amount of rejectable heat in the heat exchangers.

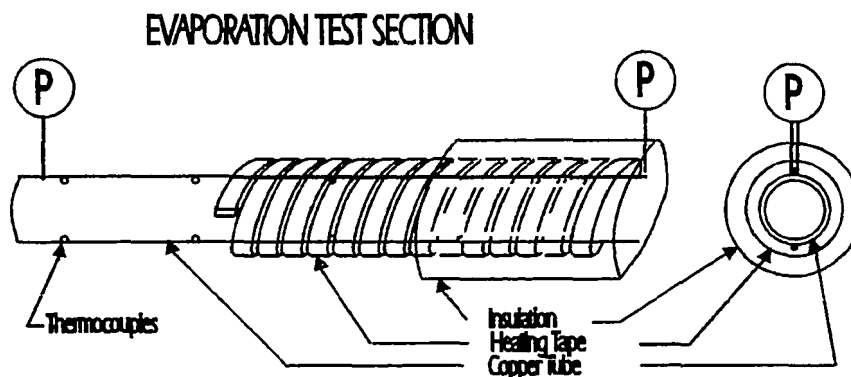


Figure 3.2 Cut Away View of the Test Section.

At low mass rates and high qualities, it was impossible to reject enough heat to condense the refrigerant at the heat exchangers when the refrigerant was flowing through the heat exchanger at the low rate. The flow rate was also adjusted by opening and closing a needle valve in the bypass line. The pressure drop through the bypass was not sufficient to create a stable flow arrangement so capillary tubing made up part of the bypass line. The short bypass arrangement with the capillary tube then had pressure losses of the same order of magnitude as the preheater and test section. The temperature of the refrigerant flowing throughout the loop was often in the  $-7.0$  °C to  $1.0$  °C ( $20$  to  $40$  °F) range. The ambient temperature ranged from  $14$  to  $33$  °C ( $60$  to  $90$  °F). A  $12$  mm ( $1/2$  inch) foam insulation was used on all piping throughout the system except for the preheater and test section. The system was closed, therefore a constant volume system.

To always have liquid at the pump inlet and the desired test pressure, the system required more refrigerant during start up than during testing. The amount of

refrigerant, the flow rate, quality, mass in the system and ambient temperature all affected the pressure in the test section. Refrigerant was removed during the start up to bring the system pressure to a desired value. If too much charge was removed then a two-phase mixture existed at the pump entrance and the flow rate could not be maintained.

The preheater consisted of a single 6.1 meter (20 foot) long, 9.5 mm (3/8 inch) OD copper pipe wrapped with heating tape and insulation. The heating tapes on the preheater were the same type used in the test section. The seven heating tapes were each controlled by a separate Staco 1020 variac. The amount of heat input was measured with an Ohio Semitronics watt meter. The heating tape was covered with 15.2 cm (6 inch) of fiberglass insulation. The refrigerant entered the preheater as a subcooled liquid. A sight glass was placed at the beginning of the preheater to verify that the refrigerant was a single phase. The temperature and pressure at the inlet were recorded. These values indicated the degree of subcooling. The amount of heat required was determined by summing the heat necessary to bring the liquid phase to a saturated liquid and the heat necessary to achieve the quality desired at the inlet to the test section.

The apparatus had two separate condensers for rejecting heat. The largest condenser consisted of an Aqua Systems 14 kW/h (four ton) and seven kW/h (two ton) single wall heat exchangers connected in series. This condenser was placed immediately upstream of the pump suction. This placement insured that the refrigerant would condense to a subcooled liquid at the pump entrance. The other side of the heat exchanger had a water-glycol chilling system. The water glycol mix was approximately 50/50 by volume. The water-glycol system consisted of a low temperature five ton R-502 chilling unit with the evaporator located in a 0.303 cubic meter (80 gallon) insulated tank. The unit was controlled by a thermostat with the thermal sensing device

placed in the tank. The 0.303 cubic meter (80 gallon) tank was connected to a 0.757 cubic meter (200 gallon) tank also containing water/glycol. The mixture was circulated between the two tanks. A small circulating pump forced the mixture from the large tank into the small one and a circulating pump controlled by a float valve in the small tank returned the mixture to the large tank. During tests, the mixture was also pumped out of the large tank by a gear pump through the condenser and back to the small tank. The temperature in this system was adjustable. The water glycol mixture temperature was usually set to  $-4\text{ }^{\circ}\text{C}$  ( $25\text{ }^{\circ}\text{F}$ ). The connecting hoses were insulated with 12 mm (1/2 inch) of foam insulation to reduce heat loss to the ambient.

A second condenser was added later after determining that the first one was too small. The second condenser was placed immediately after the test section to partially condense the refrigerant. This lowered the pressure drop of the refrigerant returning to the pump. Therefore the refrigerant could be totally condensed at a higher temperature. The second condenser differed from the first in that it was a Packless Industries, 10.5 kW/h (three ton), 1 tube, 1 pass shell and tube heat exchanger. The other side of the heat exchanger served as an evaporator for a three ton residential air conditioner that was modified for this purpose. The unit was filled with R-502 and an adjustable expansion valve was placed in line to control the evaporating temperature. The pressure in the evaporator was 276 kPa (40 psia), which corresponds to a temperature of  $-12\text{ }^{\circ}\text{C}$  ( $10\text{ }^{\circ}\text{F}$ ).

The flow rate of the refrigerant was measured using a Flow Measurements Inc. tangential turbine meter. The turbine flow meter was calibrated using water and also by comparison with a Micro Motion Model D Coriolis effect mass flow meter that remained connected to the test section for continual verification.

## OIL INJECTION AND SAMPLING

The addition of a specified amount of oil to a pressurized system was not without its own set of problems. The HFC-32/HFC-125 refrigerant was tested with oil concentrations of 0%, 2.6% and 5.4%. The oil could not be removed from the system without removing the refrigerant. Thus, all experiments that were run for 2.6% must be completed before experiments with a concentration of 5.4% could be run. The oil must be injected in prescribed quantities and the concentration must be verifiable.

The oil was injected downstream of the refrigerant pump with an air cylinder. Oil concentrations were calculated by dividing the mass of oil in the system by the mass of refrigerant. The mass of refrigerant was measured upon initial charging of the system. The mass of oil injected was determined from the diameter of the cylinder, the displacement of the cylinder and the density of the oil. The weight of the cylinder containing oil before and after injection was recorded to confirm the amount of oil added to the system. The scale used in this measurement was accurate to  $\pm 13.6$  g (0.03 lb). The oil was injected continuously as the refrigerant flowed in the system to obtain an even distribution of oil throughout the system.

The mixture was sampled periodically and the oil concentration was compared to the calculated oil concentration. These values typically matched to within 2% of each other. These samples were taken to insure that leakage of refrigerant from the system or settling out of oil in the system had not occurred. The sample was gathered just downstream of the pump at a location where the refrigerant was all liquid. The oil was assumed to be miscible in the liquid refrigerant. A schematic of the sampling vessel is shown in Figure 3.3. The sampling vessel was cylindrical with an inside diameter of 12.7 cm (5 in.) and a length of 30.5 cm (12 in.). The amount of sample gathered was 0.454 kg (1 lb)  $\pm 10\%$ . The sampling vessel was weighed prior to sampling. The vessel with the sample was weighed. And the refrigerant was vented

leaving behind the oil and vessel which were weighed again. All measurements were taken on a scale accurate to  $\pm 0.5$  g (0.001 lb). The refrigerant was vented very slowly through a 3.05 meter (10 ft) long 0.64 mm (0.025 in.) diameter capillary tube and filter. If the refrigerant were bled off quickly, there would be oil entrained in the vapor. The sampling container was then evacuated to remove any entrapped refrigerant from the oil. This procedure [Kim, 1993] for determining oil concentration was based on ASHRAE Standard 41-4-1984 [ASHRAE 1984].

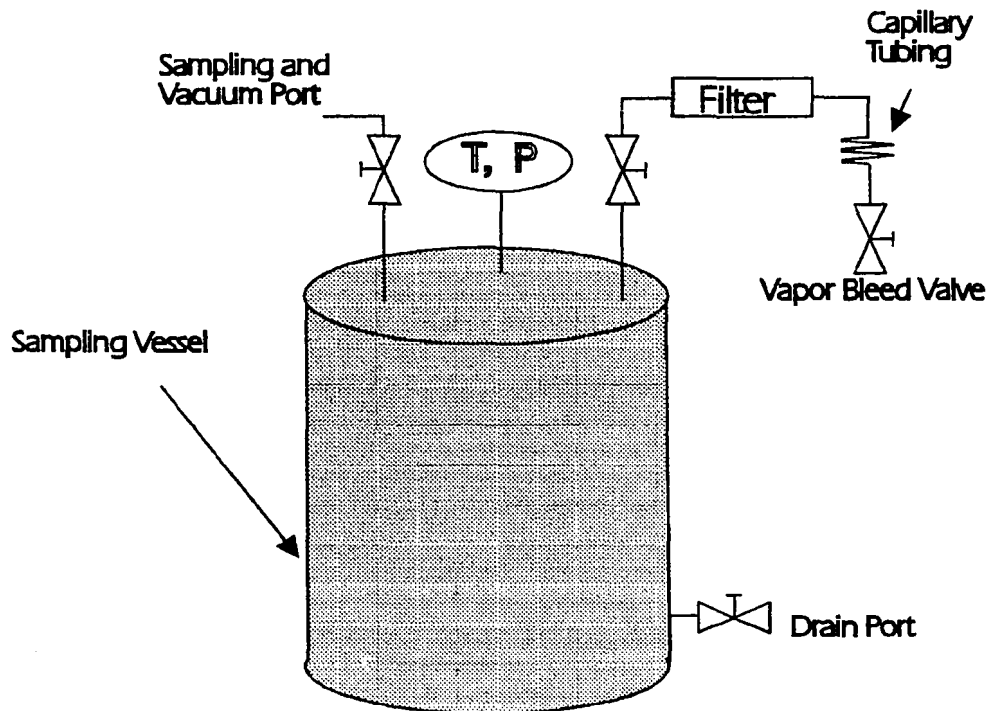


Figure 3.3 Oil Sampling Device.

## INSTRUMENTATION

The temperature, pressure, flow rate and power input were measured at different locations throughout the flow loop. These values were recorded with a data acquisition system attached to a computer. Each sensor was calibrated.

All temperature measurements were made using Type T 30 gage copper constantan thermocouples. The accuracy of the thermocouple was estimated at  $\pm 0.5$  °C (0.9 °F). The thermocouples were calibrated by inserting them in an ice water bath and adjusting a potentiometer located on the isothermal block of the input card until the temperature of 0 °C ( 32 °F) was displayed by the data acquisition unit. The surface temperature of the tube wall in the test section and the liquid refrigerant temperature were measured. The bulk refrigerant temperature was measured as shown in Figure 3.4. The thermocouple well was constructed of 1.59 mm (1/16 inch) OD capillary tubing. The tip of the well was centered in the pipe at least 5.08 cm (2 inches) from where the well entered the pipe. This was done to minimize the conduction effect of the copper. The well was partially filled with oil to ensure good thermal contact between the well and the thermocouple. The measurement of surface temperature proved to be a difficult feat. A successful technique was developed through a trial and error process. The thermocouple bead was made as small as possible. A shallow groove was cut in the exterior wall of the test section. The thermocouple was placed in the groove and the remainder of the groove space was filled with a thermally high conductivity epoxy. Electrical tape was then placed over the thermocouple and groove.

Pressure transducers were placed throughout the loop, but the most important locations were prior to the preheater and upstream and downstream of the test section. The pressure transducers were Setra Model 207, 0 to 1720 kPa (0 to 250 psig)



transducers. The transducers required an excitation voltage of 20 Vdc. This was provided by an Elenco Precision - Deluxe Regulated Power Supply model XP-650. The transducer output was 0.1-5.1 Vdc corresponding to 0 to 1720 kPa (0 to 250 psig). The transducers were individually calibrated using a dead weight tester. A least squares linear relationship between pressure and voltage output was determined and programmed into the data acquisition unit for each transducer. The estimated accuracy of the transducer was  $\pm 2\%$  of full scale or 1720 kPa (250 psig).

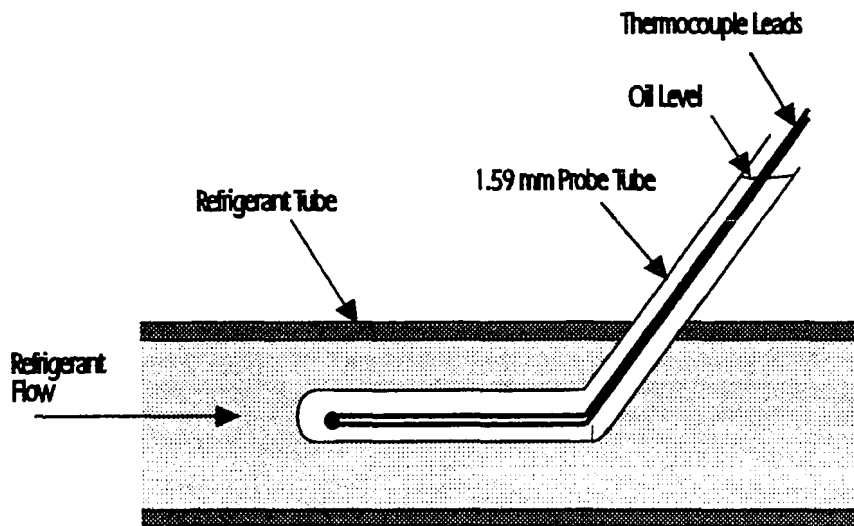


Figure 3.4 Measurement of Bulk Temperature.

The volumetric flow rate was determined using a turbine flow meter. The density of the refrigerant in the flow meter was determined from fluid temperature measurements made in close proximity to the flow meter. The flow meter was calibrated prior to purchase and subsequently calibrated with water afterward. The flow rates obtained by using the turbine flow meter were periodically checked with a

mass flow meter mounted permanently in the loop. The estimated accuracy of the flow meter is  $\pm 0.5\%$  of full scale which is  $2.84 \times 10^{-5} \text{ m}^3/\text{s}$  (0.45 gallons/minute).

The Ohio Semitronics watt meter was used to measure the total power input to the preheater and test section heating tapes. A sophisticated switching technique was used to maintain power to the tapes and still measure the individual power supplied to each one. The heating tapes are a purely resistive load. The watt meter was calibrated by connecting a bank of measured resistors in the same way that the tapes were wired. The voltages and current passing through the wire was measured and compared to the power measured by the watt meter. The estimated uncertainty of the watt meter was 0.5% of full scale or 1000 watts.

#### DATA ACQUISITION

All data points were taken with an Accurex Autocalc data acquisition system. The Autocalc read the information and stored the information on hard disk of a portable Compaq personal computer. The thermocouples, pressure transducers, flow meters and watt meter were connected to individual channels on input cards in Autocalc. Each channel could be programmed to accept a specific signal. Common signals were direct current voltage and milliamps. The channels were polled every 10 seconds. The information was displayed on the screen of the computer. This instantaneous feedback helped in adjusting the pressure, heat input and flow rate. The measurements and their respective channels are shown in Table 3.1.

After each experiment, the data file was copied to a floppy disk and stored. Instantaneous readings were made every 10 seconds. The average for each reading was calculated using a PASCAL program. The average data were used for reporting. The reduced data were then arranged for acceptance into a batch process graphing program by a combination of FORTRAN and PASCAL programs.

Table 3.1 Description of Data Acquisition Sensor Channels

Channel	Sensor	Location
00	thermocouple	preheater inlet
01-08	thermocouple	preheater surface
10-13	thermocouple	preheater surface
15-18	thermocouple	preheater surface
19	thermocouple	flow meter exit
20-23	thermocouple	preheater surface
25	thermocouple	test section inlet
26-27	thermocouple	test section surface
28	thermocouple	ambient
30-33	thermocouple	test section surface
35-38	thermocouple	test section surface
39	thermocouple	test section exit
40	watt transducer	heat tape
41	turbine flow meter	prior to preheater
42-46	pressure transducer	preheater
47	pressure transducer	test section inlet
48	pressure transducer	test section exit

## EXPERIMENTAL CONDITIONS

A systematic series of tests were run to verify the experimental apparatus and to determine the frictional and heat transfer characteristics for two-phase refrigerants. The experiments were of four types: (1) R-22 as a single phase liquid, (2) R-22 as a two phase mixture, (3) HFC-32/HFC-125 as a two phase mixture and (4) HFC-32/HFC-125 as a two phase mixture with varying oil concentrations. Operating conditions were chosen to cover a wide range. The primary emphasis was on two-phase work. Some single phase R-22 experiments were run to calculate and verify the energy balance with single phase heat transfer. These single phase experiments consist of tests where the heat input to the test section and the calculated temperature rise of a single phase liquid was compared to the measured temperature increase in the refrigerant.

The boiling heat transfer coefficient is known to change with respect to a number of different operating conditions. The variables studied in this work were mass flux, heat flux, quality, and temperature. The two-phase test conditions are outlined in Table 3.2. The basic test consists of establishing a mass flux, heat flux and quality in the test section. The experiments were run at a temperature of 4.6 °C (40 °F) at the inlet of the test section. The R-22 mass fluxes of 280 kg/m<sup>2</sup>·s (57.3 lb<sub>m</sub>/ft<sup>2</sup>·s) were run with a heat flux of 5100 and 7100 W/m<sup>2</sup> (1617 Btu/hr ft<sup>2</sup> to 2251 Btu/hr ft<sup>2</sup>). The quality varied from 0.2 to 0.6. For mass fluxes of 430 kg/m<sup>2</sup> (88.1 lb<sub>m</sub>/ft<sup>2</sup>·s) the heat flux was 7100 and 11000 W/m<sup>2</sup> (2251 Btu/hr ft<sup>2</sup> to 3488 Btu/hr ft<sup>2</sup>). This was also for quality from 0.2 to 0.6. The R-22 mass flux of 520 kg/m<sup>2</sup>·s (106.5 lb<sub>m</sub>/ft<sup>2</sup>·s) was only run with a heat flux of 11000 W/m<sup>2</sup> (3488 Btu/hr ft<sup>2</sup>) and qualities of 0.2 and 0.4. Oil was not used in the experiments with R-22. The same types of experiments were run with HFC-32/HFC-125. The same mass flux and heat flux conditions were used but a greater range of qualities were investigated. Each experiment was run for HFC-32/HFC-125 oil concentration (by mass) of 0%, 2.6% and 5.4%.

#### TESTING PROCEDURE

The parameters varied in these experiments include flow rate, quality and heat flux. Some values were measured directly and others were calculated from direct measurement. The quality could not be measured directly. The criteria for experiments with HFC-32/HFC-125 were that the quality must be calculated to 1% of the test objective, the instantaneous flow rate must not vary by more than ±10% and the average flow rate must be within ± 5% of the desired flow rate.

Table 3.2 Test Conditions for Two-phase Experiments

Refrigerant	Mass Flux kg/m <sup>2</sup>	Heat Flux W/m <sup>2</sup>	Quality	Oil Concen- tration
HCFC-22	280	5100	0.2	0%
	430	7100	0.4	
	520	11000	0.6	
HFC-32/ HFC-125	277	5100	0.1	0%
	434	7100	0.2	2.6%
	520	11000	0.3	5.4%
	700		0.4	
			0.5	
			0.6	

The average temperature in the test section must be within  $\pm 1$  degree Celsius (1.8 °F) of the test design temperature. All test data were taken under steady state conditions. The measurements were allowed to stabilize for 30 minutes prior to recording of any data. The tests were between four and eight minutes long. The data was polled and recorded every 10 seconds during that time. The average value of each measurement throughout the test was calculated.

Because the flow loop was a closed system in an unconditioned building, the pressure drops and ambient temperature affected the pressure in the system. All tests were run at a single temperature that had to correspond to a saturated pressure at that temperature. The temperature of the water-glycol and R-502 heat exchanger loops could be changed to compensate partially, but the charge in the system also had to be

adjusted. The general procedure was to start a test, adjust the charge, let the experiment stabilize, adjust charge, and so on until the refrigerant was at the correct temperature in the flow loop. The experiment was then run for 30 minutes before any data were recorded. Often small changes in quality could be made without changing the charge.

Experiments were originally run with R-22, to verify the validity of the flow loop. Once a complete series of tests were run with R-22, the system was evacuated and charged with a binary blend HFC-32/HFC-125. The HFC-32/HFC-125 refrigerant was subjected to experiments spanning a wider range of qualities. These same experiments were then repeated for oil concentrations of 2.6% and 5.4%.

The temperature of the refrigerant in the test section was calculated as the average of the inlet and exit temperatures. These temperature also corresponded to the saturation temperature determined from the measured pressure at the entrance and exit of the test section. The heat flux was determined from the power input to the heat tapes in the test section. The amount of heat necessary to change the subcooled liquid entering the preheater to a saturated liquid was calculated using Equation 3.1.  $\dot{Q}$  was the power required,  $\dot{m}$  is the mass flow rate,  $cp$  was specific heat and  $\Delta T$  was the amount of subcooling. The specific heat is a published fluid property of pure refrigerants but not for refrigerant and oil mixtures. The specific heat for the oil and refrigerant mixture was calculated using Equation 3.2. The  $W$  term is percent weight of the oil in the refrigerant [Jensen and Jackman, 1984]. The amount of heat necessary to change the quality was calculated from the flow rate and enthalpy of vaporization with no correction made for the effect of oil.

$$\dot{Q} = \dot{m} \cdot cp_l \cdot \Delta T \quad (3.1)$$

$$cp_m = cp_r W + cp_o (1 - W) \quad (3.2)$$

Since the flow rate was determined from a volumetric rate and a corresponding liquid density at that location, the density of the oil refrigerant mixture must be calculated. This was calculated using Equation 3.3 where  $\rho_m$  is the density of the mixture [ASHRAE 1986].

$$\rho_m = \frac{\rho_o}{1 + W(\rho_o/\rho_r - 1)} \quad (3.3)$$

## CHAPTER IV

### EXPERIMENTAL RESULTS FOR HCFC-22

A series of single-phase HCFC-22 heat transfer tests were conducted to provide a baseline comparison of heat transfer and pressure drop with a refrigerant that has been studied by other investigators. Two-phase flow boiling convective coefficients of HCFC-22 were determined for mass fluxes ranging from 280 kg/m<sup>2</sup>s to 520 kg/m<sup>2</sup>s (57.3 lb<sub>m</sub>/ft<sup>2</sup>·s to 106.5 lb<sub>m</sub>/ft<sup>2</sup>·s) and qualities ranging from 20 to 70 percent. The heat flux was varied from 5100 W/m<sup>2</sup> to 11000 W/m<sup>2</sup> (1617 Btu/hr·ft<sup>2</sup> to 3488 Btu/hr·ft<sup>2</sup>). The experimental heat transfer data for HCFC-22 were compared to existing flow boiling heat transfer correlations by Shah (1982), Gungor and Winterton (1986) and Kandlikar (1990). The flow pattern for each test was determined by comparing experimental data to graphs by Baker (1954) and Taitel and Dukler (1976). The experimental two-phase pressure drop was compared to a homogenous pressure drop correlation and to two separate flow correlations by Martinelli (1949) and Friedel (1979).

#### RESULTS OF SINGLE-PHASE EXPERIMENTS

The single-phase tests for HCFC-22 were conducted to provide baseline data for the experimental apparatus. HCFC-22 was used as the test fluid because the fluid properties and experimental results have previously been published. Experiments were performed by flowing a subcooled liquid HCFC-22 through the experimental test section and adding a measured amount of heat to the refrigerant. The temperature rise of HCFC-22 in the test section was recorded along with the steady state flow rate. Several experiments were run with various flow rates, subcooled temperatures and heat fluxes. The experiments were valid if the energy gain of the refrigerant and the heat input through the electrical heating tape were the same. The amount of energy input to the test section



was measured with the watt meter and the amount of energy received by the fluid was calculated from the mass flow rate, temperature rise across the test section and specific heat of liquid HCFC-22 as shown in Equation 4.1.

$$E = \dot{m} \cdot c_{pL} \cdot \Delta T \quad (4.1)$$

The single-phase heat transfer coefficients were not calculated because the difference in wall temperature and fluid temperature was the same order of magnitude as the uncertainty of temperature measurements made using the thermocouples. The average uncertainty for these tests was  $\pm 2$  percent.

#### RESULTS OF TWO-PHASE EXPERIMENTS

The two-phase tests for HCFC-22 were also conducted to validate the experimental apparatus, especially the ability to reliably determine the convective heat transfer for an evaporating refrigerant. The results of these tests were compared to published correlations and experimental research. The results also show the effect of quality, heat flux and mass flux on the convective heat transfer of HCFC-22. The convective heat transfer results were compared to existing heat transfer correlations developed by Shah (1982), Gungor and Winterton (1986) and Kandlikar (1987). The pressure drop across the test section was determined and also compared to existing correlations developed by Martinelli (1949) and Friedel (1979). Through this experimentation and subsequent analysis, an attempt was made to describe the flow boiling mechanisms taking place in HCFC-22 for the conditions studied in this analysis.

The experimental convective coefficients measured in this study were directly compared to experimental convective coefficients from published research. In Figure 4.1 the measured convective coefficients were compared to previously published convective

coefficients for HCFC-22 at the same flow conditions. All of the data were within  $\pm 17\%$  of that measured by previous investigators. The published experimental data were taken from the three references shown in the legend. The convective coefficients were determined from measured temperatures and heat flux as shown:

$$\bar{h} = q'' / (\bar{T}_{fluid} - \bar{T}_{wall}) \quad (4.2)$$

Figure 4.2 shows the effect of varying heat and mass flux on the convective coefficient for HCFC-22.

Several investigators (Hambreaus, 1991; Anderson, 1966; Wattlet, 1991) performed their experiments with inlet vapor qualities at the test section of approximately 20 percent. The experiments in this study were reported upon an average quality in the test section. This value corresponded to the vapor qualities typically found in an air conditioning evaporator. This investigation was concerned with the average convective coefficient and the use of average quality was more appropriate. The aforementioned authors used average values of quality and the convective coefficient, but limited the test section inlet quality to values close to 20 percent. The use of average quality was more appropriate here and presentation of inlet quality will only be used for viewing contrasts between the two. The trend indicated in Figure 4.2 indicated that the convective heat transfer increased as quality increased. The convective coefficient usually increased with increasing quality over specific parts of the nucleate boiling region and the convective boiling region.

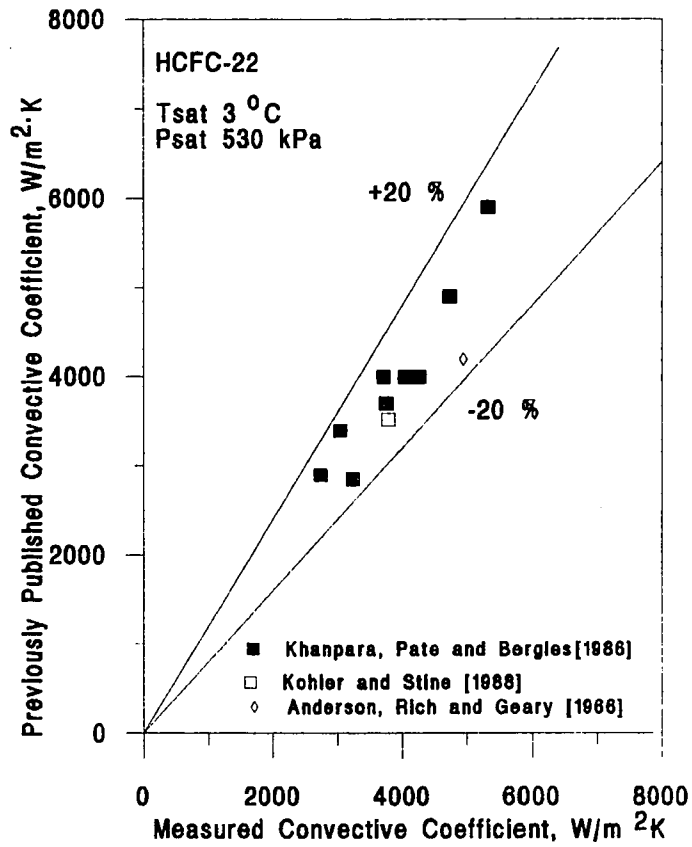


Figure 4.1 Comparison Between Measured Convective Coefficients and Previously Published Convective Coefficients for the Same Flow Conditions.

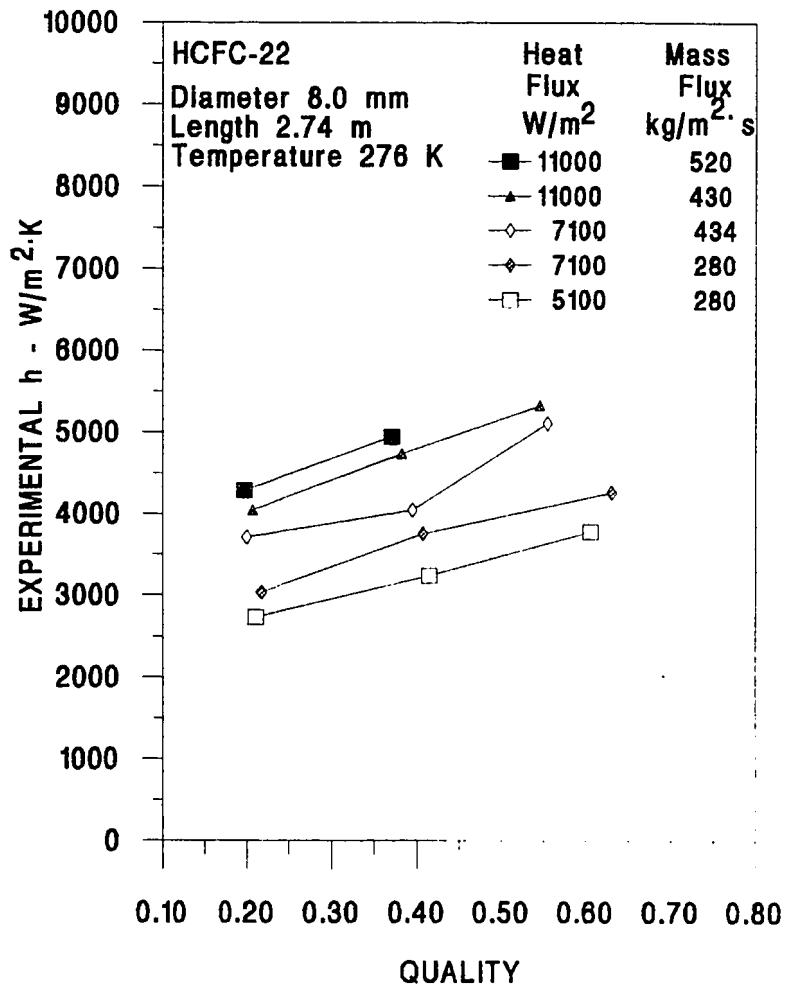


Figure 4.2 Evaporative Heat Transfer Coefficients at Various Mass Velocities and Heat Fluxes Using Test Section Inlet Qualities.

For a given mass flux, at higher qualities, the velocities must be higher. In other words, the refrigerant mixture has a lower density when the quality is high and must flow at a higher velocity to maintain the same mass flux. The higher velocities contributed to greater convective heat transfer due to the increased turbulence and fluid movement.

The convective heat transfer increased as the mass flux increased. Experiments were performed for three different mass fluxes. The mass fluxes were 280, 430 and 520  $\text{kg/m}^2\text{s}$  ( 57.3, 88.1 and 106.5  $\text{lb}_m/\text{ft}^2\cdot\text{s}$  ). By looking at the different mass fluxes for the heat fluxes of 7100 and 11000  $\text{W/m}^2$  ( 2251 and 3488  $\text{Btu/hr}\cdot\text{ft}^2$ ), the effect of the increased mass flux can be isolated. The increased mass flux translated into increased velocity, increased Reynolds numbers and increased turbulence.

The convective heat transfer also increased for higher heat fluxes. Chen [1966] and others have modeled the boiling heat transfer coefficient as a combination of nucleate boiling and convective heat transfer due to fluid motion. The higher the heat flux the greater energy available to initiate nucleate boiling. At low qualities, a higher heat flux causes more bubbles to grow from the tube wall and depart into the flow stream. The effect of heat flux can be seen by looking at the curves representing mass fluxes of 280 and 430  $\text{kg/m}^2\text{s}$  (57.3 and 88.1  $\text{lb}_m/\text{ft}^2\cdot\text{s}$  ). Two separate heat fluxes were applied at each mass flux and the effect can be noted as the higher heat flux lines corresponded to higher convective coefficients. Figure 4.3 was exactly the same graph as Figure 4.2 except that the convective coefficient was graphed against the average qualities in the test section. The curves were almost identical except using the average quality values shifted all the curves slightly to the right.

Figure 4.4 shows a comparison of all HCFC-22 data against three popular boiling models. The correlations of Gungor and Winterton (1986), Kandlikar (1987) and Shah

(1982) were fundamentally different and their differences are discussed later. In Figure 4.4, all the predicted values were calculated using the inlet quality to the test section. The experimental values were generally within  $\pm 20$  percent of the predicted values. This was the same accuracy as reported in the literature (Kandlikar, 1982). The exception was the Shah correlation which was consistently low in estimating the convective coefficients below  $4000 \text{ W/m}^2$  ( $1268 \text{ Btu/hr}\cdot\text{ft}^2$ ). Predicting two-phase convective heat transfer using a general correlation to within  $\pm 20$  percent was consistent with the results reported by Wattelet (et al, 1991). The use of inlet quality (Figure 4.4) did not seem appropriate but the comparison was made for completeness. Figure 4.5 shows the same graph as Figure 4.4 except that the average qualities were used in calculating the predicted convective coefficient. Just as in Figures 4.2 and 4.3 there seems to be little difference in reporting the heat transfer coefficient as a function of tube inlet or average quality for tests where the quality from inlet to exit does not vary more than 20 percent.

The use of the average qualities, which were naturally higher than inlet qualities, gave a higher predicted convective coefficient and thus more data points fell within the  $\pm 20$  percent error band as shown in Figure 4.5. For the rest of the study, all data were treated on an average quality basis and no further comparisons to inlet quality were made.

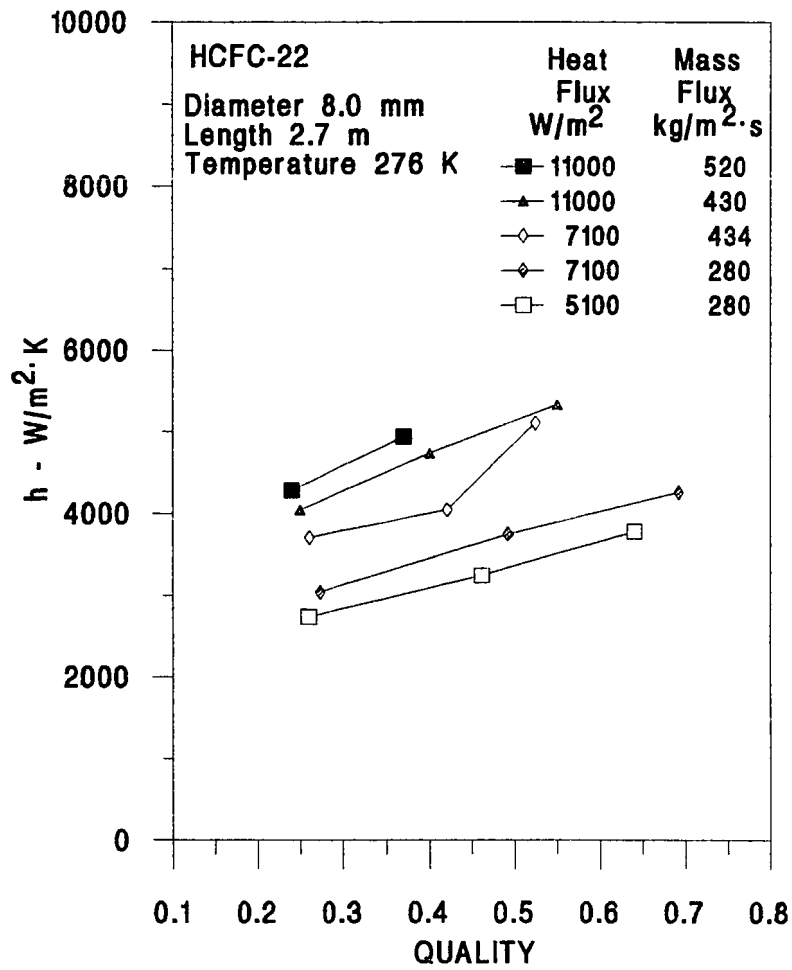


Figure 4.3 Evaporative Heat Transfer Coefficients at Various Mass Velocities and Heat Fluxes Using Average Test Section Qualities.

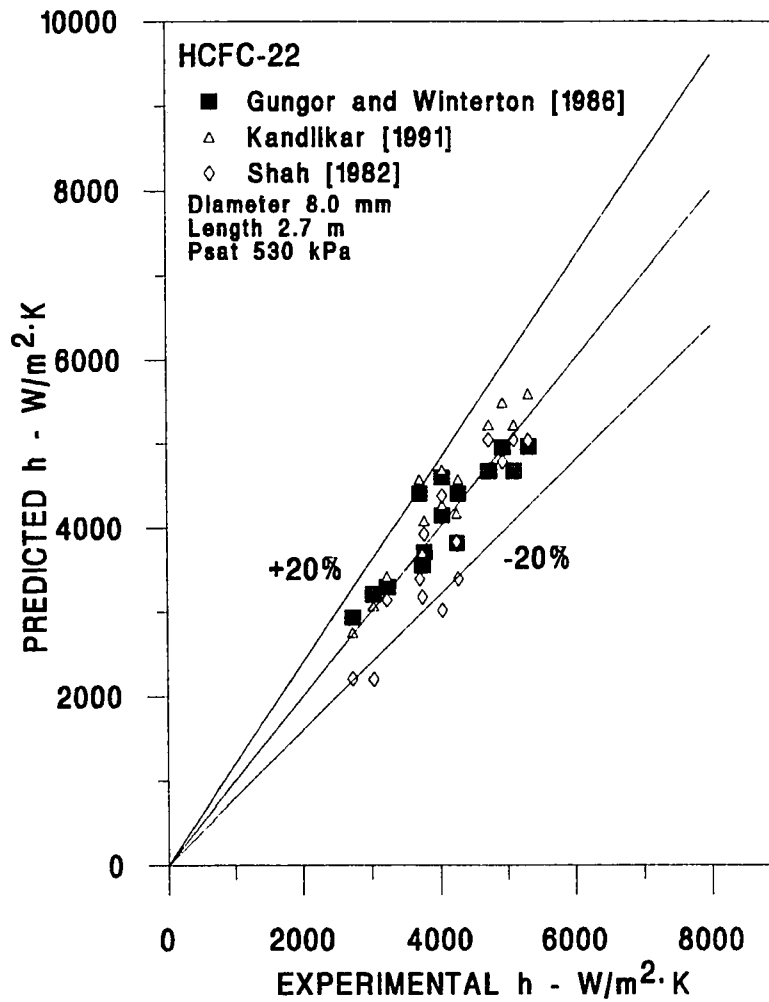


Figure 4.4 A Comparison of Evaporation Heat Transfer Data with Prediction Correlations Using Test Section Inlet Qualities.



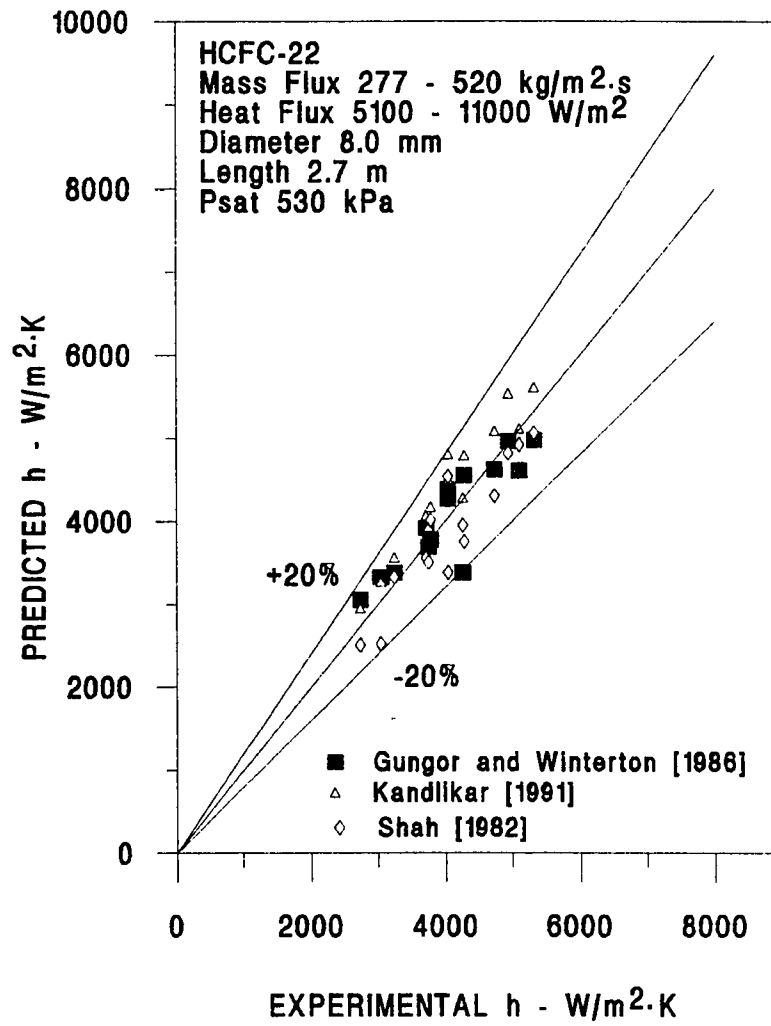


Figure 4.5 A Comparison of Evaporation Heat Transfer Data with Prediction Correlations Using Average Test Section Qualities.

Figures 4.4 and 4.5 indicated that the data and the existing correlations agreed within  $\pm 20$  percent over the test conditions studied. A larger question remained as to what the correlations predicted over a complete range of qualities for a specified mass flux and heat flux. Figure 4.6 shows the convective heat transfer coefficients predicted using the correlations of Gungor and Winterton [1986], Shah [1982] and Kandlikar [1991] over a quality range of 0 to 0.8. Figure 4.6 was generated for a heat flux of  $11000 \text{ W/m}^2$  ( $3488 \text{ Btu/ft}^2\text{-hr}$ ) and a mass flux of  $520 \text{ kg/m}^2\text{s}$  ( $106 \text{ lb}_m/\text{ft}^2\text{-s}$ ). The experimental values are also placed on this graph.

The boiling mechanisms were usually thought to be nucleate boiling dominated at low qualities and convective heat transfer dominated at higher qualities. The correlation of Kandlikar showed an abrupt drop in the convective coefficient at this transition. The Kandlikar correlation treated the nucleate boiling and convective driving mechanism separately. It contained separate equations for convective and nucleate boiling. The heat transfer coefficient was determined to be nucleate boiling dominated or convective dominated based upon whether the convection number,  $Co$ , was greater or less than 0.65. The correlation of Shah showed a smooth curve over the entire quality range. Shah's correlation also included both nucleate boiling and forced convection components where one mechanism was dominant also. The correlation of Gungor and Winterton produced a smooth curve over the entire quality range. The correlation was based upon an additive technique where the effects of both nucleate boiling and forced convection were added together.

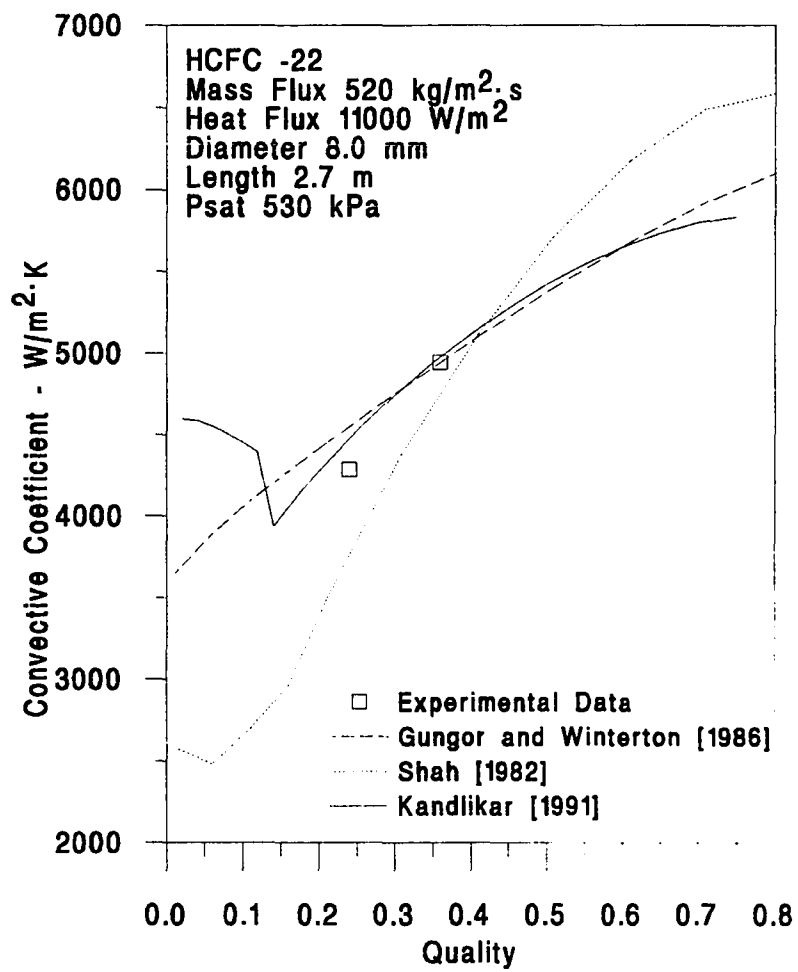


Figure 4.6 A Comparison of Evaporation Data and Prediction Correlations for a Heat Flux of 11000 W/m<sup>2</sup> and a Mass Flux of 520 kg/m<sup>2</sup>.s.

The Gungor and Winterton method was developed by curve fitting large quantities of available data. The curve fits did not necessarily attempt to represent a transition from nucleate boiling dominated heat transfer to convective dominated heat transfer. The experimental results fell between values predicted by the different correlations. As might have been expected, the experimental results were near the values of the correlations where convection was thought to be the dominant heat transfer mechanism. For the particular case in Figure 4.6 where the mass flux was  $520 \text{ kg/m}^2\text{s}$  and the heat flux was  $11000 \text{ W/m}^2$ , the prediction methods differ from each other by over  $1000 \text{ W/m}^2\text{K}$  in parts of the convective dominated region and  $1800 \text{ W/m}^2\text{K}$  in the nucleate boiling dominated region. The curves were not carried past qualities of 0.8 which would have corresponded to a the liquid deficient region. In this region, the convective coefficients decrease significantly because of a lack of liquid wetting the tube wall surface. The correlations were not recommended for use with this flow pattern.

There were some advantages in comparing the predicted convective coefficients to experimental convective coefficients as in Figure 4.6. Once the data points were graphed with the correlations, it was possible to estimate the general trend of convective coefficients between the points. All of the experimental data were compared in this same manner in Figures 4.7 through 4.10. While the data followed the overall trends of the correlations, several important points need to be made. The convective coefficients predicted with the Shah correlation were always lower for the lower qualities than the other two. The predicted convective heat transfer changed less over the entire range of qualities for lower heat and mass fluxes as was seen by viewing Figures 4.8 through 4.10. The predicted convective heat transfer for high qualities and high mass fluxes were affected by the convective forces due to increased two-phase Reynolds numbers.

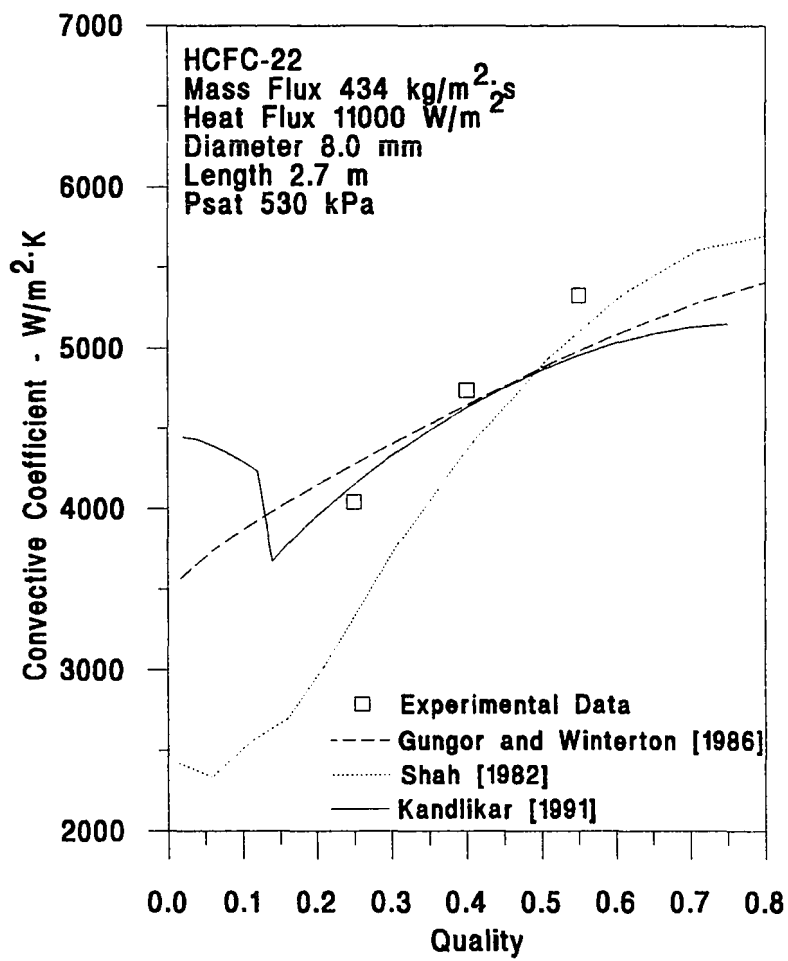


Figure 4.7 A Comparison of Evaporation Data and Prediction Correlations for a Heat Flux of  $11000 \text{ W/m}^2$  and a Mass Flux of  $430 \text{ kg/m}^2\cdot\text{s}$ .

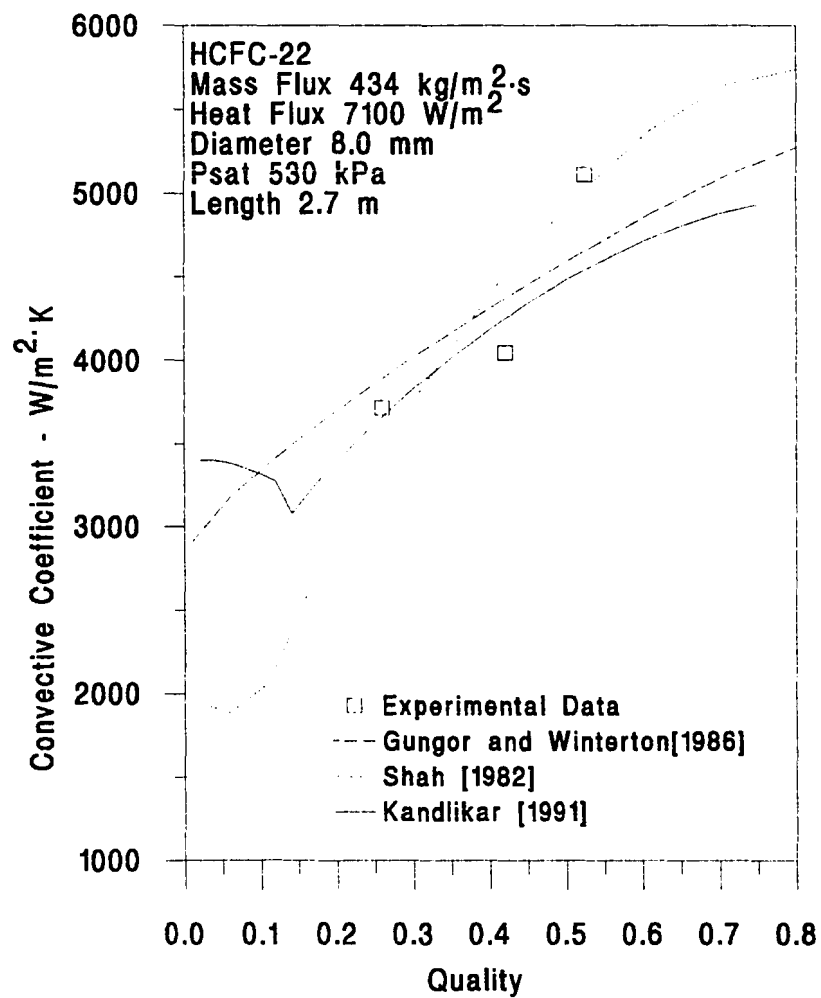


Figure 4.8 A Comparison of Evaporation Data and Prediction Correlations for a Heat Flux of  $7100 \text{ W/m}^2$  and a Mass Flux of  $434 \text{ kg/m}^2\cdot\text{s}$ .

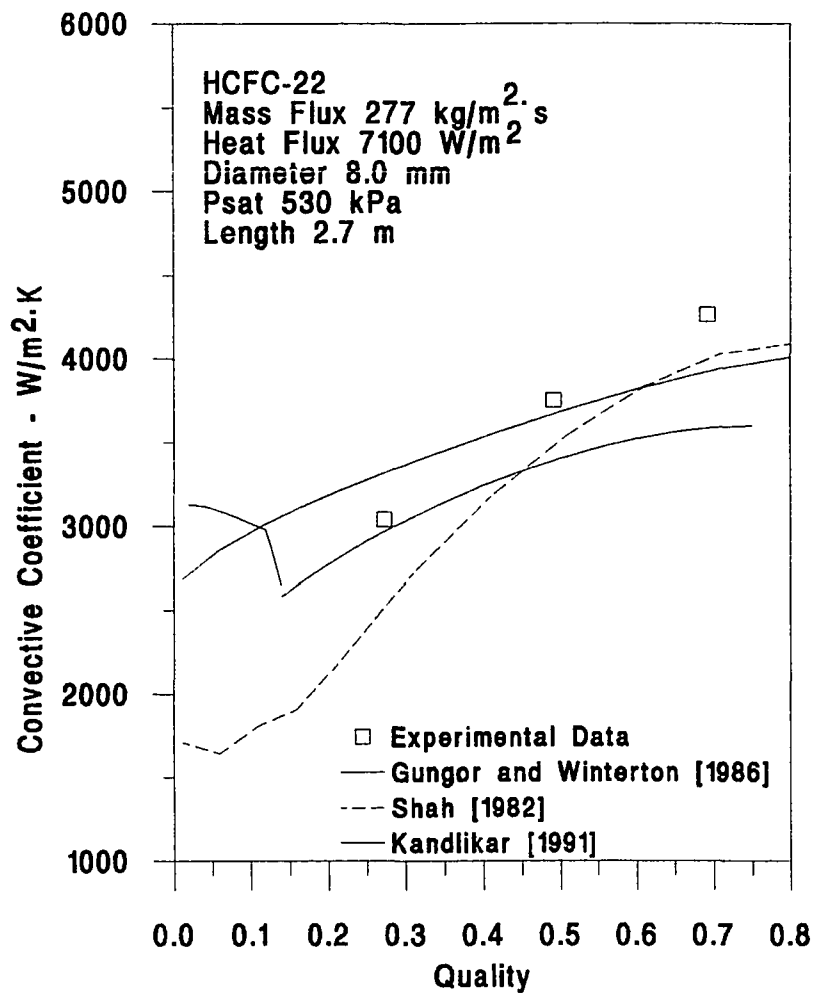


Figure 4.9 A Comparison of Evaporation Data and Prediction Correlations for a Heat Flux of  $7100 \text{ W/m}^2$  and a Mass Flux of  $280 \text{ kg/m}^2 \cdot \text{s}$ .

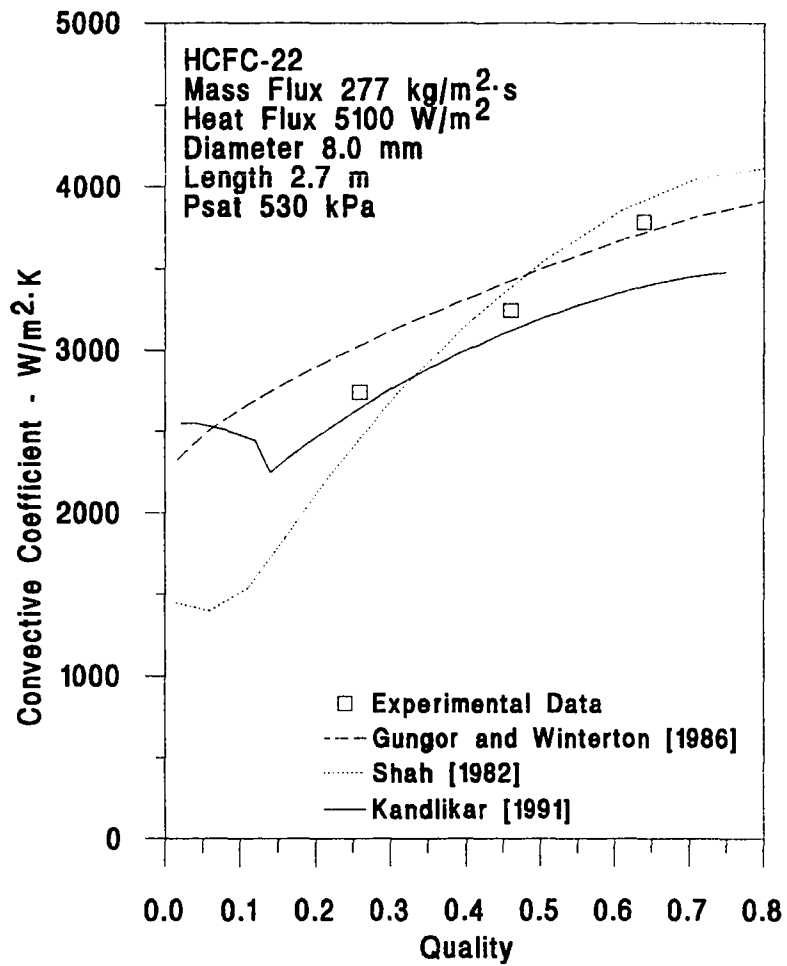


Figure 4.10 A Comparison of Evaporation Data and Prediction Correlations for a Heat Flux of  $5100 \text{ W/m}^2$  and a Mass Flux of  $280 \text{ kg/m}^2\text{s}$ .



The change or increase in convective heat transfer was much less noticeable as a function of increasing heat flux. This in itself did not represent fully suppressed nucleate boiling (FSNB) in the convective region but does lend credibility that the convective mechanism dominated at the higher qualities. If nucleate boiling was completely suppressed, then there would be no increase in convective heat transfer with increasing heat flux. (Ross, 1987)

Because convective heat transfer dominated much of the flow boiling process, most attempts to quantify its value were related back to the liquid convective coefficient. Equations to predict liquid convective heat transfer have been used over 60 years (Dittus, 1930). One of the earliest equations, known as the Dittus-Boelter equation, is shown in Equation 4.3, where the corresponding Reynolds number is a two-phase liquid Reynolds number.

$$h_L = 0.023 \text{Re}_L^{0.8} \text{Pr}^{0.4} k_L / D \quad (4.3)$$

$$\text{Re}_L = GD(1-x) / \mu_L \quad (4.4)$$

This Reynolds number represents the liquid flowing alone in the tube without the vapor. A separate Reynolds number (Equation 4.5) is sometimes used in pressure drop calculation and represents liquid flowing at the same mass flow rate as the two-phase mixture [Collier, 1982].

$$\text{Re}_{LO} = GD / \mu_L \quad (4.5)$$

The additive correlations [Chen, 1966; Kandlikar, 1991; Gungor and Winterton, 1986; Wattelet, 1994] take into account the effect convective heat transfer and nucleate boiling have on the overall heat transfer:

$$h_{tp} = h_{conv} + h_{nucleate} \quad (4.6)$$

The additive equation can be modified [Chen, 1966] by calculating the convective heat transfer from the product of the liquid convective coefficient and an enhancement factor:

$$h_{tp} = h_l \cdot E + h_{nucleate} \quad (4.7)$$

The experimental two-phase convective heat transfer coefficients are plotted against the calculated liquid convective coefficient in Figure 4.11. The curves grouped together for similar mass fluxes. Each line represented a given mass flux and heat flux. The two-phase coefficient declined as the calculated liquid convective coefficient increased. The liquid coefficient was higher at lower qualities because the liquid Reynolds number was higher at low qualities. The two-phase convective coefficient increases for higher qualities when convective heat transfer dominates the process.

The dependence of two-phase convective heat transfer upon quality and mass flow rate was shown in Figures 4.2 and 4.3. Historically, the two-phase variables were correlated to the liquid properties based on the liquid flowing at the mass flow rate equivalent to that of the two-phase refrigerant. In Figure 4.11, the experimental or calculated convective coefficient decreased with the liquid heat transfer coefficient predicted from Equation 4.3. The liquid convective coefficient decreased with increased quality.

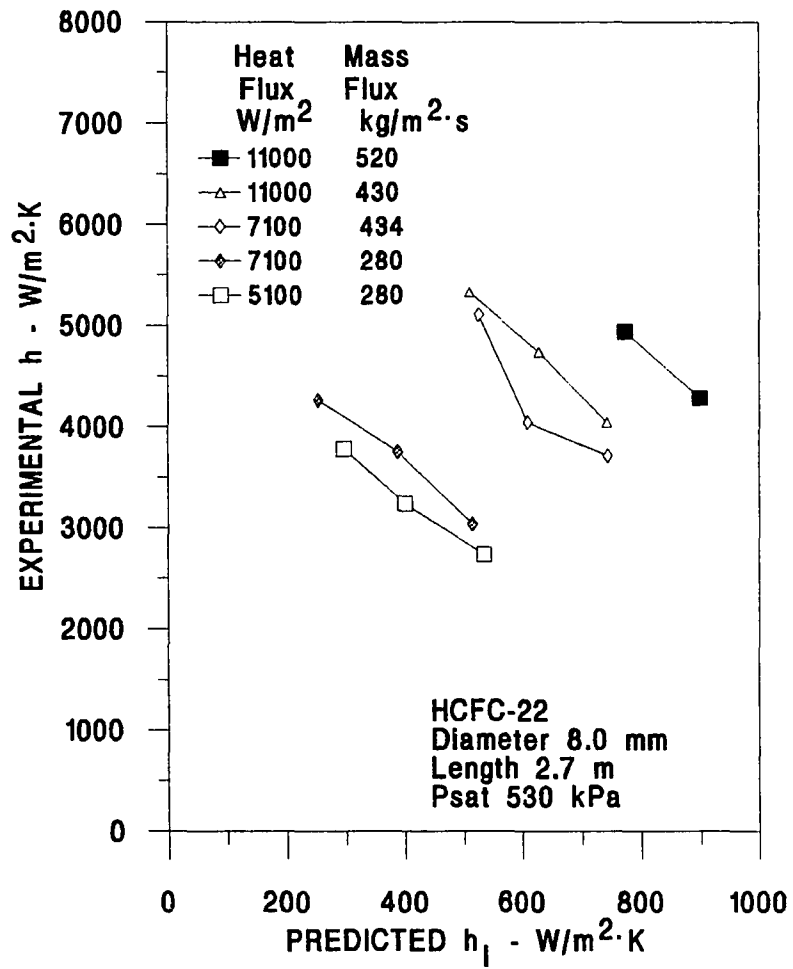


Figure 4.11 Total Evaporative Heat Transfer Coefficients Dependence as a Function of Liquid Convective Coefficient.

The comparison of two-phase and liquid convective coefficient stems from the use of additive models, where the pool boiling or nucleate boiling effects were added to the convective heat transfer contribution. The earliest use of this type of model was by Chen (1966). The effect of pool boiling upon two-phase convective heat transfer are shown in Figure 4.12.

The convective coefficient increased with increasing pool boiling convective coefficient. The effect of quality and mass flux were also evident in Figure 4.12 as shown in the vertical differences of the curves. The higher qualities and higher mass fluxes cause higher convective coefficients. It was difficult to quantify the increase in convective coefficient attributed to the nucleate boiling process. The nucleate boiling values were calculated from a pool boiling correlation given by Cooper (1984):

$$h_{pool} = 55 P_{red}^{0.12} (-\log_{10} P_{red})^{-0.55} M^{-.05} q^{0.67} \quad (4.8)$$

The only value in equation 4.8 that changed for any given refrigerant was the heat flux. The pool boiling term was not a function of mass flux or quality.

Often times two-phase convective heat transfer has been correlated using the Martinelli parameter [Martinelli and Nelson, 1948]:

$$X_{rr} = \left( \frac{1-x}{x} \right)^{0.9} \left( \frac{\rho_v}{\rho_L} \right)^{0.5} \left( \frac{\mu_L}{\mu_v} \right)^{0.1} \quad (4.9)$$

This term was originally developed and presented for the prediction of two-phase pressure drop, but has been used extensively in heat transfer as well. The experimental

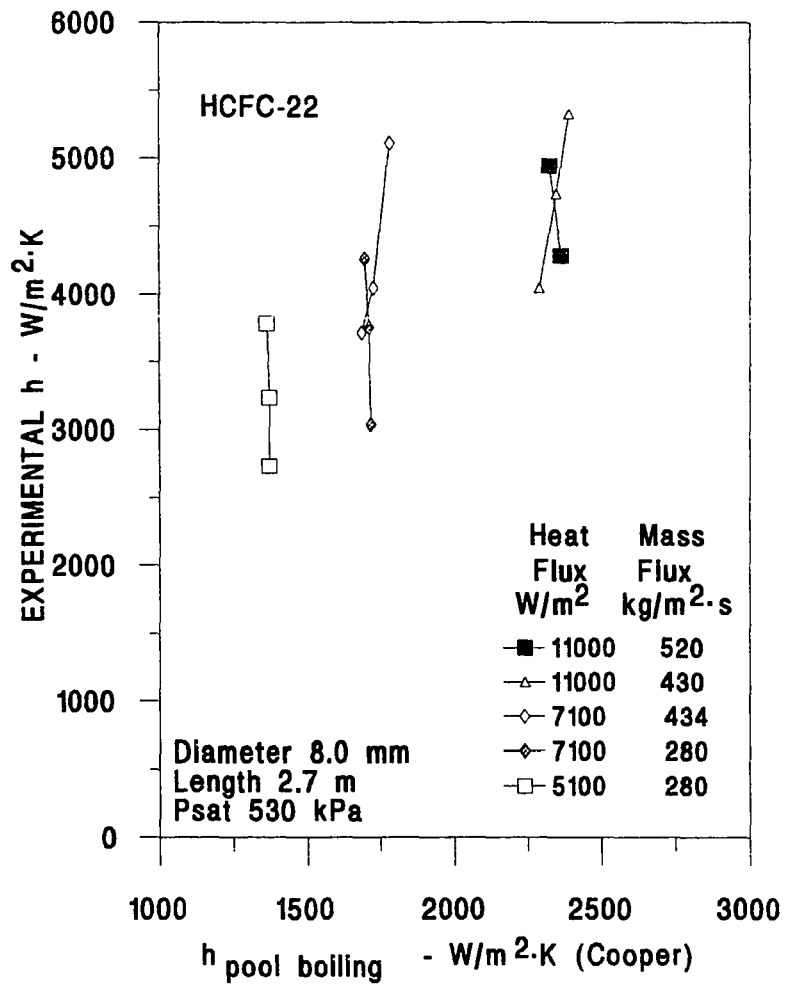


Figure 4.12 Evaporative Heat Transfer Coefficients Dependency as a Function of Pool Boiling Convective Coefficient as Calculated from Cooper (1982).

data are presented as a function of Martinelli parameter in Figure 4.13.

The convection coefficient decreased with increasing values of Martinelli parameter. The temperatures for all tests were the same and the viscosity and density terms in the Martinelli parameter did not change for any of the points. The Martinelli parameter was included to account for the differences in liquid and vapor viscosity and densities for different temperatures and refrigerants.

A common method of correlating two-phase convective coefficient is to relate the ratio of experimental two-phase convective coefficients to the calculated liquid convective coefficient to the inverse of the Martinelli parameter (Figure 4.14). Three equations from the literature are presented. Dengler and Addoms (1956) developed empirical coefficients to the equation from horizontal flow boiling experiments with water. Guerriere and Talty (1956) investigated the flow boiling of hydrocarbons in a vertical tube. Ross et al. (1987) curve fit published HCFC-22 data. The mean deviation from the experimental data to the best fit equation, the correlation by Dengler and Addoms, by Guerriere and Talty, and by Ross et al were 5.9%, 11.6%, 16.8% and 21.6 %, respectively.

Some researchers feel that improvements in the ability to predict convective coefficient and pressure drop will come by analyzing the flow for a specific flow pattern. One of the earliest attempts to map flow patterns was made by Baker (1954) and is still used today. This flow map as well as the HCFC-22 data superposed upon it is shown in Figure 4.15. The flow pattern was identified as annular and dispersed. Dispersed flow pattern was sometimes considered a subset of the annular flow. This graph reinforces the previous thought that the heat transfer for these experiments was dominated by convective mechanisms rather than nucleate boiling because convective heat transfer has been generally associated with annular flow. The annular flow regime consists of a thin layer of liquid flowing next to the tube wall and vapor flowing in the center of the tube.

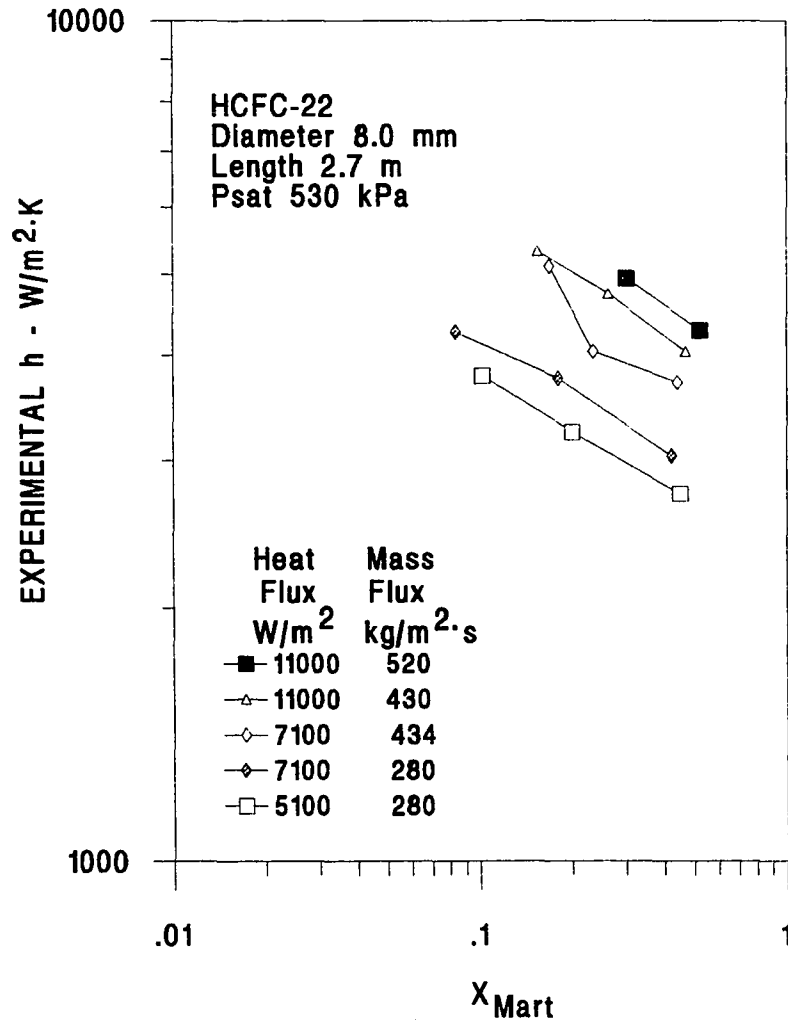


Figure 4.13 Evaporative Heat Transfer as a Function of Martinelli Parameter.

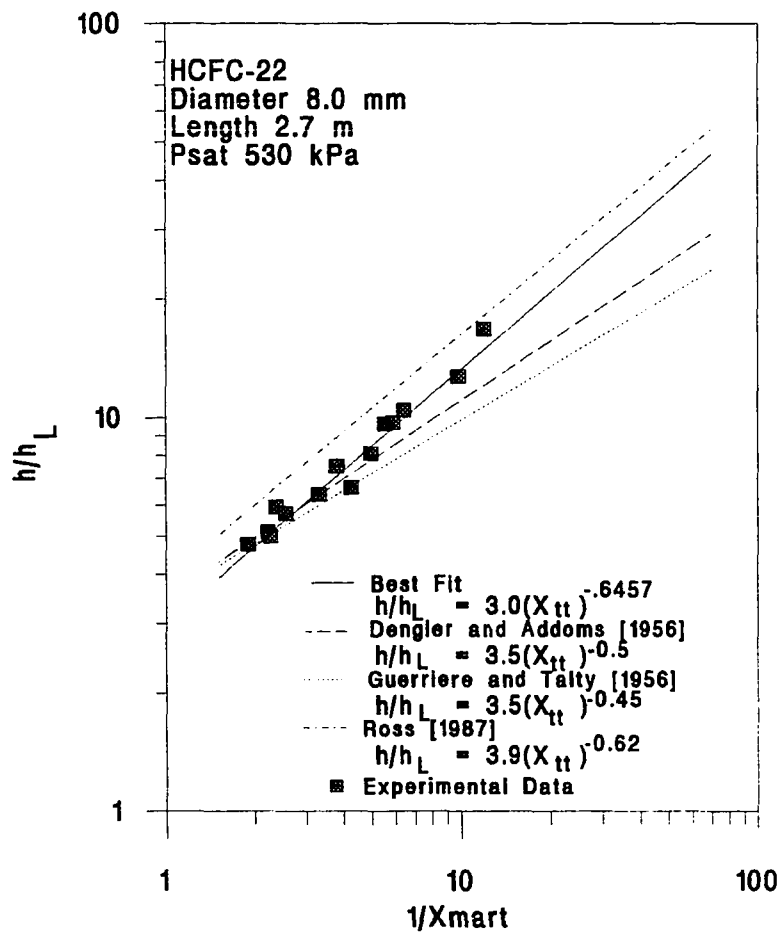


Figure 4.14 The Ratio of Two-phase to Predicted Single-phase Convective Heat Transfer Coefficient.



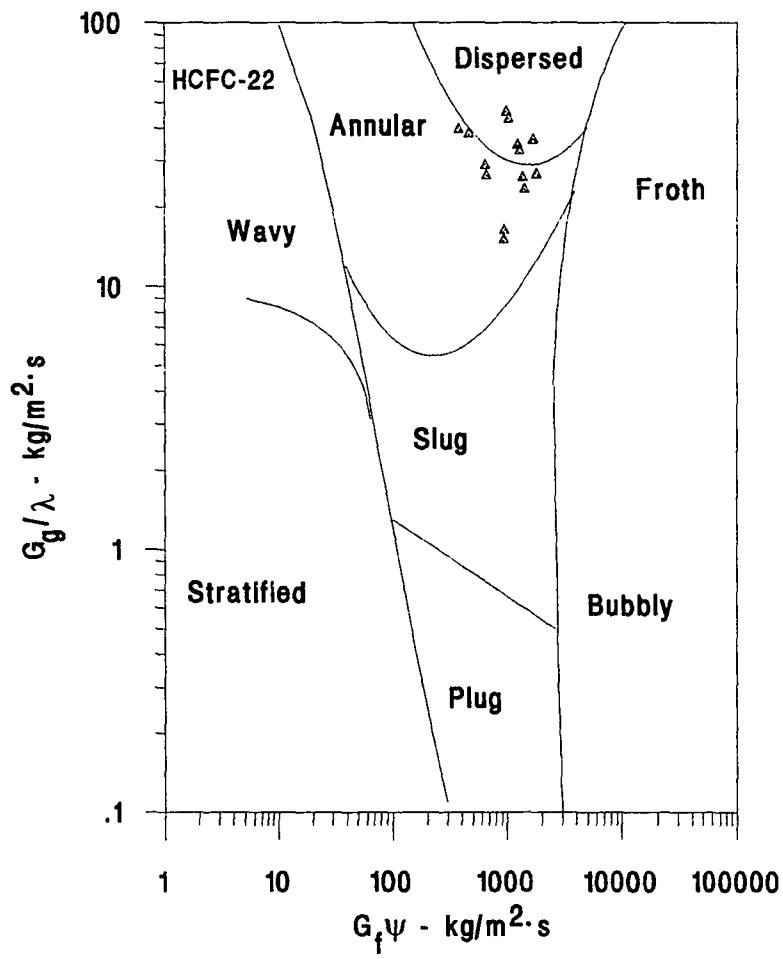


Figure 4.15 Flow Pattern Map (Baker, 1954)

Because this liquid layer is sufficiently thin, bubbles cannot grow and depart the wall. The liquid at the wall insures sufficient thermal contact so that convective heat transfer can still be reasonably high. The variables chosen for correlating the flow map are shown in Equations 4.10 and 4.11. The original work by Baker was done using air and water as the vapor and liquid, where the graphing variables were attempts to normalize the fluid properties to those of water and air.

$$G_f \Psi = G(1-x) \left( \frac{\sigma_w}{\sigma} \right) \left[ \left( \frac{\mu_f}{\mu_w} \right) \left( \frac{\rho_w}{\rho_f} \right)^2 \right]^{-\left(\frac{1}{3}\right)} \quad (4.10)$$

$$G_g / \lambda = Gx / \left[ \left( \frac{\rho_g}{\rho_a} \right) \left( \frac{\rho_f}{\rho_w} \right) \right]^{-\left(\frac{1}{2}\right)} \quad (4.11)$$

More recent work on the flow patterns of two-phase flow was performed by Taitel and Dukler (1976). The flow patten map from their work is shown in Figure 4.16 along with values of  $F_{td}$  from the current measurements on HCFC-22. The variable,  $F_{td}$ , is given as:

$$F_{td} = \left[ \frac{\rho_v j_v^2}{(\rho_l - \rho_v) \cdot D \cdot g \cdot \cos \Omega} \right]^5 \quad (4.12)$$

The value of  $F_{td}$  showed that the experimental data were entirely within the annular flow region. While these were not necessarily rigid flow pattern boundaries, the flow pattern maps of both Baker and Taitel and Dukler showed that HCFC-22 flowing under the conditions in this study were annular or dispersed annular.

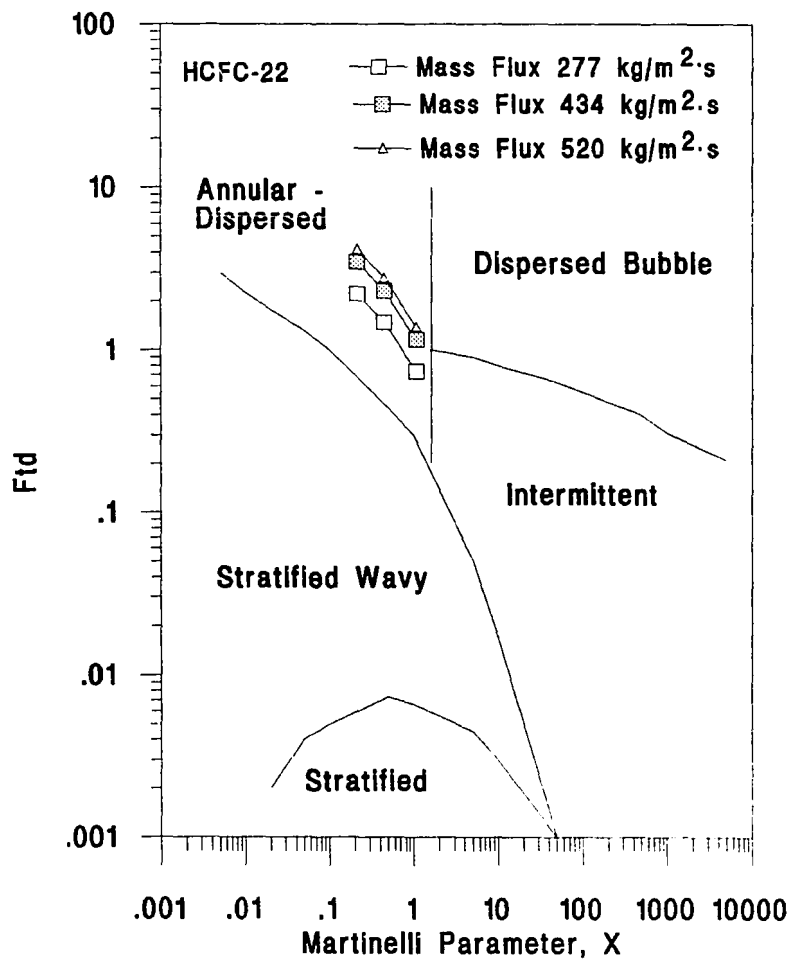


Figure 4.16 Flow Pattern Map (Taitel and Dukler, 1976)

After determining that the flow patterns were predominately annular, or possibly dispersed annular, consistent trends in the pressure drop would be expected. These trends are shown in Figure 4.17 where the measured pressure drop is shown as a function of quality with mass flow rate and heat flux as parameters. The pressure drop increased as quality increased for all cases. The higher the quality for a given mass flow rate, the higher the velocity of vapor. This increased velocity translates to more friction and the associated pressure drops. A second trend noted was that the change in heat flux has a negligible effect upon the pressure drop. The heat flux was not high enough to effectively increase the bubble nucleation sites to a point where it disrupts the flow. It can be inferred that the acceleration due to the change in quality for the qualities, heat and mass fluxes in this study were negligible. The pressure drop increased for increasing mass fluxes. This was once again due to the increased velocity and corresponding frictional pressure drop.

There are two types of pressure drop prediction models that are commonly used: a homogeneous model and separated flow models. The homogeneous model assumes that the liquid and vapor flow at some average viscosity and density and are applicable to single-phase analysis. There are several equations for determining an average viscosity and density, which in turn are used to predict the two-phase friction factor for calculating the pressure drop. The homogeneous model is considered to be accurate for conditions of high velocities and high pressures. The model is also considered applicable to flow patterns such as bubbly flow where there is a homogeneous cross section of vapor. The homogeneous model can be considered for both high and low qualities where the mixture behaves very similar to a single-phase [Collier, 1982].

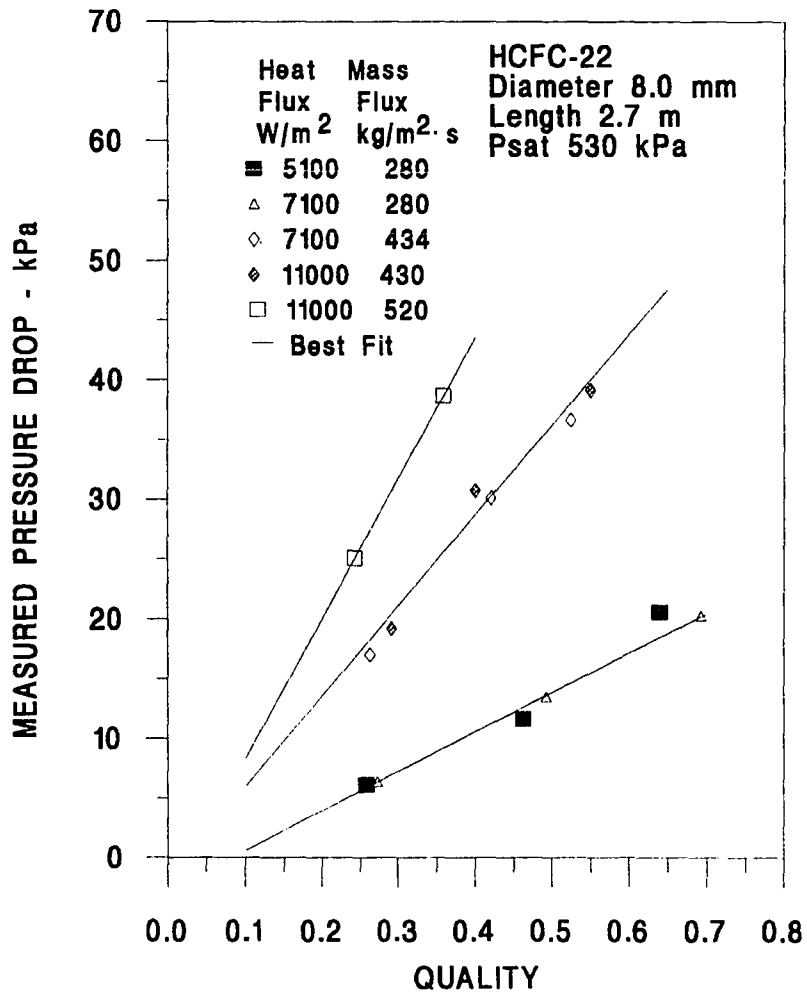


Figure 4.17 Pressure Drop for Various Mass Velocities and Heat Fluxes.

The separated flow model considers both the liquid and vapor to flow separately at constant but not necessarily equal velocities. There are several approaches to determining the pressure drop using the separated flow model. The first such attempt was proposed by Martinelli and Nelson. A more recent model by Friedel (1979) was also considered here. The experimental pressure drop was shown with the predicted pressure drop using a homogenous model and two separated flow models in Figure 4.18. The separated flow models were considered more accurate [Collier, 1982]. The Martinelli-Nelson prediction results generally fall within a  $\pm 30\%$  error band. The Friedel and homogeneous techniques under predicted the pressure drop by 65% and 50% respectively.

Just as the two-phase heat transfer was correlated to the single-phase heat transfer, so the two-phase pressure drop was correlated to the single-phase pressure drop. The early work by Martinelli (1949) found the pressure drop to be a function of the Martinelli parameter. Figure 4.18 shows the ratio of experimental pressure drop to the calculated liquid only pressure drop for all the HCFC-22 data. The use of this ratio normalized the effect of mass flux and was related to the Martinelli parameter as:

$$\Delta P / \Delta P_{LO} = 13 \cdot X_n^{-0.72} \quad (4.13)$$

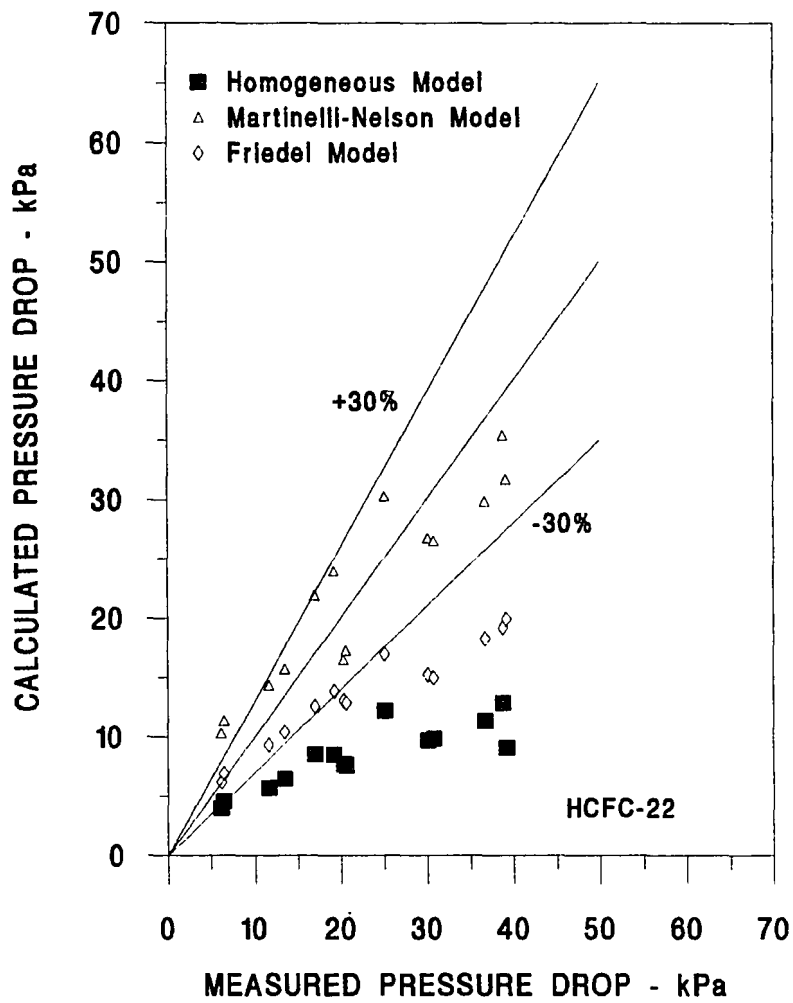


Figure 4.18 A Comparison of Pressure Drop with Predicted Pressure Drops.

## SUMMARY

The experimental heat transfer data for HCFC-22 agreed with the results of earlier investigators within eight percent. The experimental conditions were plotted on flow maps and annular flow patterns were predicted for all cases. The heat transfer coefficients responded to changes in mass flux and heat flux consistent with the response expected from annular flow. When mass flux or heat flux was increased, convective heat transfer coefficient also increased.

The pressure drop was dependent upon flow rate, where an increase in the velocity of the refrigerant corresponded to an increase in pressure drop. Heat flux appeared to have a minimal effect upon the pressure drop.



## CHAPTER V

### EXPERIMENTAL RESULTS FOR AN HFC-32/HFC-125

#### 50/50 MASS MIXTURE

One purpose of this experimental research was to obtain boiling heat transfer and flow characteristics for a 50% / 50% by mass mixture of HFC-32 and HFC-125. Two-phase flow boiling convective coefficients and the measured pressure drops of HFC-32/HFC-125 were determined for mass fluxes ranging from 277 kg/m<sup>2</sup>s to 700 kg/m<sup>2</sup>s (57 lb<sub>m</sub>/ft<sup>2</sup>·s to 143 lb<sub>m</sub>/ft<sup>2</sup>·s) and qualities ranging from 10 to 60 percent. The heat flux was varied from 5100 W/m<sup>2</sup> to 11000 W/m<sup>2</sup> (1617 Btu/hr·ft<sup>2</sup> to 3488 Btu/hr·ft<sup>2</sup>). After performing the experiments with pure HFC-32/HFC-125, a polyol ester (POE) oil was added on a mass basis in concentrations of 2.5 percent and 5.5 percent and the same series of experiments were performed. The experimental heat transfer data for HFC-32/HFC-125 were compared to existing flow boiling heat transfer correlations by Shah [1982], Gungor and Winterton [1986], Kandlikar [1987] and Chen [1966]. The flow pattern for each test was determined by comparing experimental data to graphs by Baker [1954] and Taitel and Dukler [1976]. The effect of mass flux and heat flux on pressure drop was discussed. The experimental two-phase pressure drop was compared to a homogenous pressure drop correlation and to two separate flow correlations by Lockhart and Martinelli [1949] and Friedel [1979].

Even though the operating pressures for HCFC-22 and HFC-32/HFC-125 were different, the evaporating temperatures were the same. The thermodynamic and fluid properties for these two refrigerants were very different. A direct comparison of the experimental results for heat transfer and pressure drop of these two refrigerants was included. The impact of the difference of refrigerant properties on the experimental results were also analyzed.

## HFC-32/HFC-125 MIXTURE

In this section, the experimental results for HFC-32/HFC-125 without oil were discussed. This includes examination of boiling heat transfer coefficient and pressure drop as a function of mass flux and heat flux. The ability of existing two-phase performance correlations to accurately predict the heat transfer and pressure drop were included in this discussion.

### FLOW PATTERN PREDICTION

The boiling heat transfer was dominated by forced convective effects at high qualities. This was due to two factors. First, as quality increases, the refrigerant velocity increases. The higher refrigerant velocities correspond to higher Reynolds numbers and more turbulence. Turbulence promotes convective heat transfer near the tube wall. The second factor was that annular flow patterns existed at high qualities and the shallow liquid film at the tube wall suppressed nucleation. Different heat transfer mechanisms are associated with different flow patterns. Nucleate boiling dominated heat transfer has been associated with bubbly, plug and slug flow patterns. Convective dominated heat transfer has been associated with the annular flow pattern [Carey, 1992]. Two popular flow pattern maps were compared to the experimental data. The purpose of the flow pattern maps was to help evaluate the flow pattern in the tube and to help in determining the appropriate heat transfer analytical model. The map by Baker [1954] was originally used in the petrochemical industry [Collier, 1982]. The second flow pattern map was presented by Taitel and Dukler [1976].

The flow pattern map for horizontal flow presented by Baker required graphing the superficial liquid mass velocity, (Equation 5.1), multiplied by a term,  $\Psi$  (Equation 5.2), which normalized the surface tension, viscosity and density of the refrigerant to that of water. This combination of terms was graphed on the x-axis. The y-axis term consisted of the superficial vapor velocity, (Equation 5.3), divided by  $\lambda$

(Equation 5.4), another normalizing term. The subscripts A and W represent air and water respectively. The subscripts f and g represent the refrigerant liquid and vapor, respectively. These were not dimensionless terms and the appropriate units as well as the map itself are shown in Figure 5.1.

$$G_f = G \cdot (1 - x) \quad (5.1)$$

$$\Psi = \left( \frac{\sigma_w}{\sigma_f} \right) \left[ \left( \frac{\mu_f}{\mu_w} \right) \left( \frac{\rho_w}{\rho_f} \right)^2 \right]^{\frac{1}{3}} \quad (5.2)$$

$$G_g = G \cdot x \quad (5.3)$$

$$\lambda = \left[ \left( \frac{\rho_g}{\rho_A} \right) \left( \frac{\rho_f}{\rho_w} \right) \right]^{\frac{1}{2}} \quad (5.4)$$

The terms set forth in equations 5.1 through 5.4 for determining the flow pattern were independent of heat flux. The four mass fluxes and qualities used in this study were plotted on the Baker flow pattern map for horizontal flow in Figure 5.1. The three lowest mass fluxes, 277 kg/m<sup>2</sup>s, 434 kg/m<sup>2</sup>s and 520 kg/m<sup>2</sup>s (57 lb<sub>m</sub>/ft<sup>2</sup>·s, 89 lb<sub>m</sub>/ft<sup>2</sup>·s and 108 lb<sub>m</sub>/ft<sup>2</sup>·s), all showed a transition from slug flow to annular flow at an approximate quality of 25 percent.

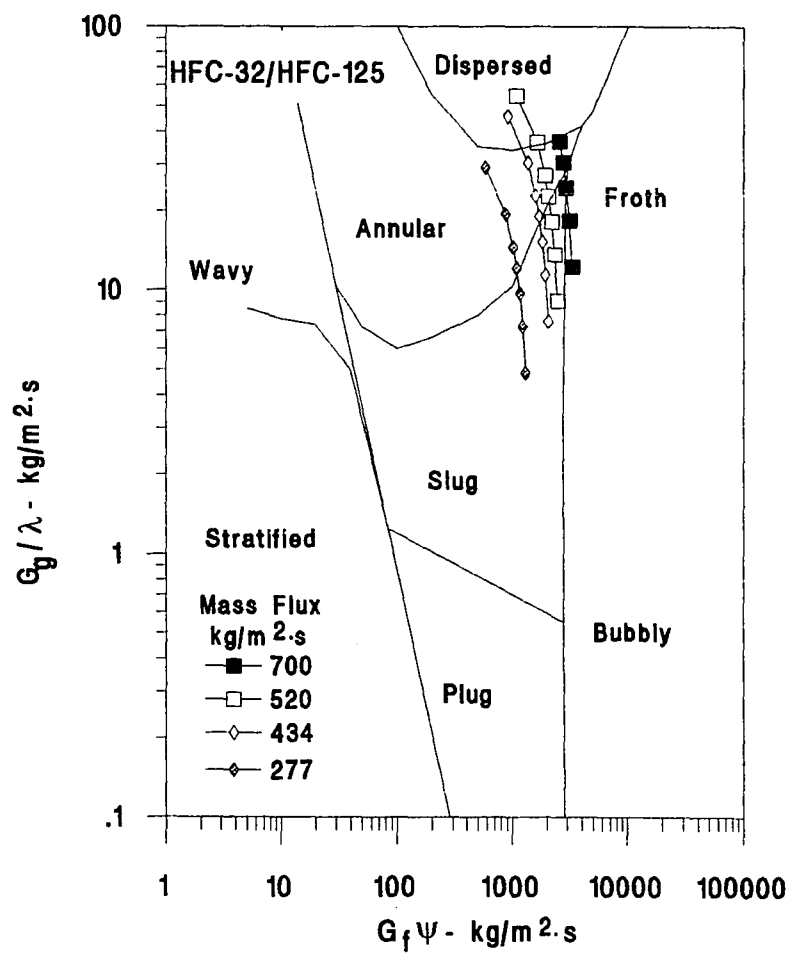


Figure 5.1 Flow Pattern Map for HFC-32/HFC-125 [Baker. 1954].

Dispersed flow is usually considered a subset of annular flow. The case of 434 kg/m<sup>2</sup>s and 520 kg/m<sup>2</sup>s mass fluxes showed a transition into the dispersed flow pattern between the qualities of 40 and 60 percent, respectively. The flow map would indicate that the highest mass flux, 700 kg/m<sup>2</sup>s (143 lb<sub>m</sub>/ft<sup>2</sup>·s), would have a transition from a froth flow pattern to an annular flow pattern at a quality of 23 percent. The flow patterns predicted from the Baker map and the transition from nucleate dominated boiling to convective dominated boiling shown in the preceding graph were from 10 to 30 percent for all but one case. The dominant heat transfer mechanism was thought to be governed by the flow pattern as well.

The Baker flow map showed the effect of quality and mass flux indicated the flow pattern. An expanded view of the Baker flow map is shown in Figure 5.2. Lines of constant quality were shown along with the data. The constant quality lines were parallel to the slug - annular transition. The experimental data were also shown in Figure 5.2. The constant quality lines indicated that for all qualities below 25 percent and mass fluxes below 600 kg/m<sup>2</sup>·s, the flow pattern should be slug, plug or stratified.

The flow pattern map for horizontal flow presented by Taitel and Dukler [1976] was shown in Figure 5.3 along with the superposed experimental data. This flow pattern map used the Martinelli parameter as the x-axis variable and a trio of calculated variables to distinguish between the various transition boundaries. Two of these variables showed that the only transitions possible were those from wavy/annular, wavy/intermittent, annular/bubbly or annular intermittent. These flow patterns could all be distinguished from the third variable,  $F_{td}$  (Equation 5.5),

$$F_{td} = \left( \frac{\rho_g}{\rho_f - \rho_g} \right)^{0.5} \frac{j_g}{(D \cdot g \cdot \cos \theta)^{0.5}} \quad (5.5)$$

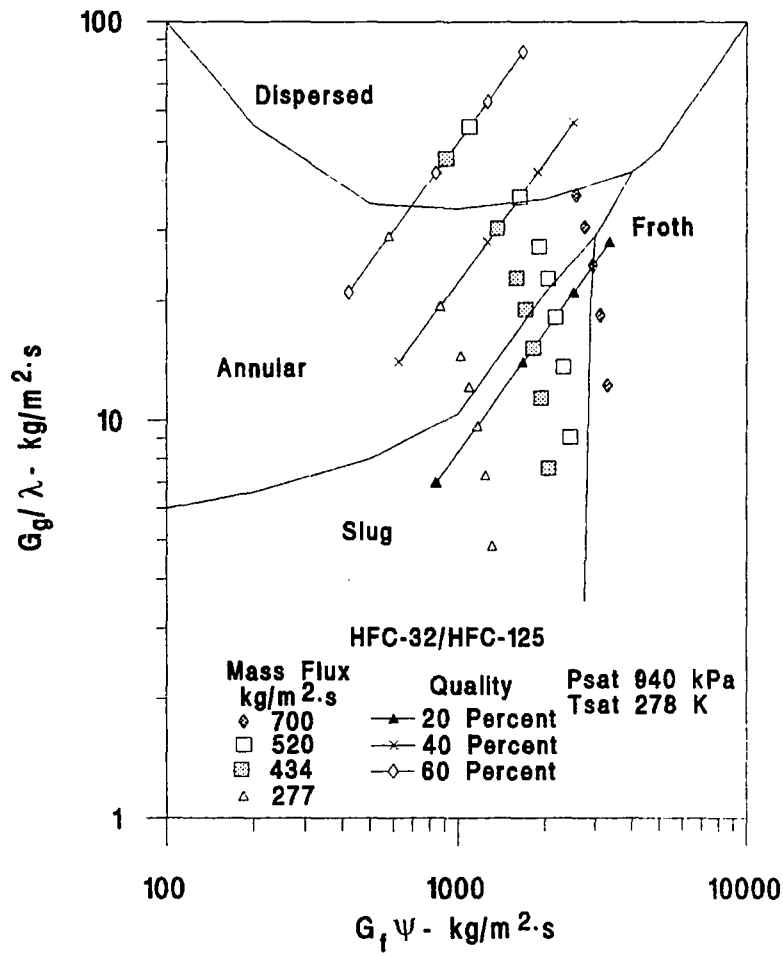


Figure 5.2 Flow Pattern Map for HFC-32/HFC-125 [Baker, 1954] with Constant Quality.

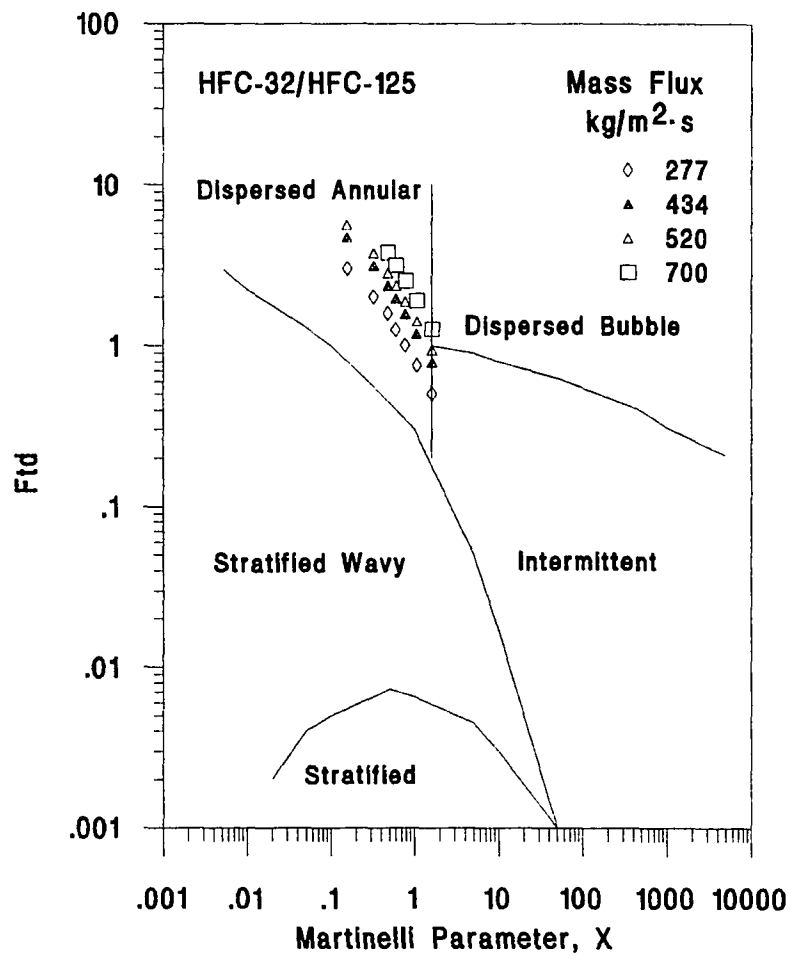


Figure 5.3 Flow Pattern Map for an HFC-32/HFC-125 Mixture [Taitel and Dukler, 1976].

and the Martinelli parameter. The  $j_g$  term represented a vapor volumetric flux. The value of  $F_{td}$  was calculated for each mass flux studied at the appropriate qualities and graphed on the flow pattern map shown in Figure 5.3. All of the data fell in the annular flow pattern except that data representing a quality of 10 percent. All the data at 10 percent fell on the boundary between annular flow and either bubbly or intermittent flow. This calculated flow pattern from this map was also independent of heat flux.

The flow pattern determined from the flow pattern maps shown in Figures 5.1 and 5.3 were not identical. The Baker flow map showed that the refrigerant should have a slug flow pattern at qualities below 25 % and annular flow pattern at higher qualities. The Baker flow map showed that a mass flux of  $700 \text{ kg/m}^2\cdot\text{s}$  was in a froth flow pattern at low qualities. The Taitel and Dukler flow pattern map showed that the flow should be annular for all qualities above 10 percent and was intermittent at all flow rates at 10 percent quality. No visual tests were performed to validate either model, but the heat transfer results appeared to support the Baker flow map better than the Taitel and Dukler flow map.

#### THE EFFECT OF MASS FLUX ON PRESSURE DROP

The pressure drop and convective coefficient are both important factors in choosing an air-conditioner working fluid. Accurate prediction of the pressure drop of a two-phase refrigerant boiling in an evaporator coil would be needed for good air-conditioner design. The pressure drop was measured and the effect of heat flux, mass flux and quality were quantified. The nature of the experimental measurements did influence the pressure drop slightly. The pressure drops in the following figures are for the average quality in the test section. The pressure drops shown for low mass fluxes and high heat fluxes represented a higher quality change across the test section than the cases of high mass flux or low heat flux. The pressure drops were reported as pressure drop per unit length,  $\Delta P/\Delta L$  in units of kPa/m. The test section length was the



same for all of the data. The pressure drop per unit length simply represented the measured pressure drop divided by the length of the test section.

The pressure drop per unit length was shown for different cases of mass flux with the same heat flux. In Figure 5.4, the pressure drop per unit length was shown for a heat flux of  $5100 \text{ W/m}^2$  ( $1617 \text{ Btu/hr}\cdot\text{ft}^2$ ) and mass fluxes of  $277 \text{ kg/m}^2\cdot\text{s}$ ,  $520 \text{ kg/m}^2\cdot\text{s}$  and  $700 \text{ kg/m}^2\cdot\text{s}$  ( $57 \text{ lb}_m/\text{ft}^2\cdot\text{s}$ ,  $108 \text{ lb}_m/\text{ft}^2\cdot\text{s}$  and  $143 \text{ lb}_m/\text{ft}^2\cdot\text{s}$ ). The pressure drop per unit length varied almost linearly for each mass flux shown. The pressure drop per unit length was higher for higher mass fluxes because of the increased frictional pressure drop. The slope of the three curves increased with increasing mass flux.

In Figure 5.5, the effect of mass flux can be seen for data representing a heat flux of  $11000 \text{ W/m}^2$  ( $3488 \text{ Btu/hr}\cdot\text{ft}^2$ ). This was the highest heat flux investigated. There were three mass fluxes shown on this figure. The same general trends were noted. The pressure drop per unit length at a given quality was higher and the slope was steeper for the curves representing higher mass fluxes. The same trends were noted for the data taken at a heat flux of  $7100 \text{ W/m}^2$  ( $2251 \text{ Btu/hr}\cdot\text{ft}^2$ ).

#### THE EFFECT OF HEAT FLUX ON PRESSURE DROP

The effect of heat flux on pressure drop was not nearly so pronounced. As shown in Figure 5.6, for a mass flux of  $520 \text{ kg/m}^2\cdot\text{s}$  ( $108 \text{ lb}_m/\text{ft}^2\cdot\text{s}$ ), the difference between the pressure drop for the lowest and highest heat flux studied was less than 10 percent. The pressure drop per unit length was within 10 percent for all heat fluxes at any given mass flux. The curves in Figure 5.6 had the same slope and the pressure drop per unit length was slightly higher for the lower mass flux. This trend was different for the other mass fluxes.

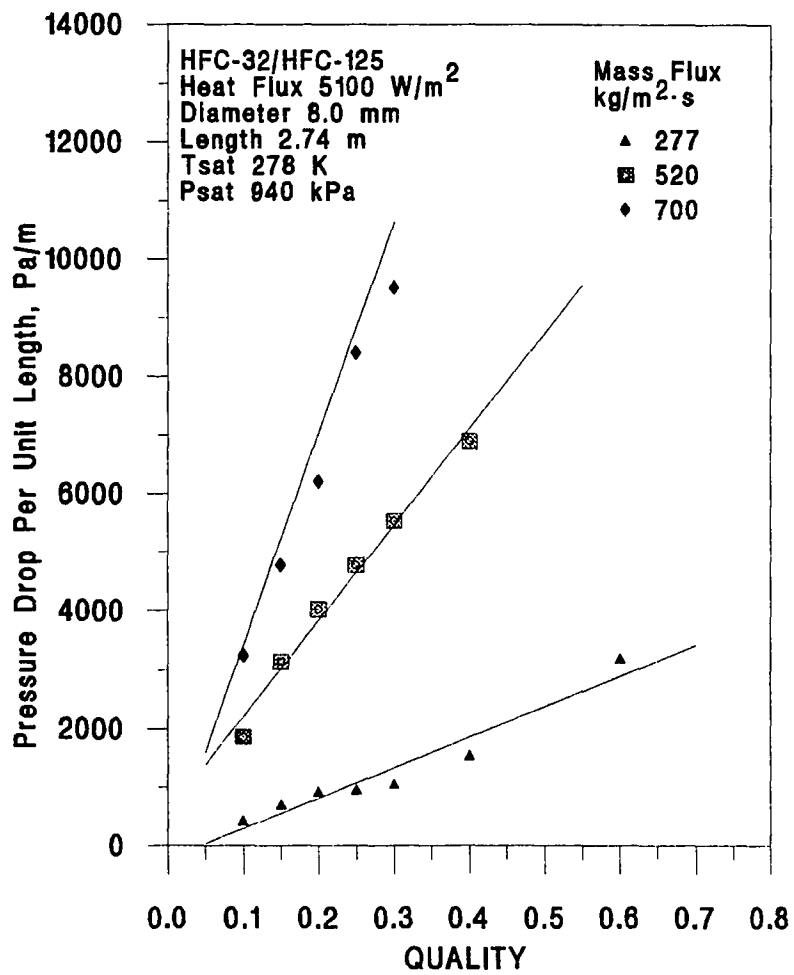


Figure 5.4 Pressure Drop Per Unit Length for Various Mass Fluxes at a Heat Flux of 5100 W/m<sup>2</sup>.

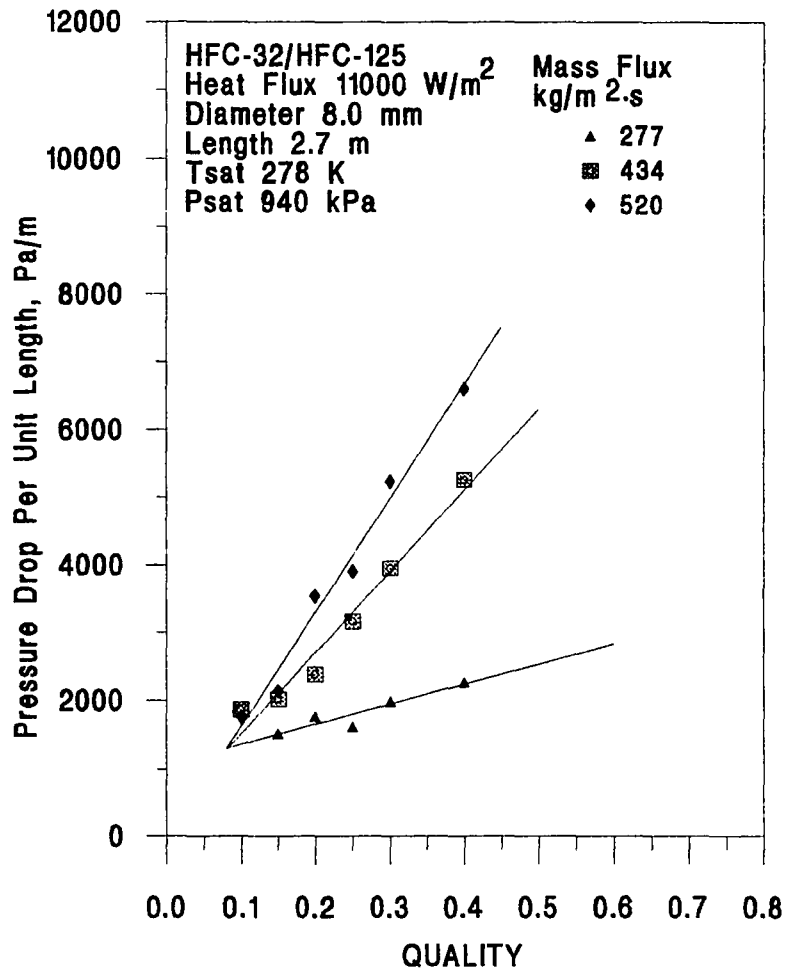


Figure 5.5 Pressure Drop Per Unit Length for Various Mass Fluxes at a Heat Flux of 11000 W/m<sup>2</sup>.

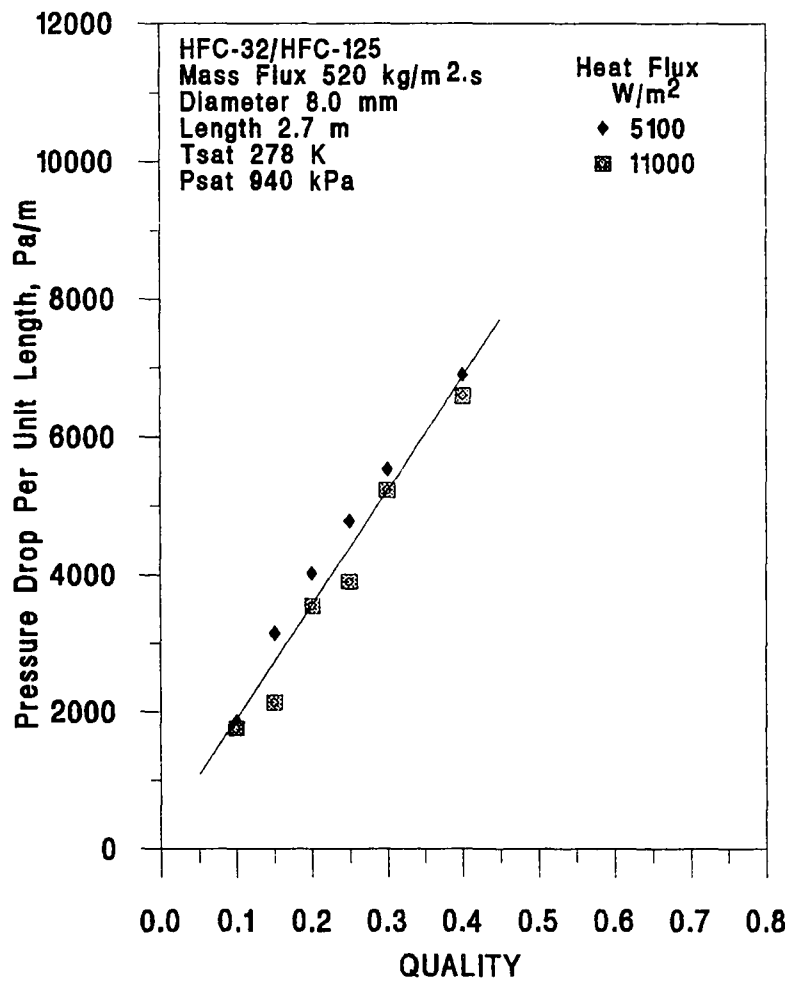


Figure 5.6 Pressure Drop Per Unit Length for Various Heat Fluxes at a Mass Flux of 520 kg/m<sup>2</sup>.s.

The mass flux had a much greater influence on the pressure drop per unit length than the heat flux. Because the same trend was noted for all the other curves showing the pressure drop for different heat fluxes at a given mass flux, they were not included.

#### PRESSURE DROP CORRELATIONS

There were two primary types of pressure drop models. The homogeneous model which assumes two-phase refrigerant flowing as single phase liquid having mean fluid properties determined from the quality, vapor and liquid properties. Separated flow models assume that the refrigerant vapor and liquid phases flow as separate streams in the tubing at constant but not necessarily equal velocities. The separated models should provide better representations of annular flow. The earliest separated flow model was developed by Lockhart and Martinelli [1949]. A version of the separated flow model introduced later by Friedel [1979] was thought to be one of the most accurate models for predicting frictional pressure drop Whalley [1987].

The separate flow model is based upon determining the ratio of two-phase pressure drop to single phase pressure drop or a two-phase multiplier as shown in Equation 5.6. This particular equation is a function of the Martinelli parameter. The two-phase pressure drop is the product of the single-phase pressure drop and the two-phase multiplier as shown in Equation 5.7.

$$\phi_l^2 = 1 + \frac{C}{\chi} + \frac{1}{\chi^2} \quad (5.6)$$

$$\left(\frac{\partial p}{\partial z}\right)_{tp} = \left(\frac{\partial p}{\partial z}\right)_{lo} \phi_{lo} \quad (5.7)$$

The liquid pressure drop is calculated using the Blasius Equation 5.8.

$$-\left(\frac{dP}{dz}\right)_{lo} = \frac{2 f_l G^2}{\rho_l D} \quad (5.8)$$

The Martinelli parameter may be a good universal variable to calculate the two-phase multiplier, but it is a function of quality, liquid and vapor viscosity and liquid and vapor density. All of the experiments with HFC-32/HFC-125 were performed at five degrees Celsius so the viscosities and densities were constant. The constant,  $C$ , used in Equation 5.6 is based upon the Reynolds number of the respective liquid and vapor phases. The Reynolds numbers in each phase were less than 15000. The constant was modified. The best fit was achieved with a value of  $C = 10.4$ . The two-phase pressure drop was divided by the calculated single-phase pressure drop and plotted against quality (Figure 5.7). The modified two phase multiplier is given by:

$$\phi_1^2 = 1 + \frac{10.4}{\chi} + \frac{1}{\chi^2} \quad (5.9)$$

Using Equation 5.9, the absolute mean error was 405 kPa/m or 11 percent error. The absolute mean error using the Separate flow model is 73% and the error with the Friedel method is 16%. The pressure drop per unit length for the data and the predicted pressure drop using the homogeneous model, the Martinelli model, the Friedel model and the proposed pressure drop calculated from Equations 5.8 and 5.9 are shown in Figure 5.8. The error lines bracketed the predicted values that fell within 30 percent of the experimental values. The pressure drop per unit length predicted by the homogeneous model was always lower than the actual pressure drop per unit length and was as low as 30 percent of the measured pressure drop per unit length. The pressure drop per unit length predicted using the Martinelli separate flow model was always higher than the measured values. The separated flow model pressure drop correlation by Friedel was more accurate for use with HFC-32/HFC-125 than the homogeneous and Martinelli technique.

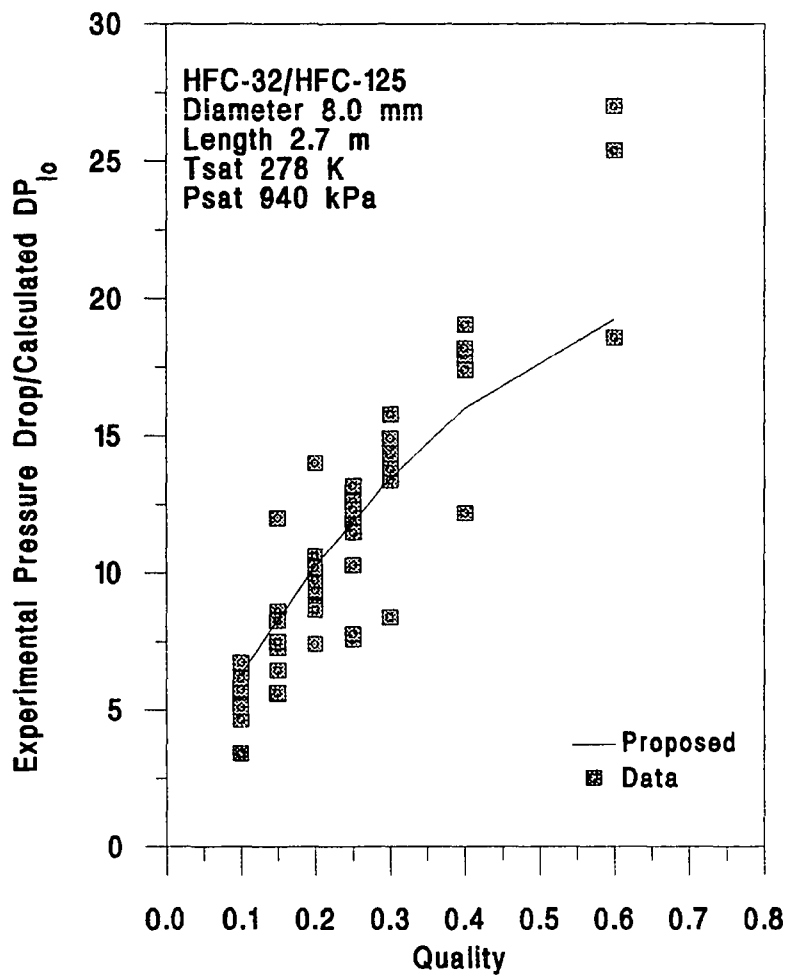


Figure 5.7 The Ratio of Two-Phase Pressure Drop to Single-Phase Pressure Drop.

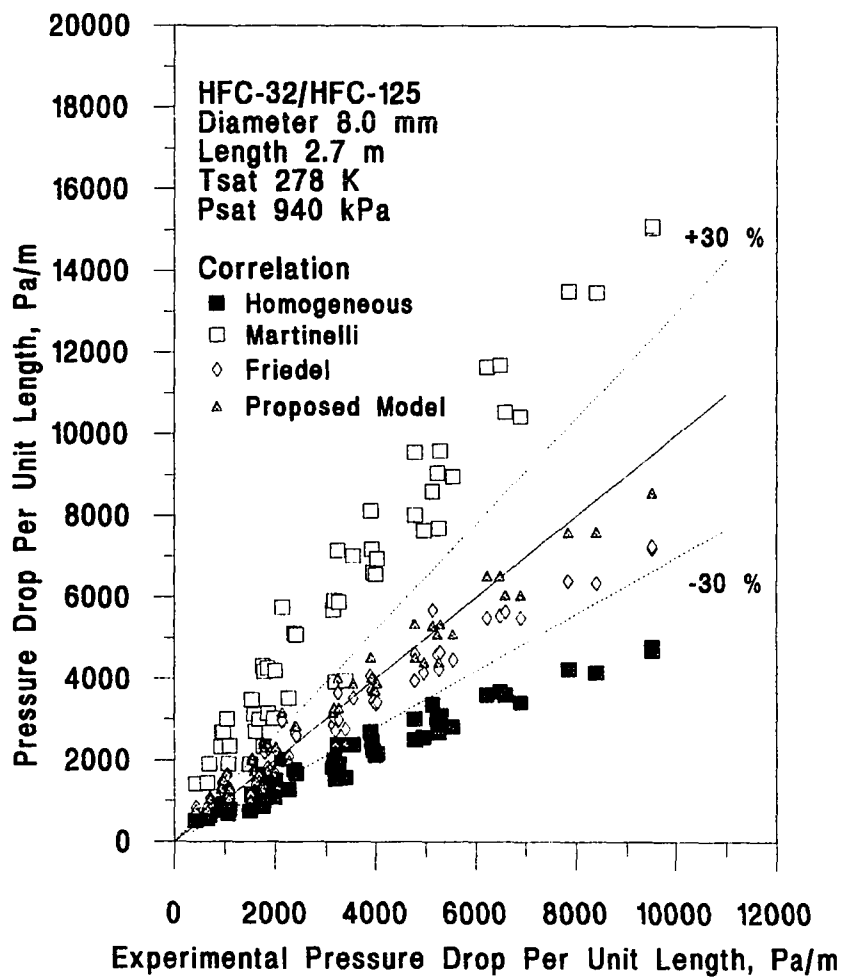


Figure 5.8 A Comparison of Experimental Pressure Drop with Predicted Pressure Drop.



The predicted values for the pressure drop correlation by Friedel tended to be less accurate at the higher pressure drops. Using the proposed changes shown in Equation 5.9, the pressure drop per unit length was predicted more accurately over the data studied. All but one of the predicted values of pressure drop per unit length fell within the 30 percent error lines.

Figure 5.9 showed the correlation of the experimental pressure drop divided by the pressure drop that would be present if there was only liquid flowing in the tubing at the same mass rate as the two-phase mixture. The calculation of single-phase pressure drop is considerably more accurate than the calculation of two-phase pressure drop. The pressure ratio, which is equivalent to the two-phase multiplier was graphed against the reciprocal of the Martinelli parameter. Chisholm [1967] originally correlated the inverse of the Martinelli parameter to the two-phase multiplier as shown in Equation 5.6. The graph showed a band of curves increasing with a decreasing Martinelli parameter. The decreasing Martinelli parameter was equivalent to an increasing quality. The data appeared to loosely band together by mass fluxes. The pressure ratio predicted using the Martinelli technique and the proposed Equation 5.9 are also shown in Figure 5.9. The Martinelli technique consistently over predicts the pressure drop ratio while the proposed technique provides for a better approximation of the data.

#### THE EFFECT OF MASS FLUX ON HEAT TRANSFER COEFFICIENT

The experiments in this study allowed the calculation of an average convective coefficient over a narrow range of quality. Many investigators, Kubanek and Miletti [1979], Anderson et al [1966], Wattlet et al [1994], and Hambræus [1991], reported an average coefficient that represented a constant inlet quality and a varying exit quality determined from the heat flux, mass flux and enthalpy of vaporization.

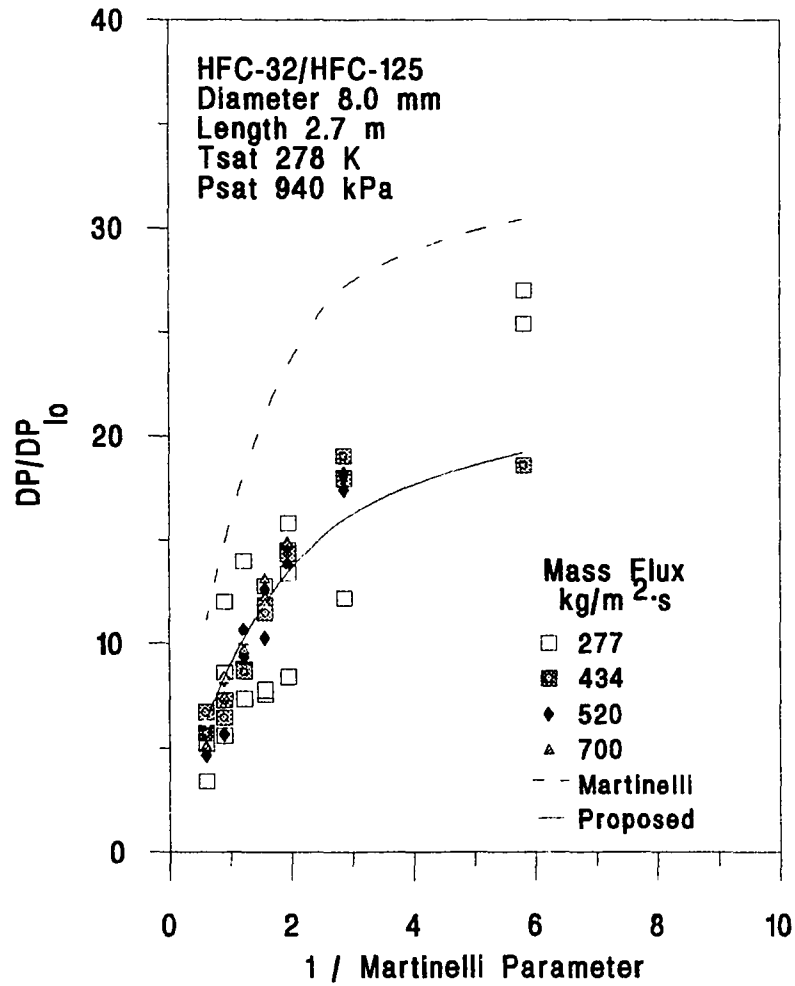


Figure 5.9 The Ratio of Two-phase Pressure Drop to the Predicted Single-phase Pressure Drop Flowing at the Same Mass Rate as the Two-phase mixture.

These studies sometimes reported a convective coefficient averaged over 60 percent range of quality. Other investigators, Ross et al [1987], Lavin and Young [1965] and Chaddock [1986], reported a local coefficient where the convective coefficient was determined from a single wall temperature measurement. The data represented herein comes from averaging the thermocouple data and calculating a representative convective coefficient over the entire test section.

The experiments in this research differed from many of the previous approaches in that the average convective coefficient was calculated over a quality change where the inlet quality was chosen as the value necessary to achieve the desired quality averaged over the test section. This means that the largest possible quality change occurred for the highest heat flux and lowest mass flux. The largest value of quality change over the test section was 27 percent. Most of the tests represented quality spans of less than 15 percent.

A small amount of literature was available that compared the local convective coefficient at a given quality for constant heat flux but examining the change in mass flux. One noted exception was the published work by Khanpara, Pate and Bergles [1988], where the convective coefficient of HCFC-22 and CFC-113 for mass fluxes and heat fluxes similar to the ones in this study were shown on the same graph. Their results show convective coefficients that did not change more than 15 percent over qualities ranging from 0 to 80 percent for any individual combination of heat flux or mass flux. These results were inconsistent with the evaporation theory and experimental work published by many others such as Riedle and Purcupile [1973], Murata and Hashizume [1990], Kandlikar [1988], Ross et al [1987], Kubanek and Miletti [1979] and Chaddock and Mathur [1980]. The research by Chaddock and Mathur reported two-phase convective coefficients for HCFC-22 over a range of qualities for different mass fluxes at the same heat flux. Their results generally

indicated a decreasing convective coefficient for low qualities and then began increasing until the liquid deficient region started at qualities of approximately 77 percent. The convective coefficient dropped rapidly once the liquid deficient region was reached. The results reported by Chaddock and Mathur were graphed for heat fluxes of  $40 \text{ kW/m}^2$  which were much higher than the highest heat flux used in this study. The effect of nucleate and convective boiling mechanisms, as shown in Figure 5.10, on the local convective coefficients over qualities of 10 to 60 percent should be evident when multiple mass fluxes are graphed with the same heat flux as function of quality. Examining the effect of mass flux on convective coefficients that were averaged over a large quality change would completely overshadow the effect of any individual flow pattern or local mechanism. The theory covering the two-phase flow boiling process has been established for over two decades [Collier, 1982]. The data obtained in this research were thought to be dominated by nucleate boiling and convective forces. The lowest quality entering the test section was 3 percent so there should not have been any subcooled boiling. The highest quality exiting the test section was 68 percent, which should have been too low for the flow pattern to have been liquid deficient or mist flow.

In Figure 5.11, the convective coefficient is shown as a function of quality. The heat flux applied to the test section for these experiments was  $5100 \text{ W/m}^2$ . The three separate curves represented mass fluxes of  $277 \text{ kg/m}^2\text{s}$  ( $57 \text{ lb}_m/\text{ft}^2\cdot\text{s}$ ),  $520 \text{ kg/m}^2\text{s}$  ( $107 \text{ lb}_m/\text{ft}^2\cdot\text{s}$ ) and  $700 \text{ kg/m}^2\text{s}$  ( $143 \text{ lb}_m/\text{ft}^2\cdot\text{s}$ ). The heat flux of  $5100 \text{ W/m}^2$  was the lowest value used in this study. The mass fluxes of  $277 \text{ kg/m}^2\text{s}$  ( $57 \text{ lb}_m/\text{ft}^2\cdot\text{s}$ ) and  $700 \text{ kg/m}^2\text{s}$  ( $143 \text{ lb}_m/\text{ft}^2\cdot\text{s}$ ) were the lowest and highest flow rates respectively. The convective coefficient remained relatively constant for the case of low flow rates and low heat flux.

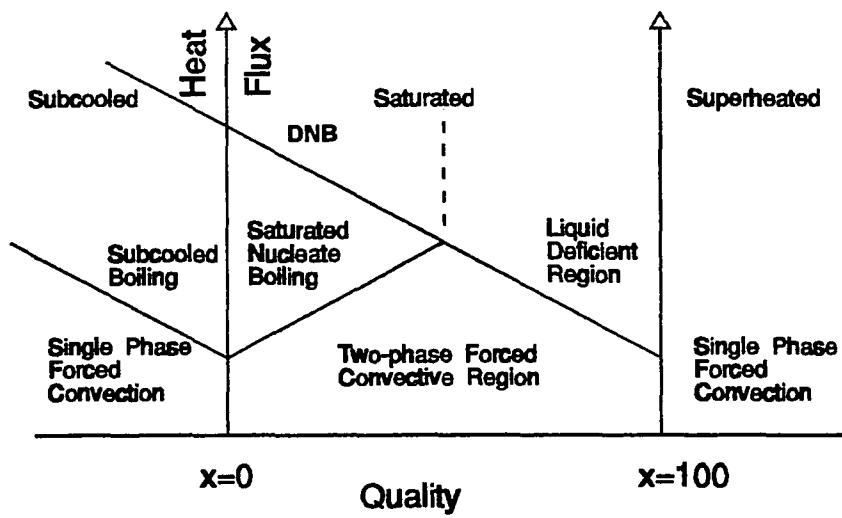


Figure 5.10 Evaporative Heat Transfer (Reprinted with permission) [Collier, 1982]

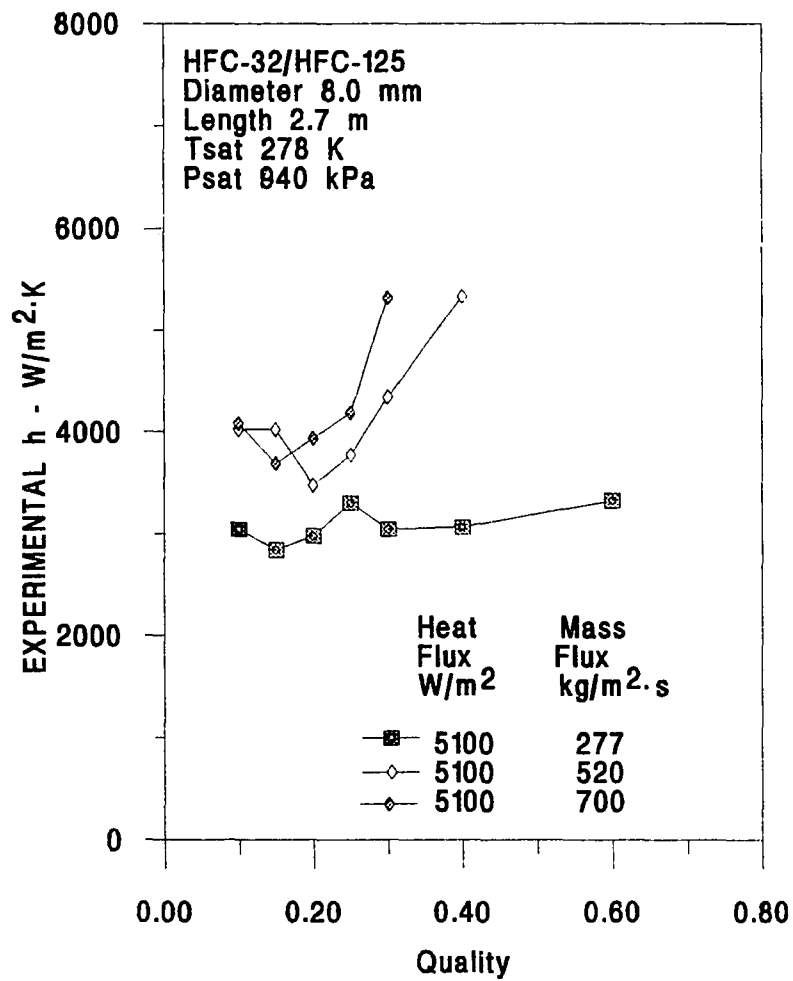


Figure 5.11 The Effect of Mass Flux upon Heat Transfer Coefficient of HFC-32/HFC-125 at a Heat Flux of  $5100 W/m^2$ .

The heat flux was not high enough to generate significant nucleate boiling effects. The mass flux for each curve remained constant but the velocity increased as quality increased because the vapor had lower densities than that of liquid.

Therefore the velocity of the two-phase mixture increased as quality increased for a single mass flux. The increased velocities should result in an increased convective heat transfer and suppression of the nucleate boiling contribution. There does not appear to be any indication of nucleate boiling or increased convective heat transfer flow rate for the data associated with the lowest mass flux ( $277 \text{ kg/m}^2\text{s}$ ) and lowest heat flux ( $5100 \text{ W/m}^2$ ) because the heat transfer coefficient showed little variation with quality. This relatively flat curve in Figure 5.11 looks similar to all of the curves presented by Khanpara, Pate and Bergles [1988]. The other two cases were quite different. The convective coefficient decreased for both cases at low qualities and then increased at higher qualities. The convective coefficient decreased up to a quality of 15 percent for the mass flux of  $700 \text{ kg/m}^2\text{s}$  ( $143 \text{ lb}_m/\text{ft}^2\cdot\text{s}$ ) then increased. The convective coefficient decreased up to a quality of 20 percent for a mass flux of  $520 \text{ kg/m}^2\text{s}$  ( $107 \text{ lb}_m/\text{ft}^2\cdot\text{s}$ ). The data indicated the minimum heat transfer coefficient shifted to lower qualities as the mass flux increased. This supported the underlying theory of higher mass velocities suppressing the nucleate boiling contribution and the convective heat transfer mechanism dominating. The higher mass flux would suppress the nucleate effect at a lower quality as was shown in Figure 5.11. The convective coefficient was higher for the highest mass flux at all qualities above 20 percent. The overall shape of the curves for mass flux of  $700 \text{ kg/m}^2\text{s}$  ( $143 \text{ lb}_m/\text{ft}^2\cdot\text{s}$ ) and  $520 \text{ kg/m}^2\text{s}$  ( $107 \text{ lb}_m/\text{ft}^2\cdot\text{s}$ ) was similar to results presented by Riedle and Purcupile [1973], Kandlikar [1991], Ross et al [1987] and Chaddock and Mathur [1980]. None of the previous authors experimented with a 50/50 mass mixture of HFC-32/HFC-125. Based upon comparison of the data with previous research and current flow boiling

theory, both: nucleate boiling and convective heat transfer appear to be significant for this refrigerant mixture.

A second graph, Figure 5.12, shows the effect of mass flux on heat transfer coefficient for a heat flux of  $7100 \text{ W/m}^2$  ( $2251 \text{ Btu/hr}\cdot\text{ft}^2$ ). This heat flux was 39 percent higher than the heat flux in Figure 5.11. The lowest and highest mass fluxes in Figure 5.12 were the same as in Figure 5.11, but the intermediate mass flux was  $434 \text{ kg/m}^2\text{s}$  ( $89 \text{ lb}_m/\text{ft}^2\cdot\text{s}$ ) as opposed to a mass flux of  $520 \text{ kg/m}^2\text{s}$  ( $108 \text{ lb}_m/\text{ft}^2\cdot\text{s}$ ) in Figure 5.11. The two curves for the low mass flux were both flat. This was the same pattern as noted in Figure 5.11 with the low mass flux case. The convective coefficient for the higher mass flux of  $434 \text{ kg/m}^2\text{s}$  ( $89 \text{ lb}_m/\text{ft}^2\cdot\text{s}$ ) was larger than the convective heat transfer coefficient for the mass flux of  $277 \text{ kg/m}^2\text{s}$  ( $57 \text{ lb}_m/\text{ft}^2\cdot\text{s}$ ). The low mass fluxes and low heat fluxes produced relatively constant convective coefficients, which was the same trend predicted by Khanpara, Pate and Bergles. For the highest mass flux the convective coefficient decreased at low qualities and increased at higher qualities (Figure 5.11). The decrease in heat transfer coefficient at low qualities could be attributed to the suppression of nucleate boiling as the refrigerant velocities increased with quality. The increase at higher qualities would correspond to conditions where the convective heat transfer takes over as the dominant mechanism. The effect of mass fluxes on the convective effects was clear at low qualities when looking at Figure 5.12. At a quality of 10 percent, the convective coefficient was higher at higher mass fluxes. If the convective contribution was negligible, the heat transfer coefficient would be a function of nucleate boiling only and the same for all three cases.

The two previous figures showed the effect of mass flux on convective heat transfer for low and medium heat flux. Figure 5.13 shows the effect of mass flux on heat transfer for a high heat flux. The mass fluxes in this figure were  $277 \text{ kg/m}^2\text{s}$ ,  $434 \text{ kg/m}^2\text{s}$  and  $520 \text{ kg/m}^2\text{s}$  ( $57 \text{ lb}_m/\text{ft}^2\cdot\text{s}$ ,  $89 \text{ lb}_m/\text{ft}^2\cdot\text{s}$  and  $108 \text{ lb}_m/\text{ft}^2\cdot\text{s}$ ). The convective



coefficients decreased at low qualities. This decrease would represent the suppression of nucleation. Higher heat fluxes promoted more nucleate boiling. If the nucleate boiling mechanism was strong enough, the convective coefficient would be independent of the mass flux. The nucleate boiling should dominate the heat transfer at low qualities under these conditions. There was a minimal difference in the convective coefficient for the data shown in Figure 5.13. The curve for a mass flux of  $520 \text{ kg/m}^2\text{s}$  ( $108 \text{ lb}_m/\text{ft}^2\text{s}$ ) was initially higher and flatter than the other two curves. The convective coefficient began to increase at a quality of 30 percent for mass fluxes of  $520 \text{ kg/m}^2\text{s}$  and  $434 \text{ kg/m}^2\text{s}$  ( $108 \text{ lb}_m/\text{ft}^2\text{s}$  and  $89 \text{ lb}_m/\text{ft}^2\text{s}$ ) after initially decreasing. The convective heat transfer decreased for a mass flux of  $277 \text{ kg/m}^2\text{s}$  ( $57 \text{ lb}_m/\text{ft}^2\text{s}$ ) for the entire range of qualities to 40 percent. These trends were generally the same trends reported by Chaddock and Mathur in their experiments with HCFC-22 at a different set of heat fluxes and mass fluxes. In air-conditioner use the refrigerant usually enters the evaporator at qualities near 20 percent. In Figure 5.13, the nucleate boiling effect could dominate the heat transfer near the entrance of the evaporator if the mass flux was below  $434 \text{ kg/m}^2\text{s}$  ( $89 \text{ lb}_m/\text{ft}^2\text{s}$ ).

#### THE EFFECT OF HEAT FLUX ON HEAT TRANSFER COEFFICIENT

The effect of heat flux on boiling the heat transfer mechanism was shown in Figure 5.10. The data in this study were all between qualities of one and 100 percent on the abscissa and heat fluxes below departure from nucleate boiling (DNB) or dryout. The data all fell in the saturated nucleate boiling and two-phase forced convection dominated region.

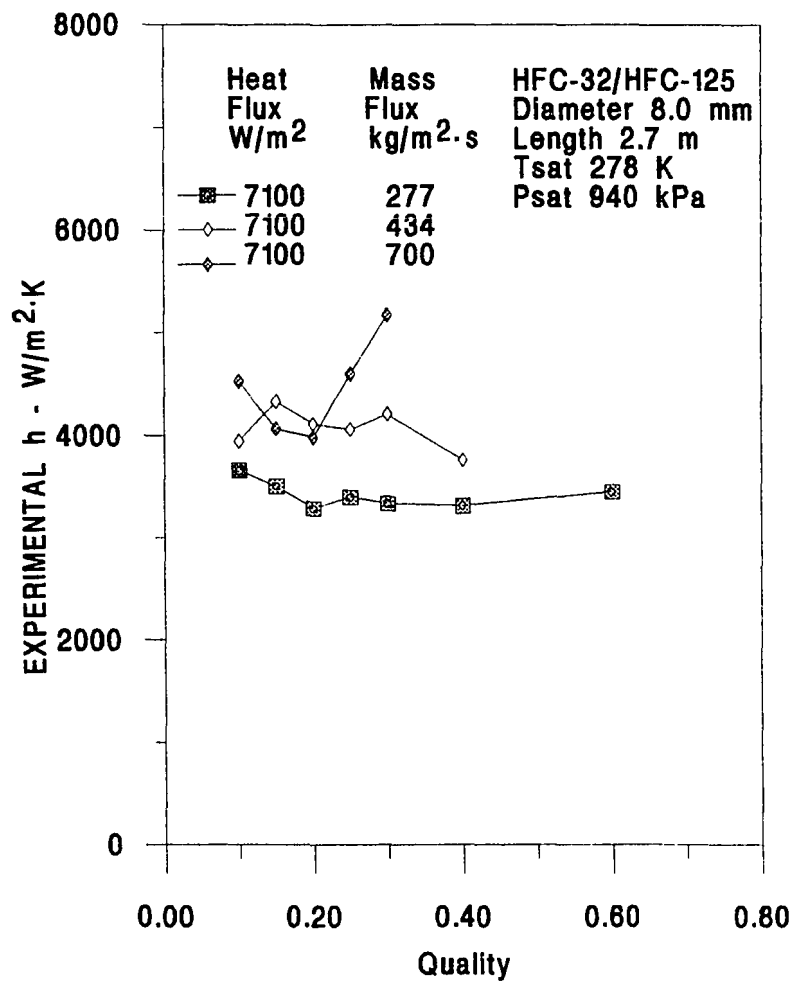


Figure 5.12 The Effect of Mass Flux upon Heat Transfer Coefficient of HFC-32/HFC-125 at a Heat Flux of 7100 W/m<sup>2</sup>.

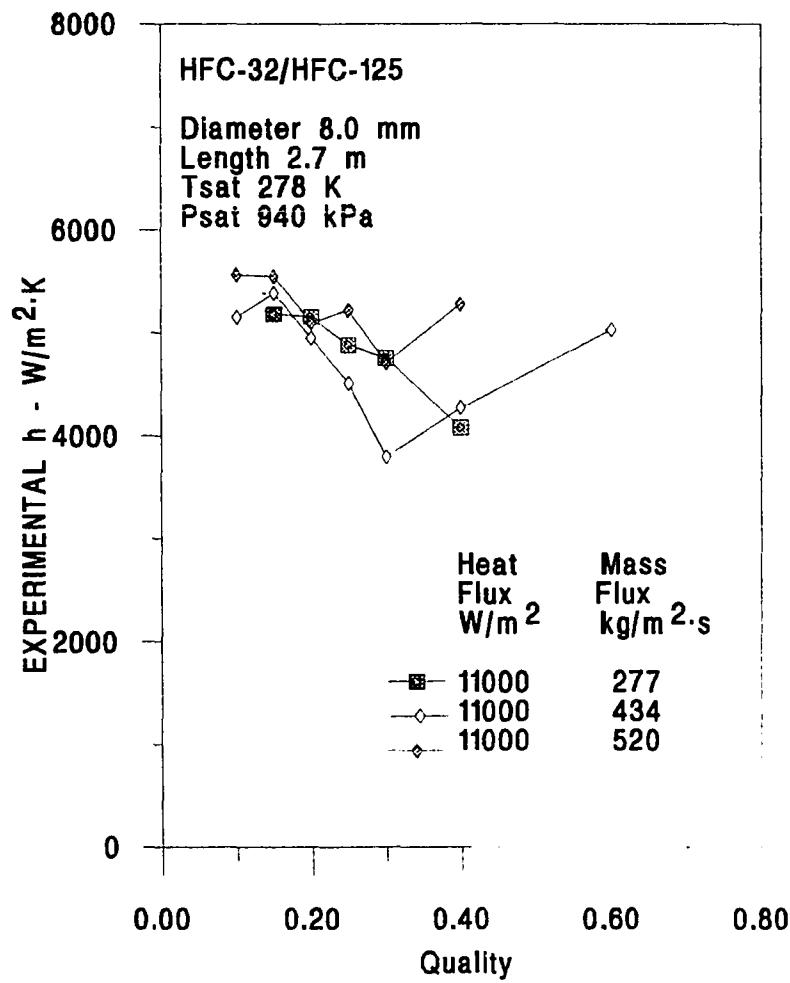


Figure 5.13 The Effect of Mass Flux upon Heat Transfer Coefficient of HFC-32/HFC-125 at a Heat Flux of 11000 W/m<sup>2</sup>.

While Figure 5.10 indicates an immediate transition from saturated nucleate boiling to two-phase forced convective boiling, the graphs showing the effect of mass flux or heat flux upon the heat transfer coefficient indicate that the distinction between nucleate boiling and convective heat transfer is transitional. The results of this study further show that this boundary was dependent upon mass flux and heat flux for the HFC-32/HFC-125 mixture in the given experimental apparatus.

Other researchers have investigated the effect of heat flux on the local heat transfer coefficient. Experimental investigations most relevant to this study were written by Ross et al [1987], Chaddock and Mathur [1980], Khanpara, Pate and Bergles [1986] and Mathur and Hashizume [1983].

The research presented by Khanpara, Pate and Bergles [1986] showed a flat trend for convective coefficient with increasing quality for a given heat flux and mass flux for refrigerants HCFC-22 and CFC-113 and mass fluxes and heat fluxes similar to the ones used in this study. Mathur and Hashizume [1983] showed a flat or increasing trend for the entire range of qualities using CFC-11 and CFC-114. The general increasing of heat transfer coefficient over a range of qualities was associated with forced convective dominated heat transfer. Neither of these two studies showed any indication of a nucleate boiling dominated heat transfer. The effect of increased heat flux was that of simply shifting the heat transfer coefficient higher for all cases. The research by Chaddock and Mathur [1980] and Ross et al [1987] showed a much different trend. Chaddock and Mathur [1980] showed a gradual increase in convective coefficient for increasing quality with low heat fluxes and also showed a decrease, then an increase for progressive values of quality with high heat fluxes. This same trend was observed by Ross et al [1987]. They also observed that the convective coefficients

merge together at high heat fluxes and moderate qualities. This trend was indicative of fully suppressed nucleate boiling.

The effect of heat flux on the convective coefficient is shown in Figures 5.14 through 5.17. Figure 5.14 shows convective coefficient for qualities between 10 and 60 percent for a mass flux of  $277 \text{ kg/m}^2\text{s}$  ( $57 \text{ lb}_m/\text{ft}^2\text{s}$ ) and heat fluxes of  $5100 \text{ W/m}^2$ ,  $7100 \text{ W/m}^2$  and  $11000 \text{ W/m}^2$  ( $1617 \text{ Btu/hr}\cdot\text{ft}^2$ ,  $2251 \text{ Btu/hr}\cdot\text{ft}^2$  and  $3488 \text{ Btu/hr}\cdot\text{ft}^2$ , respectively). This mass flux,  $277 \text{ kg/m}^2\text{s}$  ( $57 \text{ lb}_m/\text{ft}^2\text{s}$ ), was the lowest mass flux examined in this study.

The curves representing the two lowest heat fluxes showed little change as a function of quality. Of these two, the convective coefficient was higher for the higher heat flux. The average heat transfer coefficient for a heat flux of  $7100 \text{ W/m}^2$  ( $2251 \text{ Btu/hr}\cdot\text{ft}^2$ ) was  $3422 \text{ W/m}^2\text{K}$  ( $603 \text{ Btu/hr}\cdot\text{ft}^2\cdot\text{OR}$ ), which was 11 percent higher than the average heat transfer coefficient ( $3087 \text{ W/m}^2\text{K}$   $544 \text{ Btu/hr}\cdot\text{ft}^2\cdot\text{OR}$ ) for the  $5100 \text{ W/m}^2$  ( $1617 \text{ Btu/hr}\cdot\text{ft}^2$ ) heat flux. Constant convective coefficients for the higher heat fluxes were shown by Chaddock and Mathur [1980], Khanpara, Pate and Bergles [1986] and Mathur and Hashizume [1983]. The curve for the highest heat flux,  $11000 \text{ W/m}^2$  ( $3488 \text{ Btu/hr}\cdot\text{ft}^2$ ) sloped downward even to the highest quality (40 percent). The convective coefficient for the high heat flux case averaged 30 percent higher than, either the  $5100 \text{ W/m}^2$  or  $7100 \text{ W/m}^2$  curves. Results published by Ross et al [1987] and Chaddock and Mathur [1980] show this type of decreasing convective coefficient for high heat fluxes. One explanation might be that the nucleate boiling contribution was suppressed over the quality range between 15 and 40 percent as shown by Chen [1966] and explained in Chapter 2.

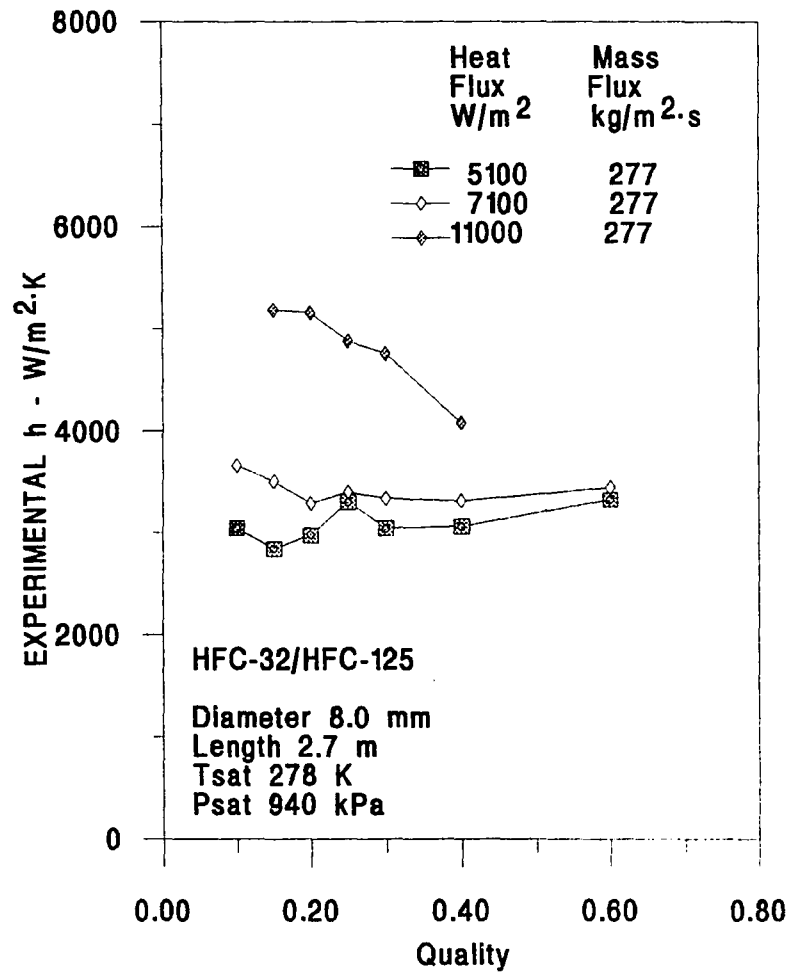


Figure 5.14 The Effect of Heat Flux upon Heat Transfer Coefficient of HFC-32/HFC-125 at a Mass Flux of  $277 \text{ kg/m}^2 \cdot \text{s}$ .

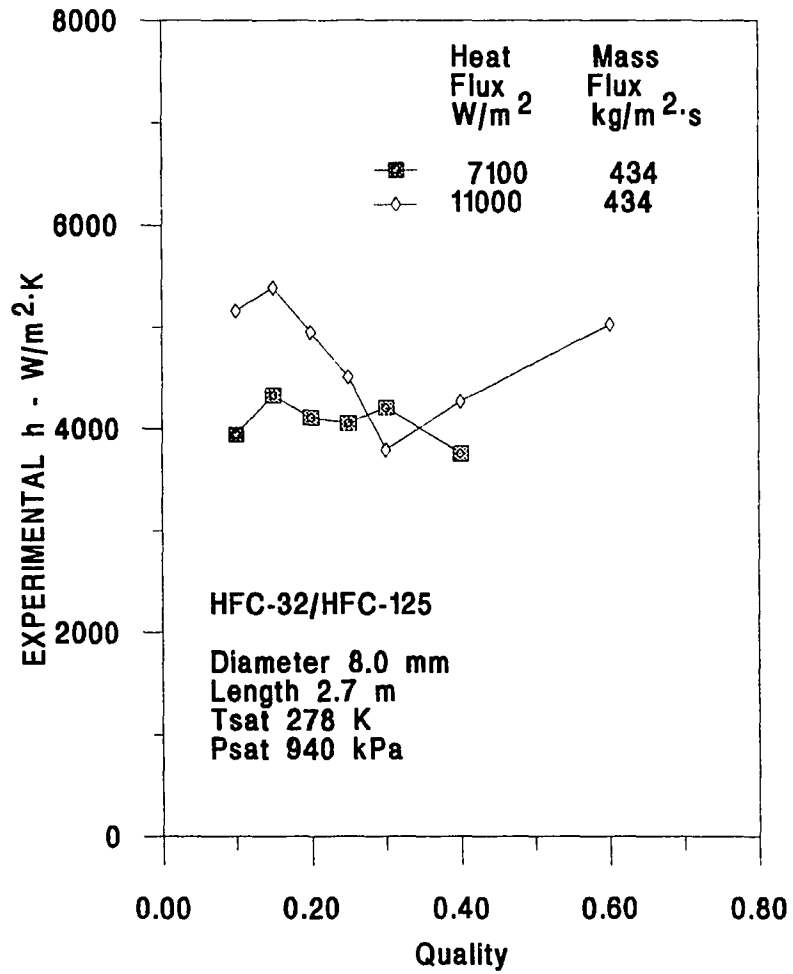


Figure 5.15 The Effect of Heat Flux upon Heat Transfer Coefficient of HFC-32/HFC-125 at a Mass Flux of  $434 \text{ kg/m}^2 \cdot \text{s}$ .

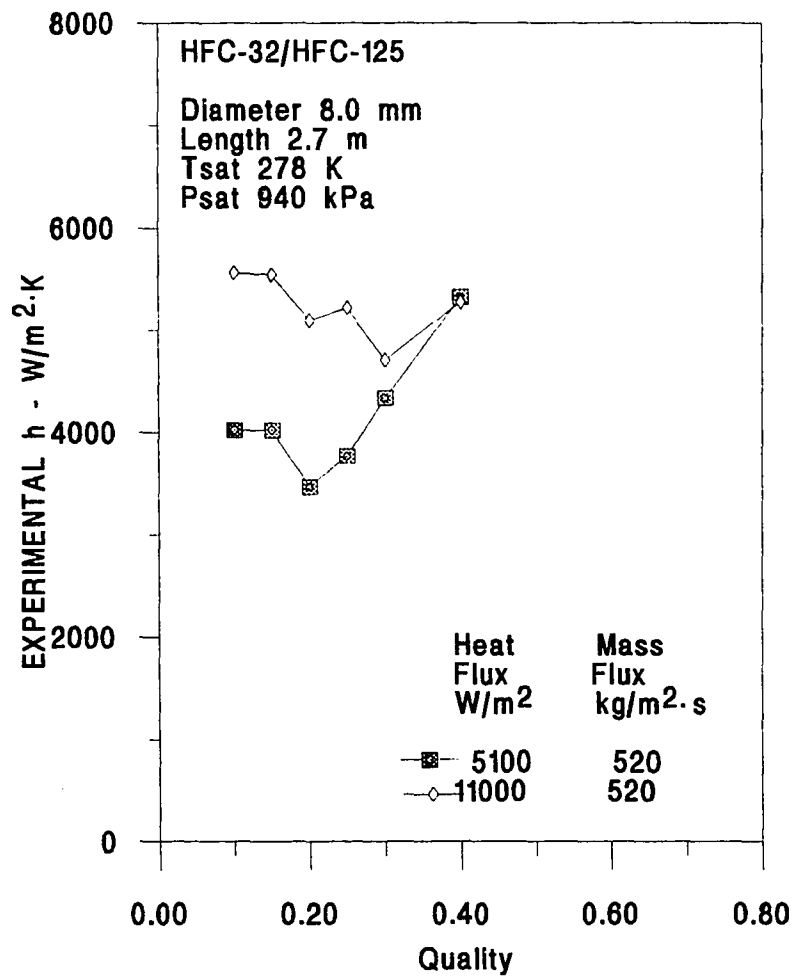


Figure 5.16 The Effect of Heat Flux upon Heat Transfer Coefficient of HFC-32/HFC-125 at a Mass Flux of 520 kg/m<sup>2</sup>·s.



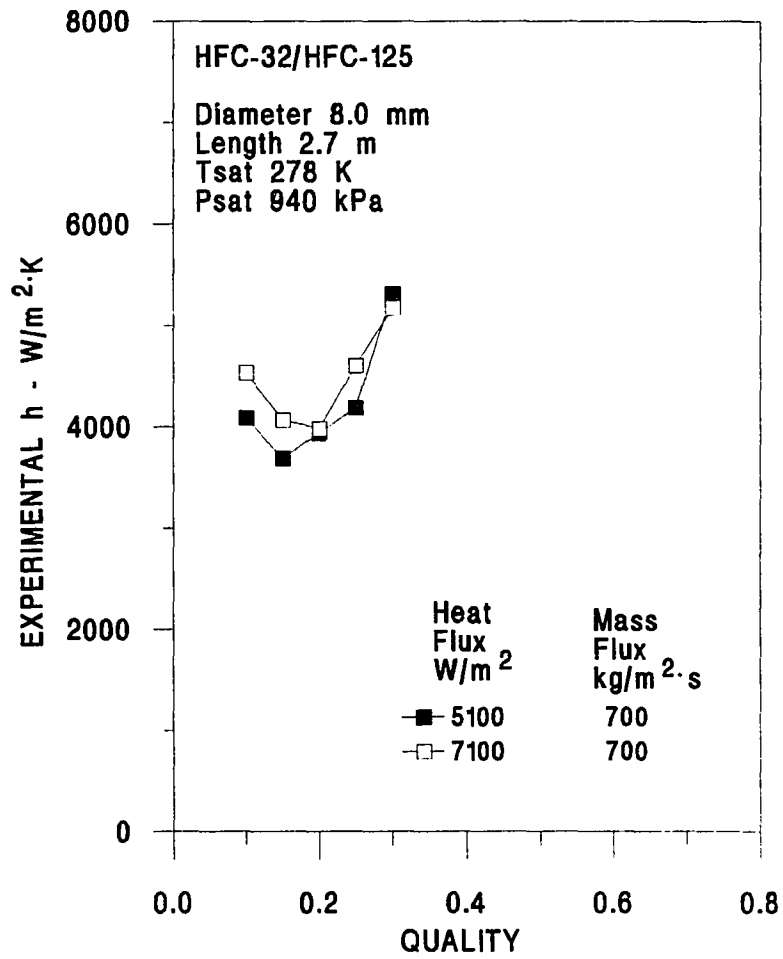


Figure 5.17 The Effect of Heat Flux upon Heat Transfer Coefficient of HFC-32/HFC-125 at a Mass Flux of 700 kg/m<sup>2</sup>·s.

Figure 5.15 showed the convective coefficient for two cases, both having a mass flux of  $434 \text{ kg/m}^2\text{s}$  ( $89 \text{ lb}_m/\text{ft}^2\cdot\text{s}$ ). The mass flux in this figure was 57 percent higher than the mass flux shown in the Figure 5.14. The two cases shown in Figure 5.15 differ in that one curve represents a heat flux of  $7100 \text{ W/m}^2$  ( $2251 \text{ Btu/hr}\cdot\text{ft}^2$ ) and the other represents  $11000 \text{ W/m}^2$  ( $3488 \text{ Btu/hr}\cdot\text{ft}^2$ ). These heat fluxes were equivalent to the two highest heat fluxes in Figure 5.14. The curve representing the lowest heat flux showed little dependency upon quality. The curve representing the higher heat flux, which was the highest heat flux tested in this study, showed a minimum heat transfer coefficient at 30 percent quality. The heat transfer coefficient increased at qualities higher than 30 percent while the lower heat flux did not. This would indicate that fully suppressed nucleate boiling [FSNB] or completely suppressed nucleation did not occur for the data subjected to a heat flux of  $11000 \text{ W/m}^2$  ( $3488 \text{ Btu/hr}\cdot\text{ft}^2$ ). If fully suppressed nucleate boiling had occurred, then the two curves would have overlaid each other after the initial separation at low qualities. This trend would suggest that the convective and nucleate heat transfer mechanisms both contributed to the heat transfer throughout the range of conditions in Figure 5.15. The curves did cross over at a quality of 30 percent. This point was where the convective coefficient was the lowest for the curve representing the higher heat flux.

Figure 5.16 shows the effect of heat flux on the convective coefficient for a mass flux of  $520 \text{ kg/m}^2\text{s}$  ( $108 \text{ lb}_m/\text{ft}^2\cdot\text{s}$ ). This mass flux was 20 percent higher than the mass flux in Figure 5.15 and 87 percent higher than the heat flux in Figure 5.14. The heat fluxes in Figure 5.16 were the lowest and highest heat fluxes measured in this research, respectively. Data were recorded for qualities ranging from 10 percent to 40 percent. The convective heat transfer coefficient for the low heat flux case had a minimum heat transfer coefficient at 20% quality. The curve representing the lower heat flux,  $5100 \text{ W/m}^2$  ( $1617 \text{ Btu/hr}\cdot\text{ft}^2$ ) had a much different shape than the curve for

11000 W/m<sup>2</sup> (3488 Btu/hr-ft<sup>2</sup>). The convective coefficient was much lower for all qualities except at 40 percent. At qualities of 10 and 15 percent, the convective coefficient for the heat flux of 11000 W/m<sup>2</sup> (3488 Btu/hr-ft<sup>2</sup>) was 38 percent higher than the convective coefficient for the lower heat flux. The convective coefficients were the same at a quality of 40 percent. The heat flux was 115 percent higher.

The convective coefficient declined 10 percent and then rose steeply for the lower heat flux case. The transition quality where the slope of the convective coefficient changed from negative to positive was 20 percent. According to the additive convective heat transfer model, the forced convective forces should dominate at lower qualities when there is a small nucleate boiling contribution. The curve representing the higher heat flux declined with a smaller slope and showed a small increase as the quality increased from 30 to 40%. The convective coefficient would be expected to be much higher at the low qualities and high heat fluxes because nucleate boiling should be much stronger and influential at those conditions. It would appear that the convective forces began to dominate at a quality of 30 percent, where the slope increased. The point where both convective coefficients were the same could be indicative of fully suppressed nucleate boiling. This suppression was discussed by Ross et al [1987]. Nucleate boiling appeared to be suppressed at lower qualities for the low heat flux case. The lower the heat flux and the higher the mass flux, the easier nucleate boiling could be suppressed. Convective forces should be completely dominant in the region of suppressed nucleate boiling.

Figure 5.17 shows the effect of heat flux on the convective coefficient for a mass flux of 700 kg/m<sup>2</sup>s (143 lb<sub>m</sub>/ft<sup>2</sup>·s). This was the highest mass flux in this study. The heat fluxes were 5100 W/m<sup>2</sup> and 7100 W/m<sup>2</sup> (1617 Btu/hr-ft<sup>2</sup> and 2251 Btu/hr-ft<sup>2</sup>). These were the two lowest heat fluxes examined in this study. The

information shown represents the highest mass flux and the lowest heat fluxes. Both curves have the same shape. They both exhibited declining then increasing convective coefficients. The convective coefficients were probably higher for the higher heat flux case at low qualities due to an increased nucleate boiling contribution. The convective coefficient for the lower heat flux case began to increase at a quality of approximately 15 percent versus 20 percent for the higher heat flux case. The lower the heat flux, the lower the quality at which convective forces began to dominate.

#### SUMMARY

The pressure dropped more at higher mass fluxes due to the increased frictional forces. Heat flux only slightly influenced the pressure drop. A modification of an existing pressure drop correlation was proposed and used with increased accuracy.

The convective coefficient increased at higher heat fluxes over almost all of the qualities. The convective coefficient varied a small amount with quality at low mass fluxes and low heat fluxes. The convective coefficient declined and then increased for the majority of the heat flux and mass flux combinations studied.

The convective coefficient began increasing at lower qualities where the heat flux was lower and the mass flux was higher. The nucleate boiling effect was significant at lower qualities and contributed to wide differences in the convective coefficient for cases with different heat fluxes and the same mass flux.

Two separate flow pattern maps were shown, one by Baker [1954], the other by Taitel and Dukler [1976]. The flow pattern map by Baker [1954] showed a transition between annular and slug flow occurring at a quality of approximately 20 percent. The flow pattern map by Taitel and Dukler showed that all of the data was dominated by annular flow patterns. The flow pattern maps were independent of heat flux and heat flux clearly affected the convective coefficient.

The pressure drop per unit length was shown for all mass fluxes and heat fluxes in this study. The pressure drop increased almost linearly as quality increased. The slope of this line was dependent upon mass flux. The higher the mass flux the higher the pressure drop per unit change in quality ( $\Delta P/\Delta x$ ). Heat flux had a minimal effect upon pressure drop. The pressure drop was compared to two types of pressure drop prediction models. The models were homogeneous flow and separate flow models. Two separate flow models, one by Lockhart and Martinelli [1949] and the other by Friedel [1979] were used to compare pressure drop. The model by Friedel [1979] was the most accurate. The homogeneous model clearly under predicted the pressure drop and the Martinelli model clearly over predicted the pressure drop.

## CHAPTER VI

### DEVELOPMENT OF A HEAT TRANSFER CORRELATION FOR HFC-32 / HFC-125

Several widely used boiling heat transfer correlations were compared to the experimentally obtained convective coefficients to understand better the heat transfer process taking place in the tube. The comparison showed the limitations of the correlations when used to predict convective coefficients for HFC-32/HFC-125. The design engineer should use a correlation over a range of heat fluxes and mass fluxes verified with experimental data [Carey, 1992]. There were many correlations available, but the four chosen were those often referenced in the literature and reviewed in Chapter II. These four correlations included: Shah [1982], Gungor and Winterton [1986], Kandlikar [1990] and Chen [1966]. Each of these correlations was capable of predicting the local coefficient as a function of quality, heat flux and mass flux. Each of the correlations required thermodynamic and fluid properties data. While the underlying theory of each correlation was different, they all were empirically determined to the extent that each contained constants obtained from curve fitting experimental two-phase heat transfer data.

A separate correlation was developed specifically for HFC-32/HFC-125. The convective coefficient showed large nucleate boiling effects at low qualities and primarily convective effects at high qualities. An asymptotic correlation such as the one originally proposed by Kutateladze [1961] and later used by Wattelet et al [1994] was found to provide an adequate fit. The general form of an asymptotic equation is shown in Equation 6.1, where  $N$  generally ranges from 1 to 3.

$$h_{tp} = \left[ h_{nuc}^N + h_{conv}^N \right]^{\frac{1}{N}} \quad (6.1)$$

The convective term (Equation 6.2) was determined from the product of the Dittus-Boelter single phase convective coefficient shown in Equation 6.3 and the two-phase convective enhancement factor developed by Chen [1966] shown in Equation 6.4.

$$h_{conv} = h_l * E \quad (6.2)$$

$$h_l = 0.023 \frac{k_l}{D} Re_l^{0.8} Pr_l^{0.4} \quad (6.3)$$

$$E = 1 + 1.925 \chi_{tt}^{-0.83} \quad (6.4)$$

The product of enhancement factor and the liquid convective coefficient is used to calculate the two phase convective contribution, which has been used in additive models by Gungor and Winterton [1982], Chen [1966], Kandlikar [1992], and Wattlet [1994].

The initial nucleate contribution was determined from Equation 6.5, where the  $h_{pool}$  equation was developed by Cooper [1984]. The pool boiling convective coefficient is not a function of quality or mass flux.

$$h_{pool} = 55 M^{-0.55} q^{0.67} P_{red}^{0.12} (-\log(P_{red}))^{-0.55} \quad (6.5)$$

Chen [1966] originally suggested a suppression factor to adjust the nucleate boiling contribution to a value less than complete nucleate boiling. Equation 6.6 shows the

nucleate boiling heat transfer coefficient equal to the product of the pool boiling term and the suppression factor.

$$h_{nucleate} = h_{pool} \cdot S \quad (6.6)$$

Chen [1966] stated that the suppression factor was dependent upon the enhancement factor,  $E$ . When the enhancement factor,  $E$ , was high, the suppression factor,  $S$ , would be low. The enhancement factor, Equation 6.4, is an inverse function of the Martinelli factor. Collier [1982] curve fit the suppression factor to data and suggested the relationship shown in Equation 6.7.

$$S = \frac{1}{1 + 2.56 \times 10^{-6} \times \text{Re}_{tp}} \quad (6.7)$$

The two phase Reynolds number is the product of enhancement factor and the liquid Reynolds number, Equation 6.8.

$$\text{Re}_{tp} = \text{Re}_l \cdot E \quad (6.8)$$

Gungor and Winterton suggested the suppression factor shown in Equation 6.9.

$$S = \frac{1}{1 + 1.15 \times 10^{-6} \times E^2 \times \text{Re}_l^{1.17}} \quad (6.9)$$



Both equations for suppression factor predict values greater than 0.4 at qualities higher than 50%. The experimental data in this study suggest that the convective forces dominate the heat transfer at these qualities. Fully suppressed nucleate boiling, FSNB, is calculated to occur at a quality of 55% [Sato and Marsumura, 1964]. All of the correlations under predict the heat transfer coefficient at low qualities and high heat fluxes. They under predict the nucleate boiling contribution. These two conditions, (1) over predicting the suppression factor at high qualities and (2) under predicting the nucleate boiling contribution at low qualities have led to the modification of the suppression equation, Equation 6,10. In the previous suppression factor equations, the enhancement factor was a function of Martinelli parameter. The two phase Reynolds number, Equation 6.7, is also a function of the enhancement factor. The liquid Reynolds number was chosen as a nondimensional variable to represent mass flow. The Martinelli parameter only changes with quality for each refrigerant in this study because the other variables that constitute Martinelli parameter were constant. This equation is of the same form as the other two suppression factor equations. The constant  $C_1$  is greater than unity and corrects for the nucleate boiling term at low qualities and high heat fluxes.

$$S = \frac{C_1}{\left[1 + C_2 \times \chi_{tt}^{n1} \times Re_l^{n2}\right]^{n3}} \quad (6.10)$$

The best fit was obtained by choosing constants and exponents that minimized the error in Equation 6.10 in conjunction with determining the exponent N in Equation 6.1. The two phase nucleate boiling contribution contains only the variables,  $\chi_{tt}$  and  $Re_l$ . Equation 6.11 shows the result of minimizing the error between equation

6.12 and the data. An exponent value of  $N = 2.0$  was found to best match the data to Equation 6.12. The convective coefficient is a function of the mass flux, quality and fluid properties. The nucleate contribution is a function of heat flux, quality and the suppression from high velocities and qualities.

$$S = \frac{1.4}{\left[1 + 2.3 \times 10^{-6} \cdot \chi_{tt}^{-3.7} \cdot \text{Re}_l^{1.07}\right]^2} \quad (6.11)$$

$$h = \left[ (h_{pool} \cdot S)^2 + (h_l \cdot E)^2 \right]^{1/2} \quad (6.12)$$

The asymptotic model is dominated by the greater contributor; if the nucleate boiling forces are much greater than the convective forces, the total convective heat transfer takes on a value close to that of the nucleate boiling contribution. The Shah correlation [Shah, 1982] proposed using the dominant heat transfer mechanism as the two phase heat transfer coefficient. Figure 6.1 shows the calculated nucleate contribution and convective contribution for low heat flux, low mass flux conditions. The asymptotic model approaches the nucleate boiling values at low qualities and the convective values where the nucleate boiling contribution is zero. The curve shows a declining heat transfer coefficient where the quality is low and the nucleate boiling contribution is decreasing. The two phase heat transfer coefficient increases at higher qualities where the convective forces begin to dominate. The point where the nucleate boiling reaches zero is the point of fully suppressed nucleate boiling (FSNB) [Ross, 1987].

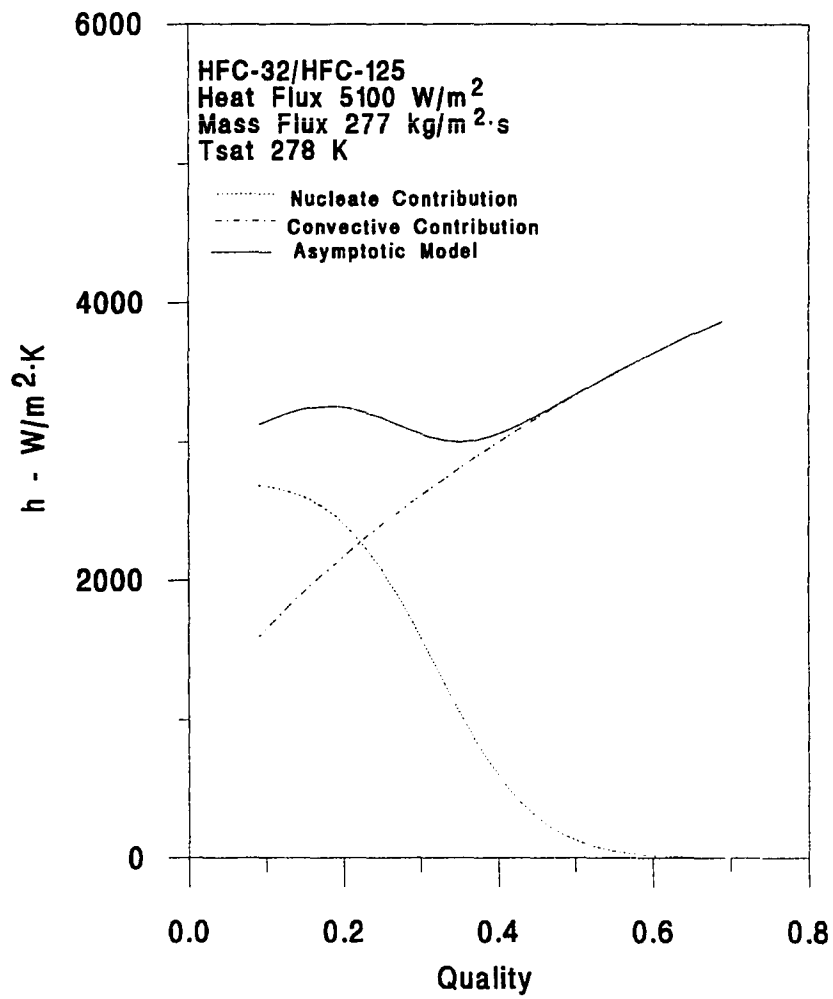


Figure 6.1 The Effect of Nucleate Boiling and Convective Forces on Heat Transfer Coefficient.

The nucleate boiling contribution calculated from Equation 6.6 and the convective contribution calculated from Equation 6.4 are shown in Figure 6.2 and Figure 6.3, respectively, as a function of quality. Figure 6.2 shows the nucleate boiling term for heat fluxes of 5100 and 11000 W/m<sup>2</sup> (1620 and 3490 Btu/h·ft<sup>2</sup>).

The nucleate boiling contribution is higher at low qualities. It is also higher at high heat fluxes. The nucleate contribution approaches numbers close to zero at qualities near 50%. Figure 6.3 shows the convective term for mass fluxes of 277 kg/m<sup>2</sup>·s and 520 kg/m<sup>2</sup>·s (57 and 108 lb<sub>m</sub>/ft<sup>2</sup>·s). The convective contribution increases with increasing quality. The convective contribution is also higher for a higher mass flux.

The proposed correlation predicted the convective coefficient more accurately than the other correlations. The mean deviation was 345 W/m<sup>2</sup>K and the percent mean deviation was 8.4 percent as shown in Table 6.1. The McJimsey correlation predicts the nucleate effects as well as the convective effects.

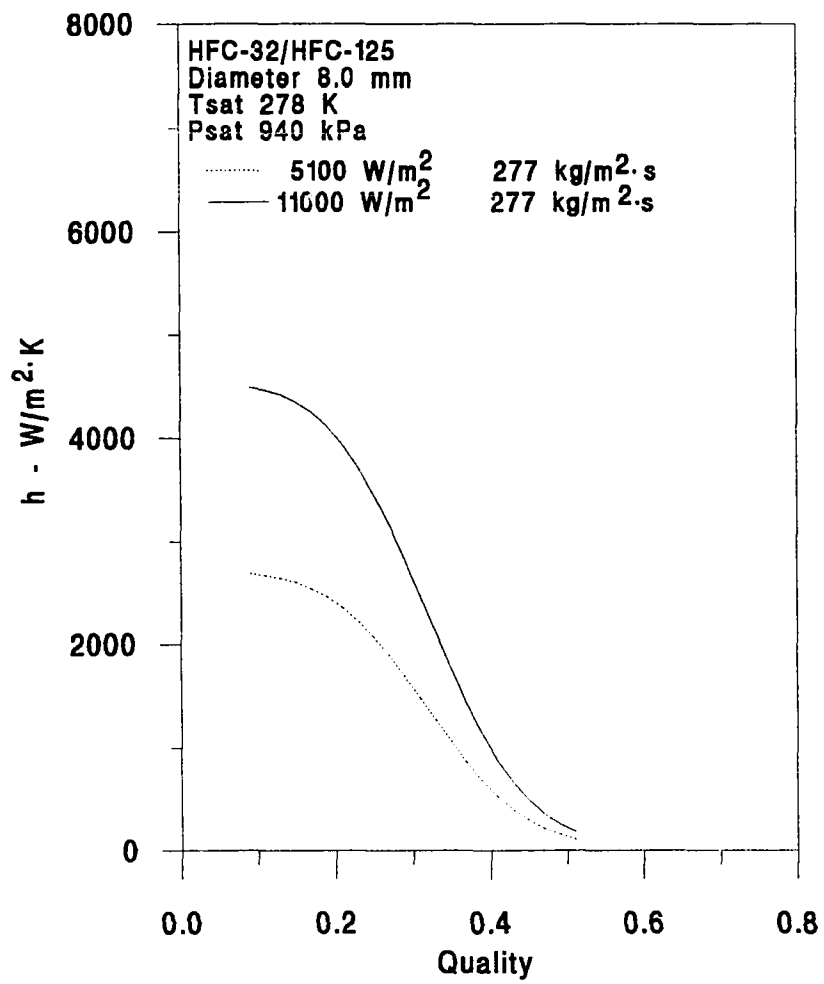


Figure 6.2 The Effect of Mass Flux and Heat Flux on the Nucleate Contribution to Heat Transfer.

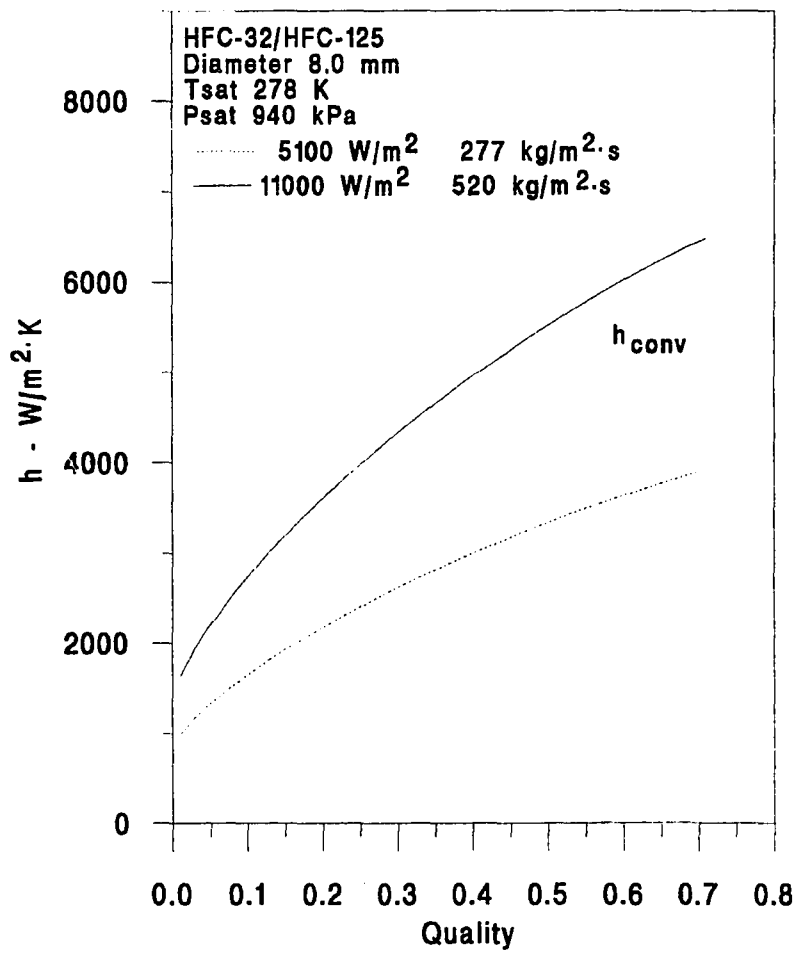


Figure 6.3 The Effect of Mass Flux and Heat Flux on the Convective Contribution to Heat Transfer.

Table 6.1 - Error Comparison of Heat Transfer Correlations

Correlation	Mean Deviation, W/m <sup>2</sup> K	Mean Deviation, Percent
Shah	1100	26.2
Gungor and Winterton	425	10.1
Kandlikar	715	17.0
Chen	876	20.8
McJimsey	345	8.4

Figure 6.4 shows convective heat transfer for the mass flux of 277 kg/m<sup>2</sup>s (57 lb<sub>m</sub>/ft<sup>2</sup>·s) and a heat flux of 5100 W/m<sup>2</sup> (1617 Btu/hr·ft<sup>2</sup>). This was the lowest heat flux and lowest mass flux used in this study. The convective coefficient varied little over the entire range of qualities from 10 to 60 percent. All of the correlations were based upon the effect of nucleate boiling at low qualities and forced convection at higher qualities.

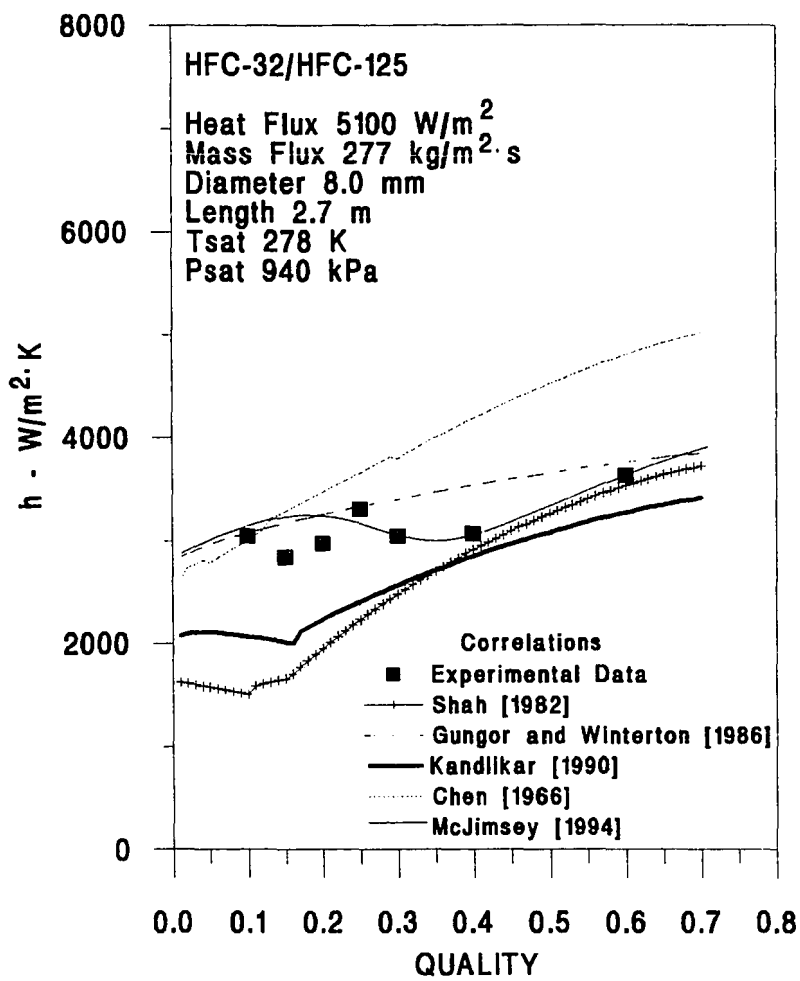


Figure 6.4 A Comparison of Evaporation Heat Transfer Data with Prediction Correlations for a Heat Flux of  $5100 \text{ W/m}^2$  and a Mass Flux of  $277 \text{ kg/m}^2 \cdot \text{s}$ .



The convective coefficients predicted by the Chen correlation were the highest over the range of qualities. The convective coefficients predicted by the correlation developed in this study were the highest at low qualities, decreased for qualities up to 30%, then increased as the convective component began to dominate.

The Gungor and Winterton [1986] correlation and Chen [1966] correlation did not show any significant abrupt changes in slope or shifts in convective coefficient. The convective coefficients by Shah [1982] and Kandlikar [1990] did show abrupt changes in the slope. These changes were due to the predicted transition from nucleate boiling dominated heat transfer to convective dominated heat transfer. This predicted transition was shown to occur over a very small quality change. The convective coefficients predicted by Shah [1982] were the lowest at low qualities. The convective coefficient predicted by Gungor and Winterton [1986], Shah [1982], Kandlikar [1990] and this study all tended toward the same value at the higher qualities. These correlations showed similar trends in the convective dominated heat transfer region. The trend that was not consistent in this study was the small variation in the heat transfer coefficient. This was only seen in this study in the low mass flux and low heat flux cases. The flat convective coefficient was shown in published research by Chaddock and Mathur [1980] and Khanpara, Pate and Bergles [1986]. In the research by Chaddock and Mathur [1980], the convective coefficient showed little dependence on quality for the low heat flux and low mass flux experimental data. This trend was also noted for the cases of mass fluxes of  $277 \text{ kg/m}^2\text{s}$  and  $434 \text{ kg/m}^2\text{s}$  ( $57 \text{ lb}_m/\text{ft}^2\text{s}$  and  $89 \text{ lb}_m/\text{ft}^2\text{s}$ ) and heat flux of  $7100 \text{ W/m}^2$  ( $2251 \text{ Btu/hr}\cdot\text{ft}^2$ ). Since these curves looked essentially the same they were not plotted.

Figure 6.5 showed a very different trend. The convective coefficients predicted by Kandlikar [1990], Gungor and Winterton [1986], Chen [1966] and Shah [1982] showed the same shapes and relative positioning. The experimental convective coefficients for this high heat flux and low mass flux case showed a declining slope to a quality of 40 percent. There were two points of interest in comparison with the correlations. The first was that only the current correlation predicted the magnitude of the effect nucleate boiling had on the convective coefficient. The second point of interest was that the suppression or decline continued to a larger quality than predicted by either the correlation by Shah [1982] or Kandlikar [1990]. The suppression of nucleate boiling was thought to occur at a lower quality for mixtures than for pure substances [Wattlet et al, 1994]. The contribution of nucleate boiling was significant for a 50/50 mass mixture of HFC-32/HFC-125 at high heat fluxes and low mass fluxes to a quality of 40 percent.

The nucleate boiling contribution to the convective coefficient was continually under predicted for this refrigerant mixture at the heat fluxes and mass fluxes studied. Figure 6.6 showed experimental data for a moderate mass flux,  $434 \text{ kg/m}^2\text{s}$  ( $89 \text{ lb}_m/\text{ft}^2\text{s}$ ), and the highest heat flux used in this study,  $11000 \text{ W/m}^2$  ( $3488 \text{ Btu/hr}\cdot\text{ft}^2$ ). In Figure 6.6, the experimental convective coefficient was  $1000 \text{ W/m}^2$  ( $317 \text{ Btu/hr}\cdot\text{ft}^2$ ) lower than the highest predicted heat transfer coefficient, except for the method proposed in this study, and twice as high as the lowest predicted value for qualities of 10 and 15 percent. The quality at which convective forces began to dominate was also under predicted by Shah [1982] and Kandlikar [1990]. There were two important conclusions to draw from Figure 6.6.

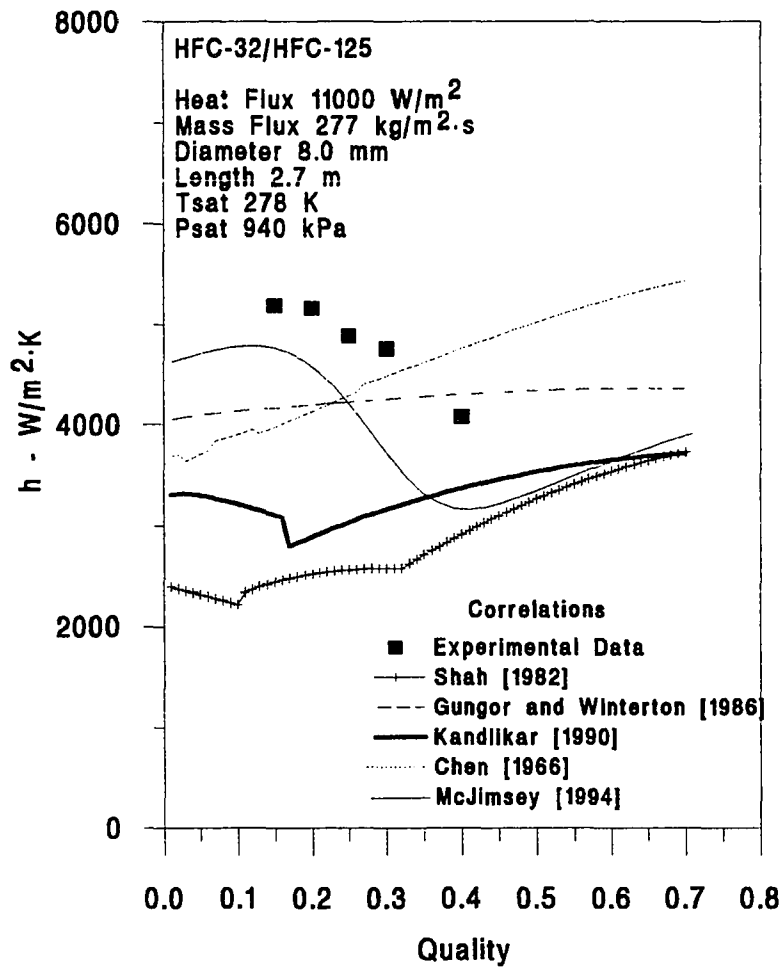


Figure 6.5 A Comparison of Evaporation Heat Transfer Data with Prediction Correlations for a Heat Flux of  $11000 \text{ W/m}^2$  and a Mass Flux of  $277 \text{ kg/m}^2\cdot\text{s}$ .

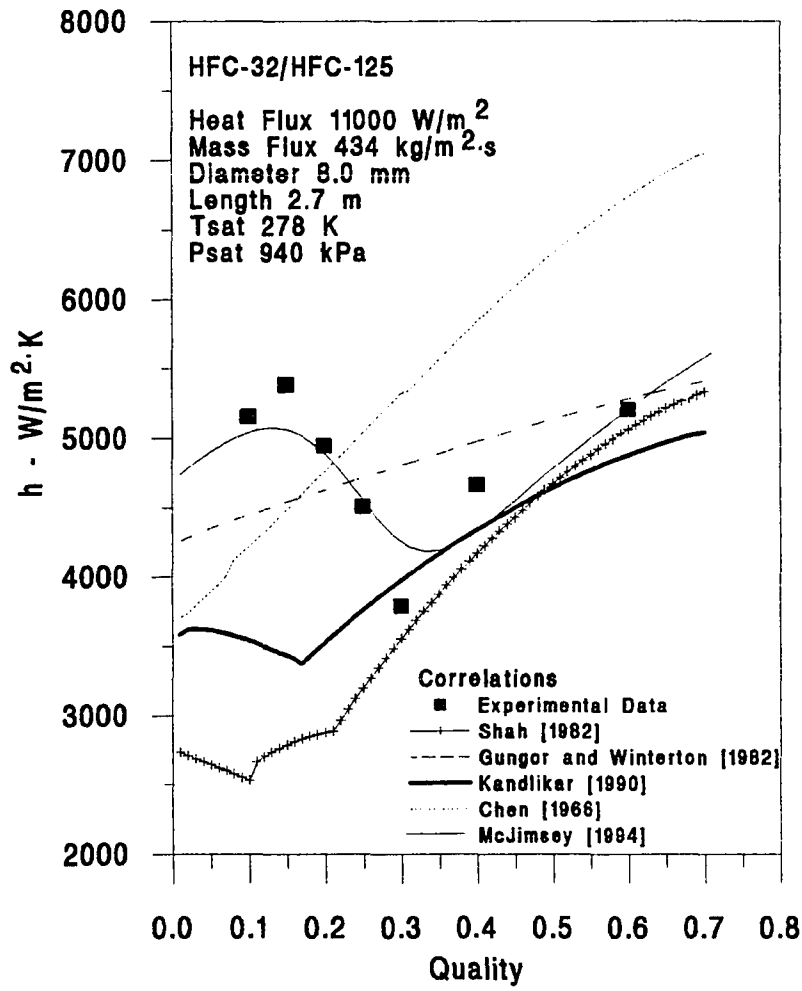


Figure 6.6 A Comparison of Evaporation Heat Transfer Data with Prediction Correlations for a Heat Flux of  $11000 \text{ W/m}^2$  and a Mass Flux of  $434 \text{ kg/m}^2\cdot\text{s}$ .

The first conclusion was the previous prediction correlations under predicted the nucleate contribution for the low qualities. This would not be extremely devastating to air-conditioner designers because the entering quality to an evaporator was usually around 20 percent. The under prediction of convective coefficient will cause the designer to over design a heat exchanger or design an evaporator larger than necessary. The second point was that once the convective forces begin to dominate the heat transfer process, the correlations did an adequate job predicting the convective coefficient. The worst case was the Chen [1966] correlation, where it was off by 30 percent.

The final comparison of data and prediction results showed convective coefficients for high mass flux and low heat flux. In Figure 6.7, the convective coefficient was shown for a mass flux  $700 \text{ kg/m}^2\text{s}$  ( $143 \text{ lb}_m/\text{ft}^2\cdot\text{s}$ ) and a heat flux of  $5100 \text{ W/m}^2$  ( $1617 \text{ Btu/hr}\cdot\text{ft}^2$ ), which were the highest mass flux and the lowest heat flux used in this study.

The convective dominated region was predicted to within 10 percent by all of the correlations except that of Chen [1966]. The quality at which convective forces begin to dominate was under predicted by the correlations of Shah [1982] and Kandlikar [1990].

#### SUMMARY OF CORRELATION DEVELOPMENT

The heat transfer characteristics for a HFC-32/HFC-125 mixture were examined for heat fluxes  $5100 \text{ W/m}^2$  to  $11000 \text{ W/m}^2$  ( $1617 \text{ Btu/hr}\cdot\text{ft}^2$  to  $3488 \text{ Btu/hr}\cdot\text{ft}^2$ ) and mass fluxes of  $277 \text{ kg/m}^2\text{s}$  to  $700 \text{ kg/m}^2\text{s}$  ( $57 \text{ lb}_m/\text{ft}^2\cdot\text{s}$  to  $143 \text{ lb}_m/\text{ft}^2\cdot\text{s}$ ).

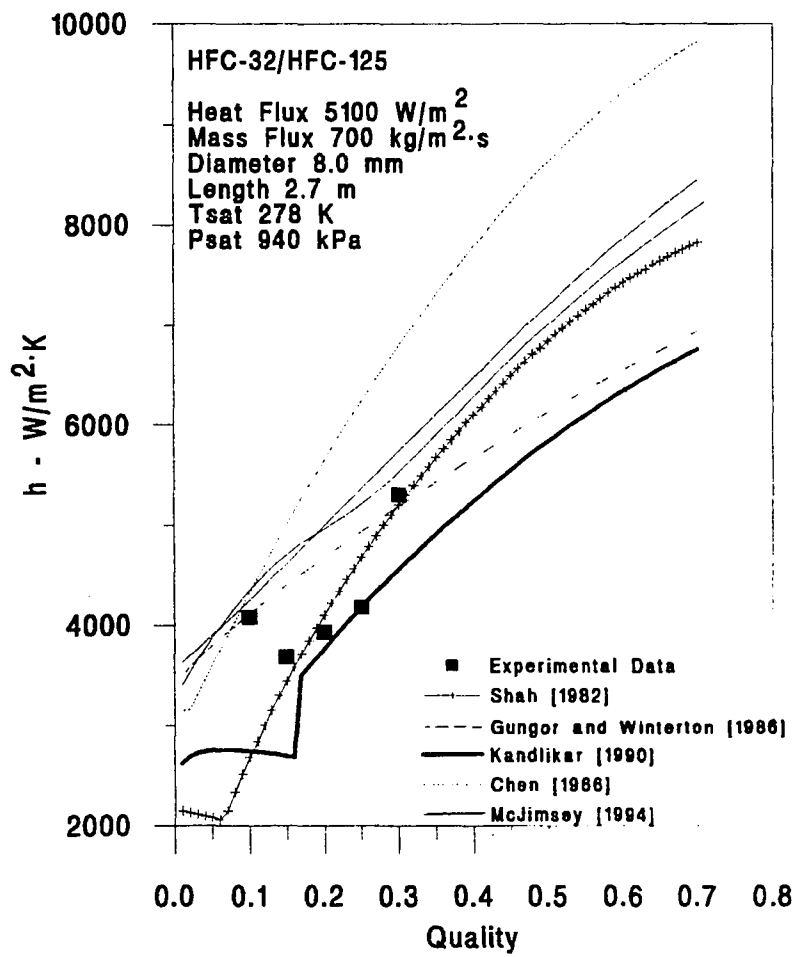


Figure 6.7 A Comparison of Evaporation Heat Transfer Data with Prediction Correlations for a Heat Flux of  $5100 \text{ W/m}^2$  and a Mass Flux of  $700 \text{ kg/m}^2\cdot\text{s}$ .

In non oil experiments there were two patterns of heat transfer performance. The major pattern consisted of heat transfer coefficient declining at low qualities and increasing at higher qualities. This pattern was explained as suppression of nucleate boiling as the convective coefficient decreased and convective dominated heat transfer as the convective coefficient increased. The other trend that was noted at low mass fluxes and low heat fluxes was a constant or nonchanging convective coefficient for all qualities. The convective coefficient began to increase at lower qualities when the heat flux was lower and the mass flux was higher. High heat fluxes caused a higher convective coefficient at low qualities.

The convective coefficient was compared to five prediction correlations. The correlations used were by Shah [1982], Gungor and Winterton [1986], Kandlikar [1990], Chen [1966] and the proposed correlation. Only the proposed correlation predicted the convective coefficient effectively at low qualities.

## CHAPTER VII

### EXPERIMENTAL RESULTS FOR HFC-32/HFC-125 50/50 MASS

#### MIXTURE WITH A POLYOL ESTER (POE)

After performing the experiments with pure HFC-32/HFC-125, Mobil EAL Arctic 32 a POE oil was added on a mass basis in concentrations of 2.6 percent and 5.4 percent and the same series of experiments were carried out. The effect of mass flux and heat flux on pressure drop and heat transfer was measured.

The choice of a HCFC-22 replacement refrigerant could not be made without considering the effect of oil on the heat transfer coefficient and the pressure drop. The lubrication and miscibility of the oil would also have to be considered, but were beyond the scope of this study. The addition of oil increases the surface tension and viscosity of the mixture. The oil changes the density of the refrigerant mixture and changed the vapor pressure / temperature relationship. However, Chaddock [1986] stated the vapor pressure and temperature relationship doesn't change much until a significant amount of oil was added. Neither the P(T) relationship or the amount of oil was quantified. The oil in refrigerant systems is needed to lubricate the compressor. The oil stays in a liquid phase as it circulates through an air conditioning system. The oil needs to be miscible in the liquid refrigerant. The oil was added directly to the refrigerant in the test apparatus. The effect of oil on heat transfer coefficient was shown along with the effect of heat and mass flux. The oil was of a different viscosity than the refrigerant, thus the effect of oil on pressure drop was shown as well.



Table 7.1 Properties of HFC-32/HFC-125 and a POE Oil

Fluid Property	HFC-32/HFC-125	Mobil EAL Arctic 32
Liquid Density kg/m <sup>3</sup> lb <sub>m</sub> /ft <sup>3</sup>	1176.7 73.75	993.0 62.00
Liquid Specific Heat kJ/kg·K Btu/lb <sub>m</sub> ·°F	1.286 0.307	1.84 0.44
Liquid Viscosity μNs/m <sup>2</sup> lb <sub>m</sub> /ft·hr	0.202 0.488	0.316 0.764
Liquid Thermal Conductivity W/m·K Btu/hr·ft·°F	0.108 0.062	0.140 0.080
Surface Tension mN/m lb <sub>f</sub> /ft	8.51 5.83 E-04	30.4 20.8 E-04

#### THE EFFECT OF OIL PROPERTIES UPON MIXTURE PROPERTIES

The oil viscosity is higher than the liquid refrigerant viscosity as shown in Table 7.1. According to Equations 7.1 and 7.2 the addition of oil to the refrigerant would increase the mixture viscosity.

$$f_{Lr} = \frac{\text{mass liquid refrigerant}}{\text{mass liquid refrigerant} + \text{mass oil}} \quad (7.1)$$

$$\mu_{mix} = \mu_{Lr} \cdot \exp \left[ (1 - f_{Lr}) (\mu_{Lr} / \mu_{oil})^{0.3} \right] \quad (7.2)$$

The two phase Reynolds number, Equation 7.3, would decrease with increasing viscosity.

$$\text{Re}_{tp} = \frac{G D}{\mu_{tp}} \quad (7.3)$$

The lower Reynolds number calculated using a higher viscosity due to the addition of oil used in Equation 7.4 would calculate a higher two phase friction factor.

$$f_{tp} = 0.079 \cdot \text{Re}^{-0.25} \quad (7.4)$$

The oil density is less than the refrigerant liquid density, also shown in Table 7.1. The addition of oil would decrease the mixture density. The lower density and higher two phase friction factor due to the addition of oil would both work to increase the frictional pressure drop calculated in Equation 7.5.

$$-\left(\frac{dP}{dz}\right)_{fr} = \frac{2 f_{tp} G^2}{\rho_l D} \quad (7.5)$$

Oil affects the heat transfer in a more complex manner. The heat transfer mechanism can be described as a combination of nucleate boiling and convective heat transfer as shown in Equation 7.6.

$$h_{tp} = h_{conv} + h_{nucleate} \quad (7.6)$$

The higher viscosity that results from the addition of oil will decrease the convective heat transfer. The oil thermal conductivity and specific heat are both higher than the refrigerant thermal conductivity and specific heat and would increase the heat transfer to the refrigerant. The surface tension for the oil is over three times higher than the refrigerant surface tension. The increased surface tension would restrain the bubble growth at the wall during nucleate boiling.

The addition of oil is thought to suppress nucleate boiling because of the increased surface tension. The flow pattern map, Figure 7.1, was recalculated using liquid properties determined from the oil and refrigerant properties. The oil should not be a vapor under the temperature and pressure values used in this research. Qualities from 10 percent to 60 percent all fall in the annular or dispersed flow pattern. The annular flow pattern is associated with convective heat transfer.

#### THE EFFECT OF OIL ON PRESSURE DROP

Schlager et al [1987] found that the addition of oil to refrigerant usually increased the pressure drop over that of a pure refrigerant. The POE oil had a higher viscosity ( $316 \mu\text{Ns}/\text{m}^2$ ) than that for the pure refrigerant ( $202 \mu\text{Ns}/\text{m}^2$ ).

The addition of oil only slightly changed the pressure drop relationships with heat flux and mass flux combinations in this study. Figure 7.2 shows the pressure drop per unit length for the lowest heat flux and the lowest mass flux used in this study. The pressure drop per unit length increased with increasing qualities. Velocity of the vapor should increase at higher qualities for the same mass flux. The frictional pressure drop should increase with quality because the frictional pressure drop is a function of the square of velocity. The frictional pressure drop variation with quality is shown in Figure 7.2. The more oil that was added to the refrigerant, the higher the viscosity and the higher the frictional pressure drop.

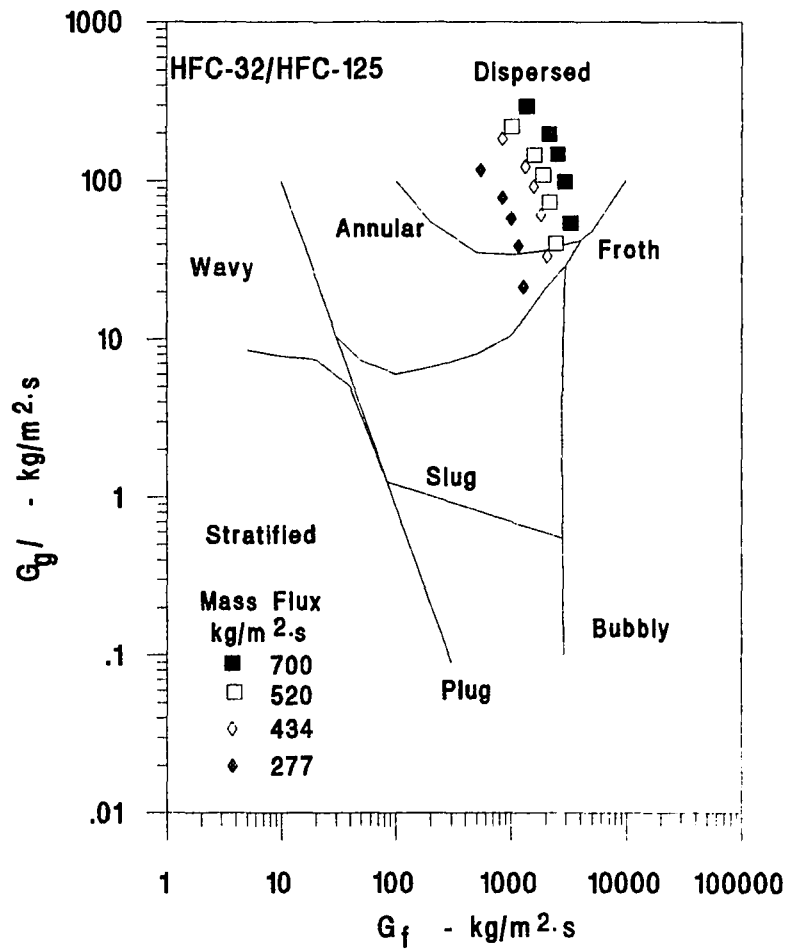


Figure 7.1 Flow Pattern Map for HFC-32/HFC-125 with 2.5 Percent POE Oil (Baker, 1954)

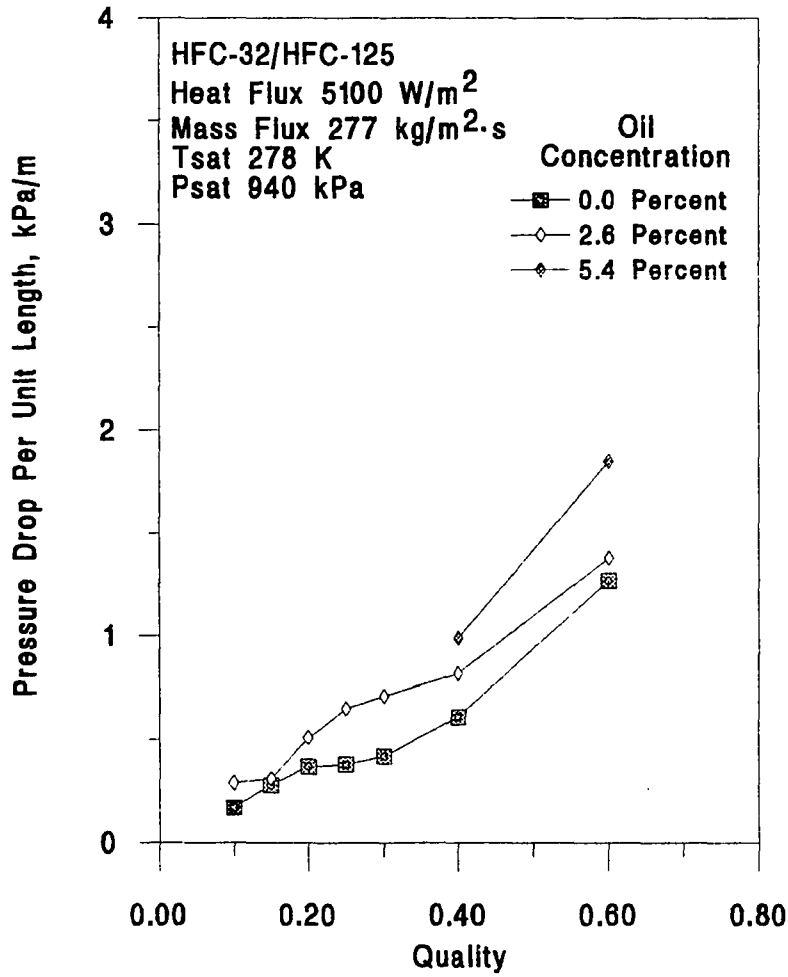


Figure 7.2 The Effect of Oil Concentration on Pressure Drop Per Unit Length for a Heat Flux of  $5100 \text{ W/m}^2$  and a Mass Flux of  $277 \text{ kg/m}^2 \cdot \text{s}$ .

The pressure drop per unit length was highest for the higher oil concentration and lowest for the pure HFC-32/HFC-125. The pressure drop per unit length for the refrigerant with a mass concentration of 2.6 % oil was 33 % higher than the pure refrigerant. The pressure drop per unit length for the refrigerant with a concentration of 5.4 % oil was 51 % higher than the refrigerant without oil at qualities of 40 and 60 percent.

The ratio of pressure drop of oil laden refrigerant to that of a pure refrigerant for a heat flux of  $5100 \text{ W/m}^2$  and a mass flux of  $277 \text{ kg/m}^2\text{-s}$  is shown in Figure 7.3. The pressure drop ratio was smaller for oil concentrations of 2.6 percent. The general trend was that the ratio falls between 1.1 and 1.75 and decreases as quality increases.

The effect of oil on pressure drop was the same for all cases. The effect of oil on pressure drop was plotted in Figure 7.4 for high mass fluxes and high heat fluxes. The pressure drop per unit length increased as quality increased. The pressure drop per unit length was higher for refrigerant containing oil. There was very little difference in the pressure drop per unit length for oil concentrations of 2.6 and 5.4 percent at the higher mass fluxes and heat fluxes. The pressure drop per unit length for the refrigerant containing oil averaged 21 percent higher than the pressure drop of the pure refrigerant.

The ratio of pressure drop for oil laden refrigerant to pure refrigerant for heat fluxes of  $11000 \text{ W/m}^2$  and mass fluxes of  $520 \text{ kg/m}^2\text{-s}$  is shown in Figure 7.5. The pressure drop ratios were all above 1.0. There was minimal difference in the two oil concentrations. Both ratios decreased as quality increased. The ratios were between 1.1 and 1.6.

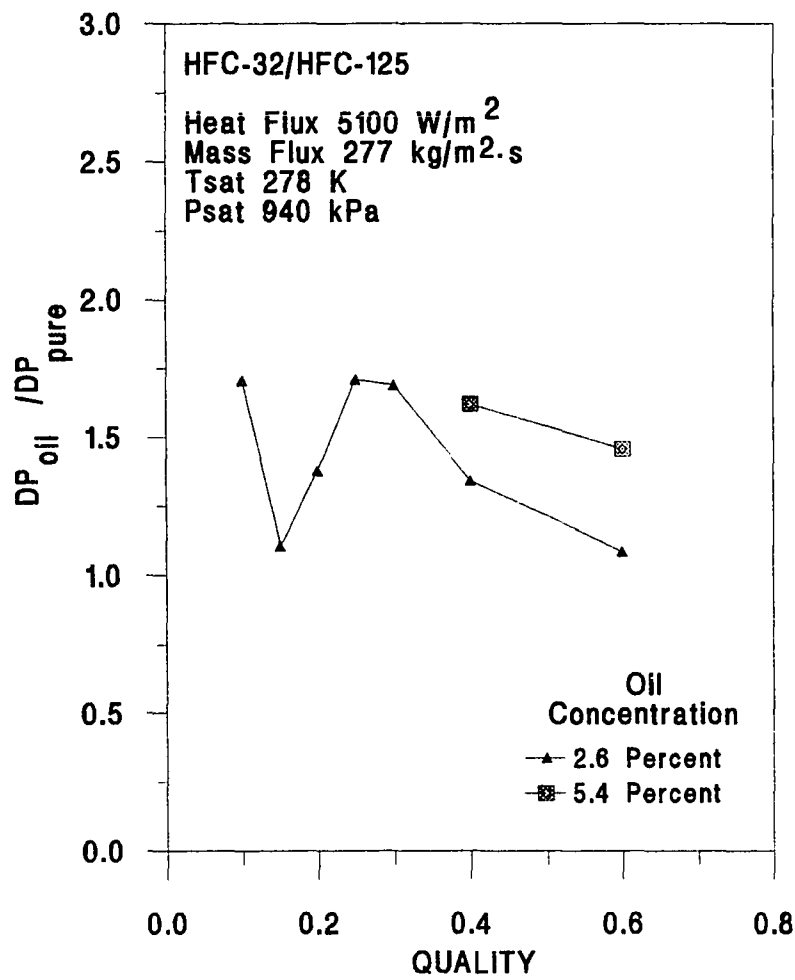


Figure 7.3 The Ratio of Pressure Drop for Heat Flux of 5100 W/m<sup>2</sup> and a Mass Flux of 277 kg/m<sup>2</sup>.s.

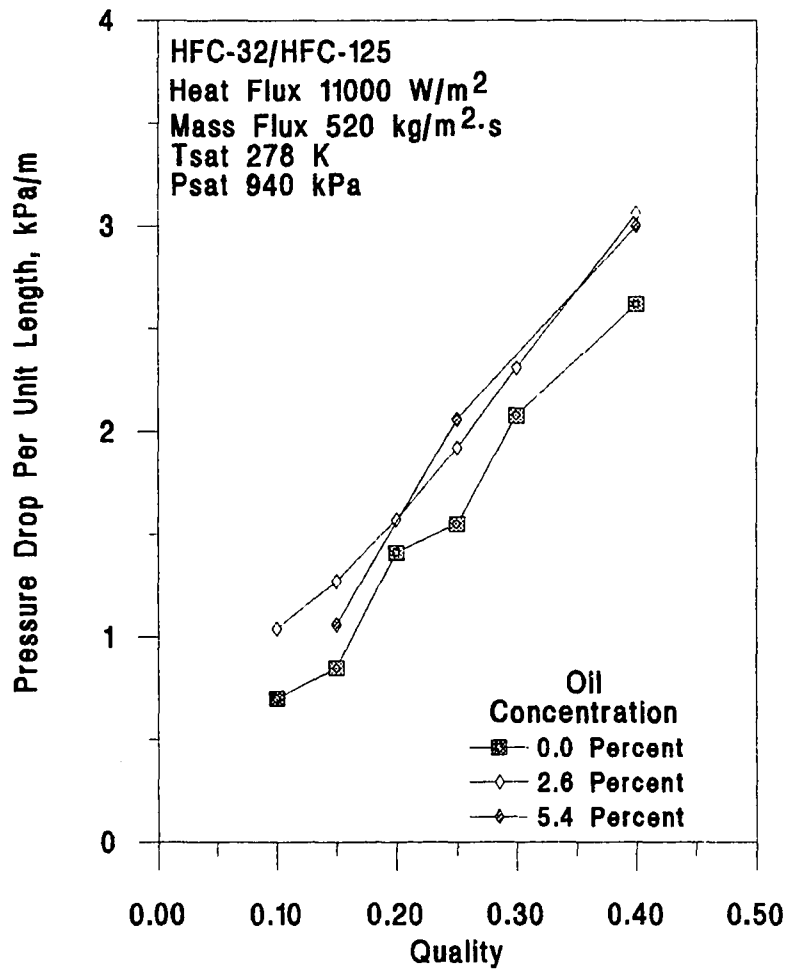


Figure 7.4 The Effect of Oil Concentration on Pressure Drop Per Unit Length for a Heat Flux of  $11000 \text{ W/m}^2$  and a Mass Flux of  $520 \text{ kg/m}^2\cdot\text{s}$ .



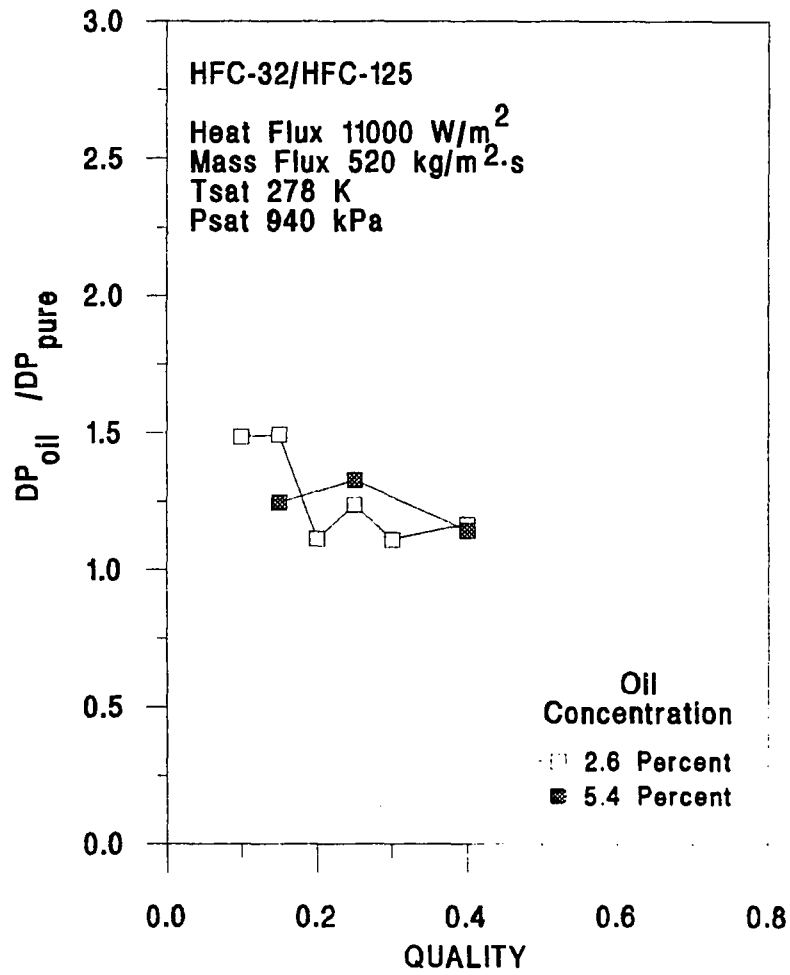


Figure 7.5 The Ratio of Pressure Drop for Heat Flux of 11000 W/m<sup>2</sup> and a Mass Flux of 520 kg/m<sup>2</sup>.s.

## THE EFFECT OF MASS FLUX ON HEAT TRANSFER

The effect of mass flux was shown in the same manner as the pure HFC-32/HFC-125. The heat transfer coefficients for a constant mass flux were graphed as a function of mass flux and quality. Figure 7.6 shows the convective coefficients for a 2.6 percent oil concentration.

The heat flux in this figure was the lowest one used in this study,  $5100 \text{ W/m}^2$  ( $1617 \text{ Btu/hr}\cdot\text{ft}^2$ ). The convective coefficient increased for the three higher mass fluxes. The slope of the curve representing a mass of  $700 \text{ kg/m}^2\text{s}$  ( $143 \text{ lb}_m/\text{ft}^2\cdot\text{s}$ ) was higher than the other two curves. The convective heat transfer effects appeared to dominate at a lower quality for the 2.6 % oil concentration compared to the pure case. The addition of oil should induce an annular flow pattern at a lower quality than for a pure refrigerant [Chaddock, 1986]. Figure 7.7 shows the effect of mass flux on heat transfer coefficient for the highest heat flux,  $11000 \text{ W/m}^2$  ( $3488 \text{ Btu/hr}\cdot\text{ft}^2$ ). The heat transfer coefficient for the curve representing the lowest mass flux,  $277 \text{ kg/m}^2\text{s}$  ( $57 \text{ lb}_m/\text{ft}^2\cdot\text{s}$ ), first increased with quality, peaked, then decreased with quality. This same shape was noted for low mass fluxes and low oil concentrations by Chaddock and Mathur [1980]. One possible explanation for this increasing convective coefficient at low qualities and then decreasing at higher qualities might have been that convective forces increase with the higher velocities as quality increases. At some point the liquid layer against the tube wall becomes oil laden and the high oil concentrations in the liquid hinder the convective forces at the tube wall. The curve representing the highest heat flux also showed this increasing trend. The curve representing the mass flux between these two,  $434 \text{ kg/m}^2\text{s}$  ( $89 \text{ lb}_m/\text{ft}^2\cdot\text{s}$ ), increased until quality reached 20 percent and convective coefficient peaked at  $5800 \text{ W/m}^2$  and then decreased. No other data showed these trends.

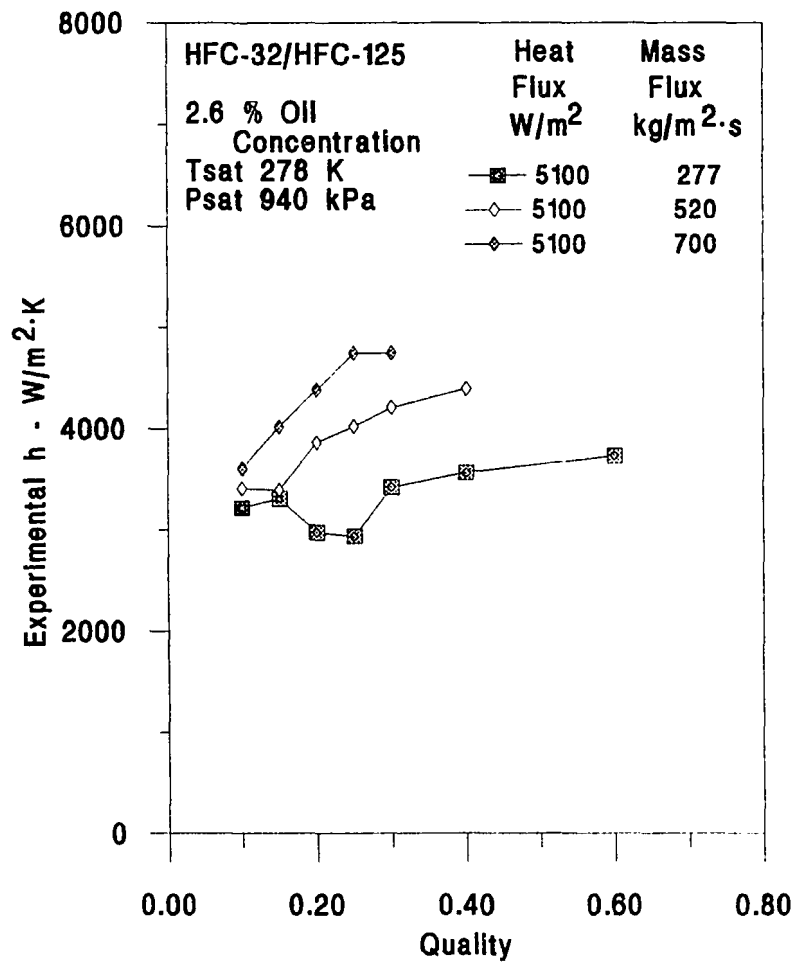


Figure 7.6 The Effect of Mass Flux upon Heat Transfer Coefficient of HFC-32/HFC-125 Containing a 2.6 Percent Oil Concentration at a Heat Flux of  $5100 W/m^2$ .

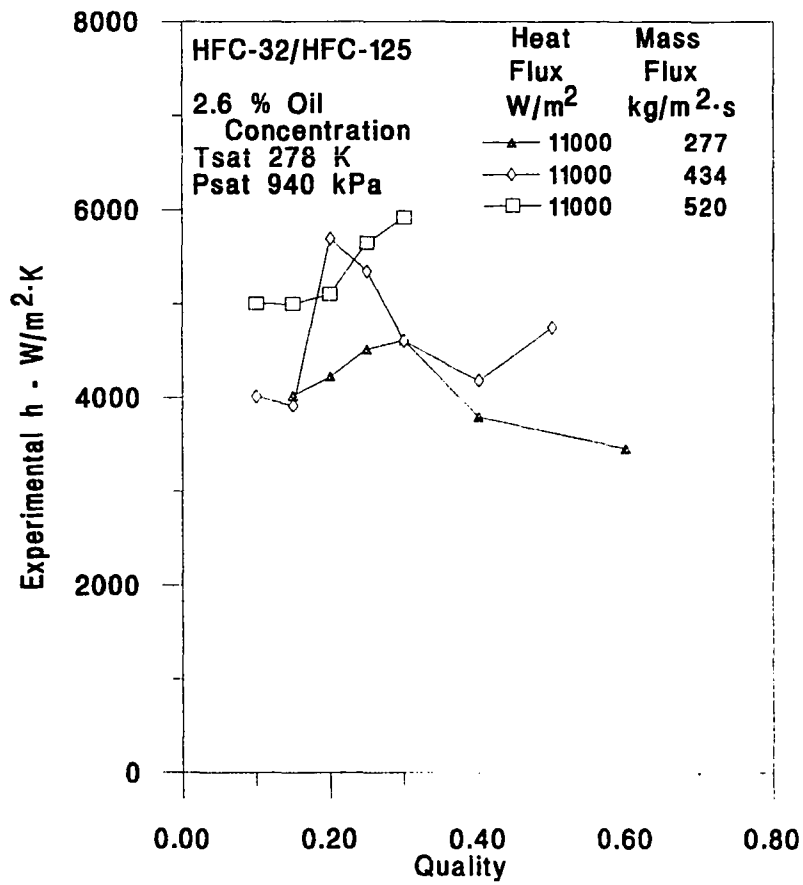


Figure 7.7 The Effect of Mass Flux upon Heat Transfer Coefficient of HFC-32/HFC-125 Containing a 2.6 Percent Oil Concentration at a Heat Flux of  $11000 W/m^2$ .

## THE EFFECT OF HEAT FLUX ON HEAT TRANSFER

The effect of heat flux on heat transfer coefficient for a HFC-32/HFC-125 mixture with 2.6 percent oil concentration is shown in Figures 7.8 and 7.9. Each data point is graphed at the point corresponding to a mean quality in the test section.

In Figure 7.8, the heat transfer coefficients for mass fluxes of  $277 \text{ kg/m}^2\text{s}$  ( $57 \text{ lb}_m/\text{ft}^2\text{s}$ ) are shown. The same heat fluxes that were used in the non oil experiments were used with the refrigerant/oil mixtures. These heat fluxes were  $5100 \text{ W/m}^2$ ,  $7100 \text{ W/m}^2$  and  $11000 \text{ W/m}^2$  ( $1617 \text{ Btu/hr}\cdot\text{ft}^2$ ,  $2251 \text{ Btu/hr}\cdot\text{ft}^2$  and  $3488 \text{ Btu/hr}\cdot\text{ft}^2$ ). The heat transfer coefficients for the curves representing the lowest two heat fluxes showed little variation with quality. The values never differed by more than 15 percent. The heat transfer coefficients shown for the highest heat flux started out higher than the other two. The values increased linearly from  $4024 \text{ W/m}^2\text{K}$  ( $709 \text{ Btu/hr}\cdot\text{ft}^2\text{OF}$ ) to  $4610 \text{ W/m}^2\text{K}$  ( $812 \text{ Btu/hr}\cdot\text{ft}^2\text{OF}$ ) for qualities of 15 to 30 percent, respectively. It then decreased as the qualities increased from 40 percent to 60 percent. The heat transfer coefficients were within eight percent of the mean values at qualities of 40 and 60 percent. This would indicate that the nucleate boiling contribution was no longer influential and the forced convective mechanism was now dominating the heat transfer process. The nucleate boiling effects were still in effect at a quality of 40 percent for pure HFC-32/HFC-125 at a mass flux of  $277 \text{ kg/m}^2\text{s}$  ( $57 \text{ lb}_m/\text{ft}^2\text{s}$ ) and a heat flux of  $11000 \text{ W/m}^2$  ( $3488 \text{ Btu/hr}\cdot\text{ft}^2$ ). The introduction of oil in small quantities should promote annular flow and the corresponding suppression of nucleate boiling at lower qualities than for a pure case [Chaddock, 1986].

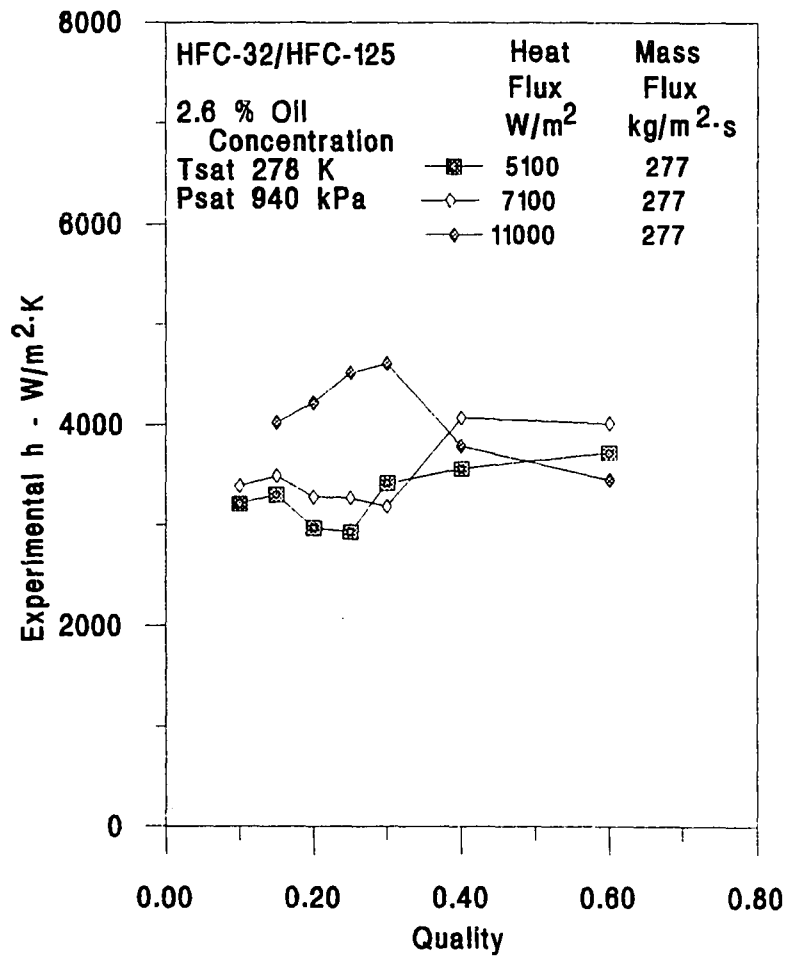


Figure 7.8 The Effect of Heat Flux upon Heat Transfer Coefficient of HFC-32/HFC-125 Containing a 2.6 Percent Oil Concentration at a Mass Flux of  $277 \text{ kg/m}^2 \cdot \text{s}$ .

The effect on the heat transfer was even more pronounced at higher mass fluxes. In Figure 7.9, the heat transfer coefficient was shown for a mass flux of 520  $\text{kg/m}^2\text{s}$  ( $108 \text{ lb}_m/\text{ft}^2\cdot\text{s}$ ) and the highest and lowest heat fluxes used in this study. The curves looked similar in shape up to a quality of 30 percent. The curves both increased approximately 20 percent over a quality change from 10 to 30 percent.

The heat transfer coefficients for heat fluxes of  $5100 \text{ W/m}^2$  ( $1617 \text{ Btu/hr}\cdot\text{ft}^2$ ) and  $7100 \text{ W/m}^2$  ( $2251 \text{ Btu/hr}\cdot\text{ft}^2$ ) were nearly identical for the highest mass flux studied at low qualities (Figure 7.10). The heat transfer coefficient increased 27 percent over a quality change from 10 to 30 percent. The heat transfer coefficient for these two heat fluxes never differed by more than five percent at any quality studied. The convective contribution to heat transfer appeared to completely overshadow the difference in heat fluxes.

#### THE EFFECT OF OIL ON HEAT TRANSFER

Experiments were performed with HFC-32/HFC-125 at oil concentrations of 0, 2.6 and 5.4 percent. The effect of the oil concentration on heat transfer coefficient was shown through a series of graphs representing different combinations of heat fluxes and mass fluxes at all three oil concentrations. These graphs were organized by the relative values of heat flux and mass flux. A high mass flux low heat flux case, a low mass flux low heat flux case, a high mass flux high heat flux case and a low mass flux high heat flux case were chosen to illustrate the effect of oil on the heat transfer coefficient. Each graph shows the ratio of two-phase heat transfer coefficient with oil divided by the two-phase heat transfer coefficient for pure refrigerant. The oil could have caused foaming in the two-phase refrigerant that created turbulence and promoted nucleation. Schlager et al [1987] hypothesized that the added turbulence and increased nucleation were the main reasons that the heat transfer coefficient was sometimes higher for moderate oil concentrations .

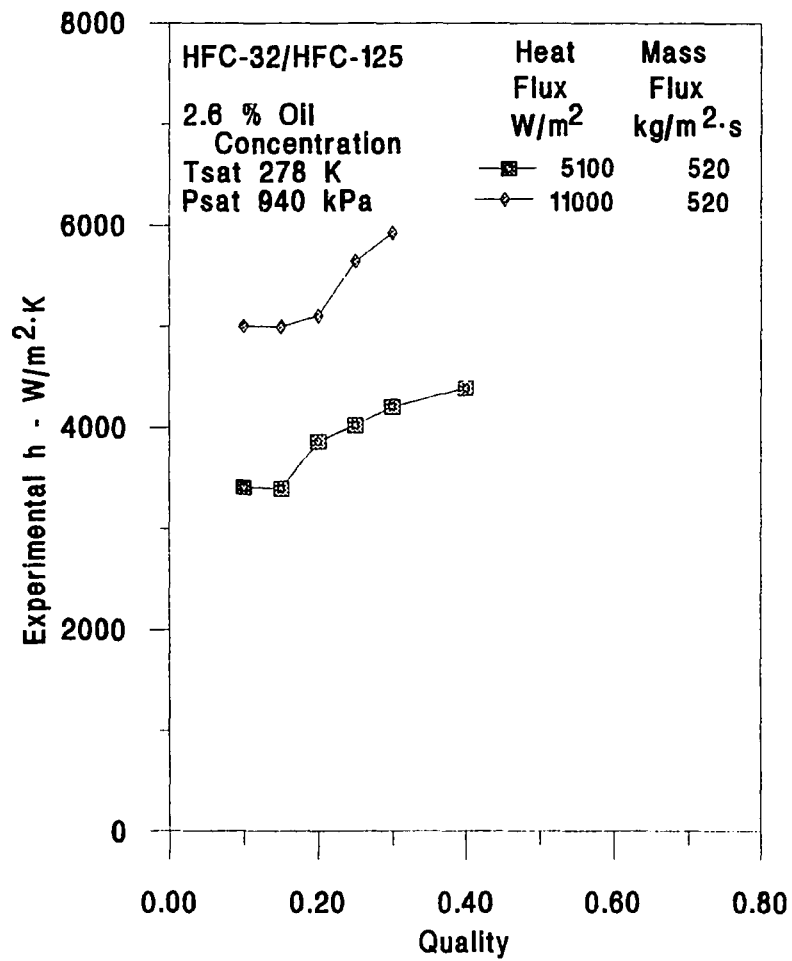


Figure 7.9 The Effect of Heat Flux upon Heat Transfer Coefficient of HFC-32/HFC-125 Containing a 2.6 Percent Oil Concentration at a Mass Flux of 520 kg/m<sup>2</sup>·s.



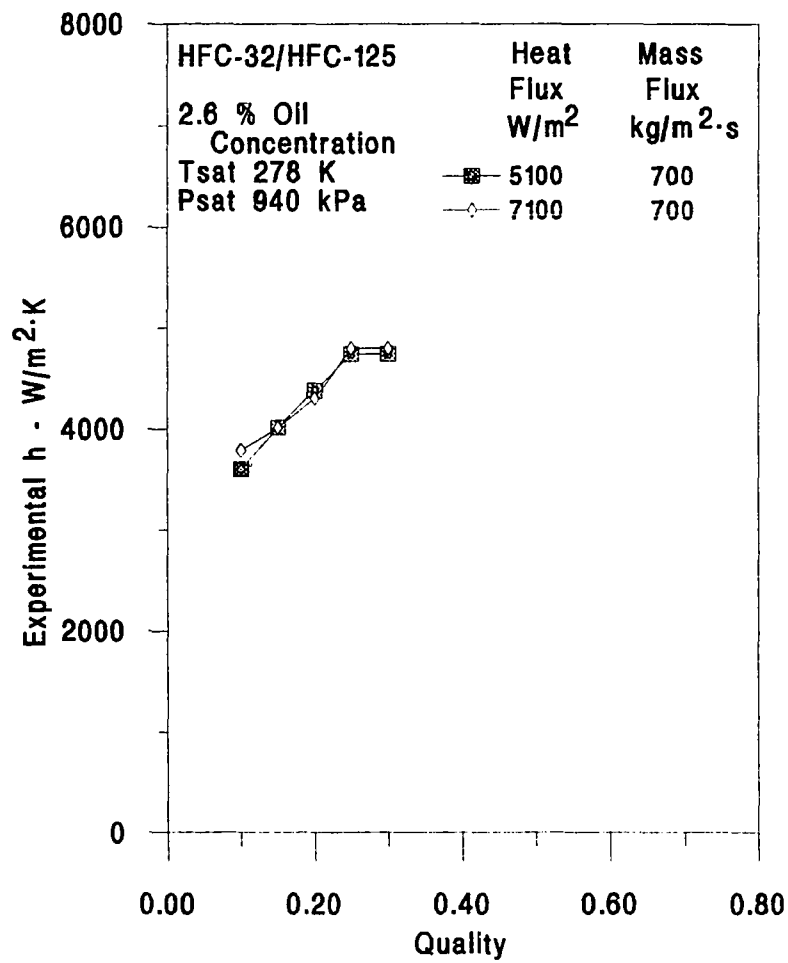


Figure 7.10 The Effect of Heat Flux upon the Heat Transfer Coefficient of HFC-32/HFC-125 Containing a 2.6 Percent Oil Concentration at a Mass Flux of 700 kg/m<sup>2</sup>·s.

The ratio of the heat transfer coefficient for low mass flux and low heat flux is shown in Figure 7.11. The heat flux was  $7100 \text{ W/m}^2$  ( $2251 \text{ Btu/hr}\cdot\text{ft}^2$ ) and the mass flux was  $277 \text{ kg/m}^2\cdot\text{s}$  ( $57 \text{ lb}_m/\text{ft}^2\cdot\text{s}$ ). The data for the same mass flux and a heat flux of  $5100 \text{ W/m}^2$  ( $1617 \text{ Btu/hr}\cdot\text{ft}^2$ ) showed exactly the same trends for the two oil concentrations, 2.6 and 5.4 percent. The heat transfer coefficient ratio was close to one for the lower oil concentration over the quality range from 10 to 30 percent. The heat transfer coefficient for the HFC-32/HFC-125 mixture with a 2.4 percent concentration was 23 percent higher than that for the pure refrigerant case coefficient at qualities from 40 and 60 percent. The heat transfer coefficient for the mixture having 5.4 percent oil concentration was 40 percent higher than the pure refrigerant at these same qualities. The overall significance of this figure was that at low qualities, low heat fluxes and low mass fluxes the heat transfer coefficient was not affected by oil concentration. At moderate qualities, the increased oil concentration caused a slight increase in heat transfer coefficient. It was possible that at these low mass fluxes the foaming action discussed by Schlager et al [1987] that increased turbulence did not effectively begin until the velocity reached some minimum level.

The effect of a high heat flux and low mass flux on the heat transfer coefficient for two oil HFC-32/HFC-125 mixtures are shown in Figure 7.12. The heat flux and mass flux were the highest and lowest, respectively, used in this study. The heat transfer coefficient for the 2.6 percent oil concentration was lower than the coefficient for the pure refrigerant and that for the 5.4 percent oil concentration was higher. The general trend was that the heat transfer coefficient for refrigerant containing oil increased with respect to the pure case as quality increased. This was evident from the positive slope of both curves in Figure 7.12.

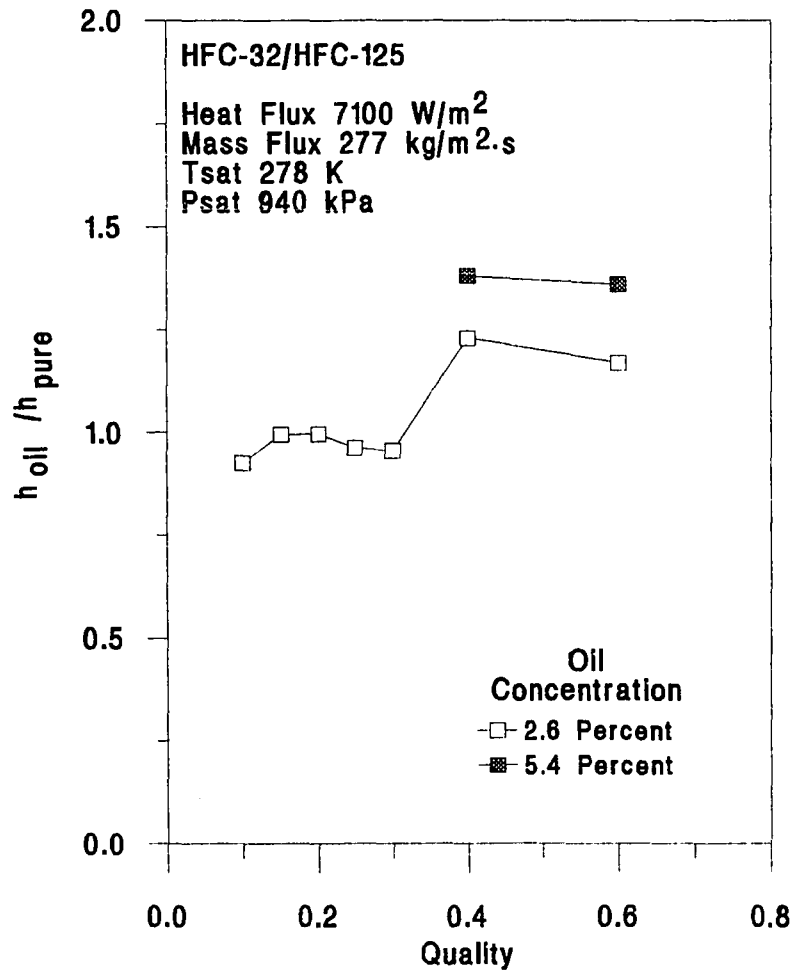


Figure 7.11 The Effect of Oil Concentration upon Heat Transfer Coefficient for a Heat Flux of  $7100 \text{ W/m}^2$  and a Mass Flux of  $277 \text{ kg/m}^2\cdot\text{s}$ .

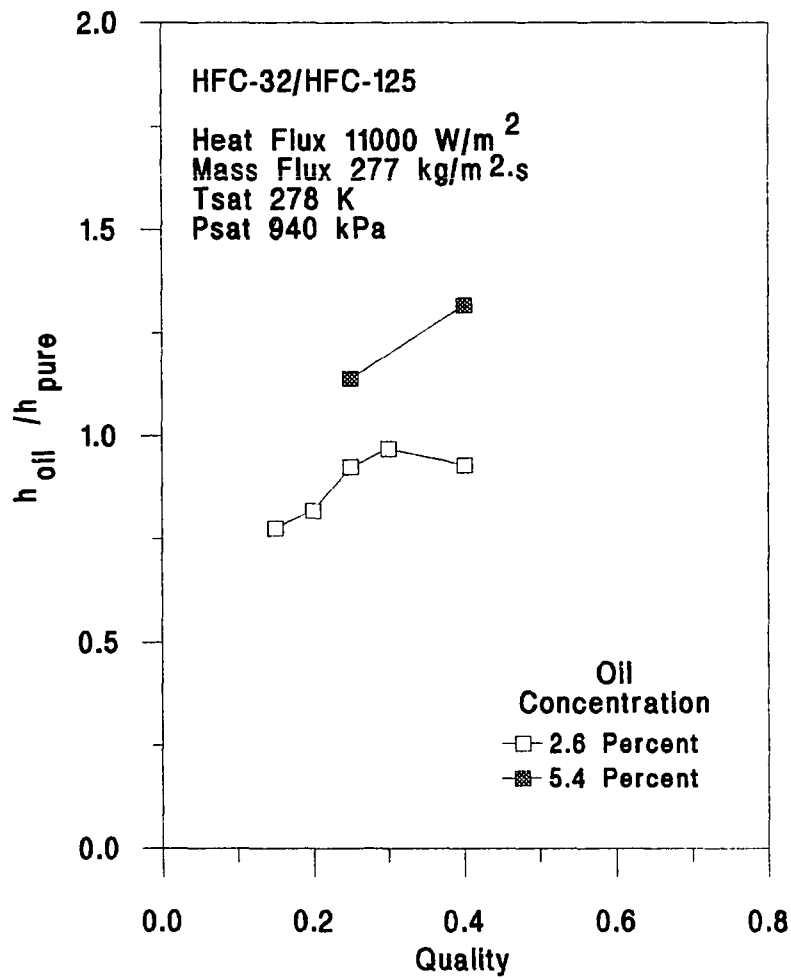


Figure 7.12 The Effect of Oil Concentration upon Heat Transfer Coefficient for a Heat Flux of  $11000 \text{ W/m}^2$  and a Mass Flux of  $277 \text{ kg/m}^2\cdot\text{s}$ .

The high mass flux results were different. The characteristics of high mass flux and low heat flux could have been shown with a mass flux of 520 kg/m<sup>2</sup>s or 700 kg/m<sup>2</sup>s (108 lb<sub>m</sub>/ft<sup>2</sup>·s to 143 lb<sub>m</sub>/ft<sup>2</sup>·s ) and a heat flux of 5100 W/m<sup>2</sup> and 7100 W/m<sup>2</sup> (1617 Btu/hr·ft<sup>2</sup> or 3488 Btu/hr·ft<sup>2</sup>). The trends were the same for all these conditions. In Figure 7.13, the ratios declined at qualities above 20 percent. The ratios for a 5.4 percent oil concentration were lower than that of the 2.6 percent oil concentration. The ratio at higher oil concentrations was higher at mass fluxes, low heat fluxes and low qualities. The ratio for lower oil concentrations was lower at low qualities and high mass fluxes.

The final conditions examined were at high mass fluxes combined with high heat fluxes. This comparison was made in Figure 7.14. The heat transfer coefficient for the pure case declined at low qualities and increased at high qualities (Figure 5.13). The heat transfer coefficient for an oil concentration of 5.4 percent followed this same trend and the curve was parallel to the pure case in the higher qualities. High oil concentrations appeared to have a negligible effect on the heat transfer once nucleation was suppressed. The heat transfer coefficient for the 2.6 percent oil mixture increased to a value of 6000 W/m<sup>2</sup>K at a quality of 30 percent (Figure 7.9). This increase was attributed to the increased nucleation associated with low concentrations of oil in refrigerant. The ratio of these heat transfer coefficient show a marginally increasing ratio of the 5.4 percent oil with an absolute value less than one. The ratio of heat transfer coefficients for the lower oil concentration, 2.6 percent, increased to a factor of 1.3 at a quality of 30 percent.

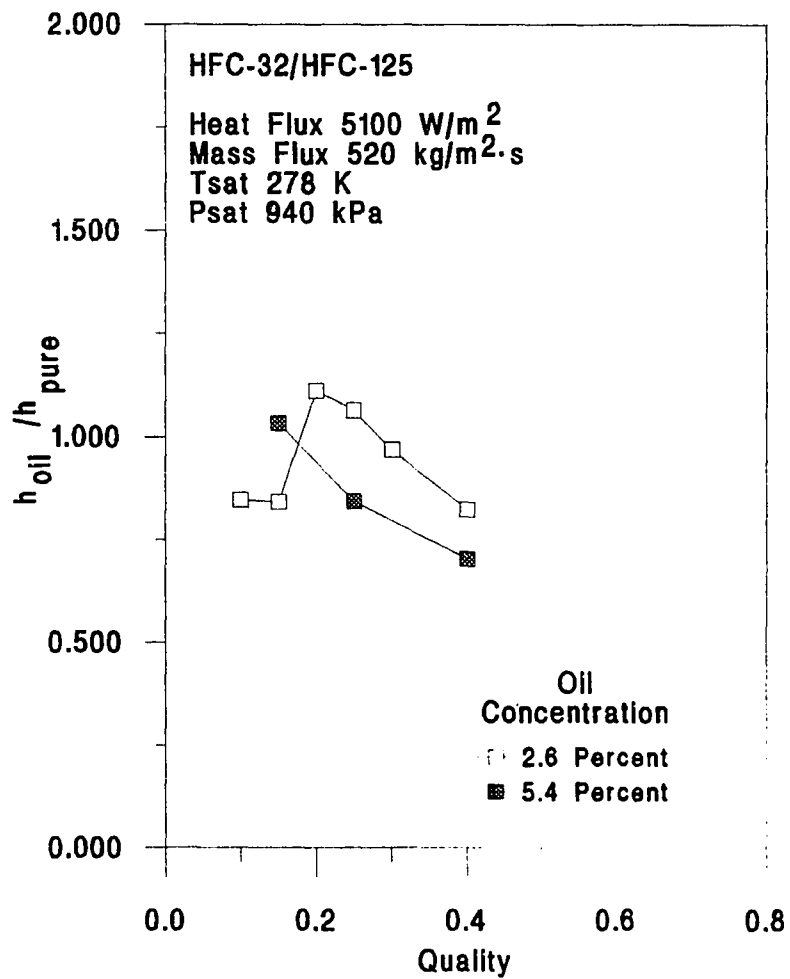


Figure 7.13 The Effect of Oil Concentration upon Heat Transfer Coefficient for a Heat Flux of  $5100 \text{ W/m}^2$  and a Mass Flux of  $520 \text{ kg/m}^2\cdot\text{s}$ .

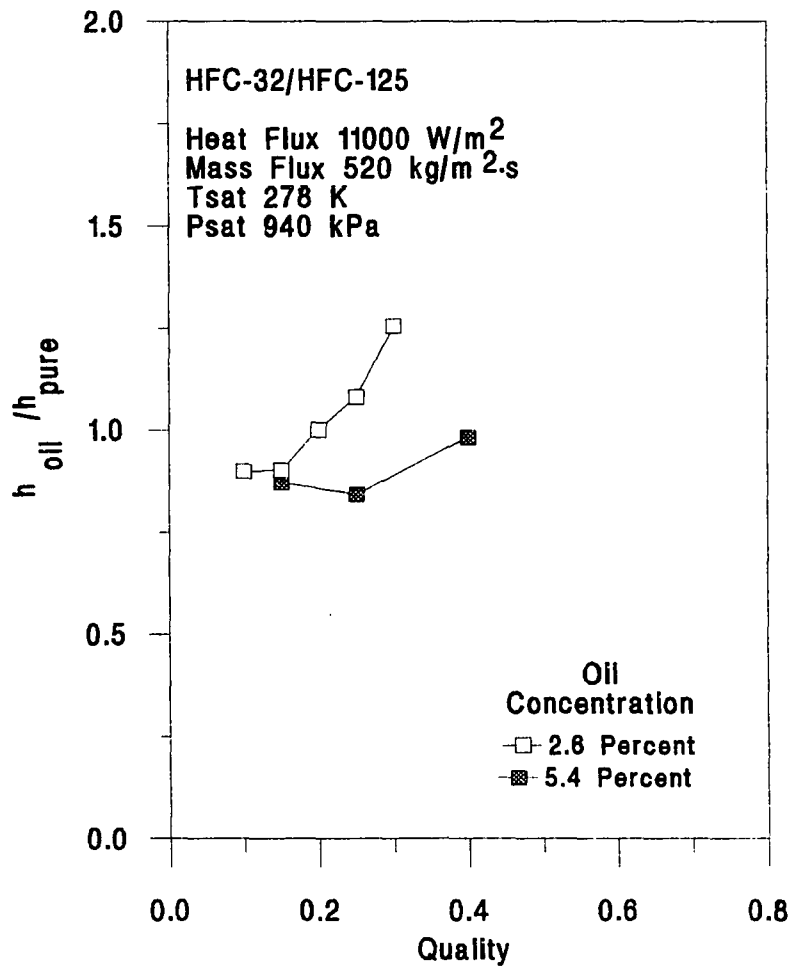


Figure 7.14 The Effect of Oil Concentration upon Heat Transfer Coefficient for a Heat Flux of 11000 W/m<sup>2</sup> and a Mass Flux of 520 kg/m<sup>2</sup>.s.

## SUMMARY OF EXPERIMENTAL RESULTS

The heat transfer and pressure drop characteristics for a HFC-32/HFC-125 mixture with oil concentration of 0, 2.6 and 5.4 percent were examined for heat fluxes  $5100 \text{ W/m}^2$  to  $11000 \text{ W/m}^2$  ( $1617 \text{ Btu/hr}\cdot\text{ft}^2$  to  $3488 \text{ Btu/hr}\cdot\text{ft}^2$ ) and mass fluxes of  $277 \text{ kg/m}^2\text{s}$  to  $700 \text{ kg/m}^2\text{s}$  ( $57 \text{ lb}_m/\text{ft}^2\cdot\text{s}$  to  $143 \text{ lb}_m/\text{ft}^2\cdot\text{s}$ ). The heat transfer coefficient and pressure drop across the test section were recorded.

Oil was added in a batch process to obtain concentrations of 2.6 and 5.4 percent. The addition of oil should have promoted an annular flow pattern where convective heat transfer would dominate. Flow visualization was not conducted to verify the flow pattern. The oil caused a foaming of the refrigerant. The addition of oil increased heat transfer coefficient at low mass fluxes, but caused mixed results at higher mass flux. The effect of oil was generally less than 15 percent on the convective heat transfer coefficient for the mass fluxes and heat fluxes in this study. The addition of oil increased the pressure drop because the oil was more viscous than the refrigerant.



## CHAPTER VIII

### COMPARISON OF HFC-32/HFC-125 EXPERIMENTAL RESULTS WITH HCFC-22 EXPERIMENTAL RESULTS

The operating pressures for HCFC-22 would be approximately 60 % lower than those of HFC-32/HFC-125 for the same evaporator temperatures in a residential air-conditioner. The thermodynamic and fluid properties for these two refrigerants were very different. A direct comparison of the experimental results for heat transfer and pressure drop of these two refrigerants is included. The differences in experimental results were attributed to the difference in refrigerant properties when possible. The performance of each refrigerant in the ideal vapor compression cycle for each refrigerant was also analyzed.

The heat transfer and pressure drop characteristics of HFC-32/HFC-125 were investigated because it was a possible HCFC-22 replacement in residential air-conditioners. The question of interest to design engineers was "How does it compare to HCFC-22?" The boiling heat transfer data for HCFC-22 was dominated by convective forces. The nucleate effect was more pronounced in the heat transfer data for the HFC-32/HFC-125. The fluid properties of both refrigerants are shown in table 8.1.

The three fluid properties that should influence the nucleate boiling most were liquid thermal conductivity, viscosity and surface tension. A high liquid thermal conductivity promotes heat transfer at the wall.

Table 8.1 Fluid Properties of HCFC-22 and HFC-32/HFC-125 at  
4.5 °C (40 °F)

Fluid Property	HFC-32/HFC-125	HCFC-22
Liquid Viscosity		
$\mu\text{Ns/m}^2$	202.0	213.0
$\text{lb}_m/\text{ft}\cdot\text{hr}$	0.489	0.515
Surface Tension		
$\text{mN/m}$	8.51	10.6
$\text{lb}_f/\text{ft}$	5.83E-04	7.26E-04
Liquid Thermal Conductivity		
$\text{W/m}\cdot\text{K}$	0.108	0.100
$\text{Btu/hr}\cdot\text{ft}\cdot^\circ\text{F}$	0.062	0.058
Enthalpy of Vaporization		
$\text{kJ/kg}$	214.0	199.2
$\text{Btu/lb}$	92.1	85.7
Vapor Pressure		
$\text{kPa}$	942	572
$\text{psia}$	137	82.9
Liquid Density		
$\text{kg/m}^3$	1177	1272
$\text{lb}_m/\text{ft}^3$	73.5	79.4
Vapor Density		
$\text{kg/m}^3$	35.0	24.5
$\text{lb}_m/\text{ft}^3$	2.18	1.53
Liquid Specific Heat		
$\text{kJ/kg}\cdot\text{K}$	1.66	1.19
$\text{Btu/lb}_m\cdot^\circ\text{F}$	0.396	0.284
Liquid Prandtl Number	3.10	2.53

Equation 8.1, developed by Forster and Zuber [1955] shows that increasing thermal conductivity increases the nucleate boiling convective coefficient.

$$h_{mic} = 0.00122 \left( \frac{k_L^{0.79} C_{pL}^{0.49} \rho_L^{0.49} g_c^{0.25}}{\sigma^{0.5} \mu^{0.29} \lambda^{0.24} \rho_v^{0.24}} \right) (\Delta T_e)^{0.24} (\Delta P_e)^{0.75} \quad (8.1)$$

At 4.5 °C (40 °F), the liquid thermal conductivity for a HFC-32/HFC-125 mixture was seven percent higher than the liquid thermal conductivity for HCFC-22. Lower liquid viscosity causes less restraining forces against bubble growth. The liquid viscosity of a HFC-32/HFC-125 mixture was 5.5 percent lower than the liquid viscosity of HCFC-22. According to Equation 8.1, a lower viscosity would increase nucleate boiling heat transfer.

Lower surface tension also lowers restraining forces against a bubble growing at the wall of the tube and eventually departing the wall. The surface tension for a HFC-32/HFC-125 mixture was 20 percent lower than the surface tension of HCFC-22 at 4.5 °C (40 °F). These fluid properties were part of the reason behind the higher nucleate boiling contribution for the HFC-32/HFC-125 mixture. Decreasing the surface tension in the Forster and Zuber [1955] equation would increase the nucleate heat transfer. The effect of individual properties helped explain why the nucleate boiling effect was higher with the HFC-32/HFC-125 mixture. The vapor compression cycle required much more information than just refrigerant properties at a single temperature.

Cooper's [1984] pool boiling correlation related the heat transfer coefficient to the molecular weight, reduced pressure and heat flux:

$$h = 55 P_r^{0.12} (\log_{10} P_r)^{-0.55} M^{-0.5} q^{0.67} \quad (8.2)$$

Comparing the ratio of pool boiling values from Equation 8.2 for HFC-32/HFC-125 to HCFC-22, Equation 8.3, the pool boiling contribution for HFC-32/HFC-125 should be 1.5 times the pool boiling contribution of HCFC-22. The HFC-32/HFC-125 mixture operated at a 48 percent higher reduced pressure.

$$\frac{h_{\text{Nucleate - HFC-32/HFC-125}}}{h_{\text{Nucleate - HCFC-22}}} = \frac{\left[ P_r^{0.12} (\log_{10} P_r)^{-0.55} M^{-0.5} \right]_{\text{HFC-32/HFC-125}}}{\left[ P_r^{0.12} (\log_{10} P_r)^{-0.55} M^{-0.5} \right]_{\text{HCFC-22}}} \quad (8.3)$$

The pressure ratio of the expected evaporator pressure to the expected condenser pressure for the mixture was slightly lower than for HFC-32/HFC-125, even though the absolute pressure change was much higher.

The nucleate contribution to heat transfer was higher for a HFC-32/HFC-125 mixture than for HCFC-22. Figure 8.1 showed that the heat transfer coefficient for a HFC-32/HFC-125 mixture was higher than the heat transfer coefficient of HCFC-22 at qualities of 20%. In Figure 8.1, the ratio of the heat transfer coefficient of HFC-32/HFC-125 to that of HCFC-22 was greater than one at qualities of 20 percent but lower than one for qualities of 40 and 60 percent. The lowest ratio was 0.82 and the highest ratio was 1.22. The average ratios of heat transfer coefficient at a quality of 20 percent was about 1.10.

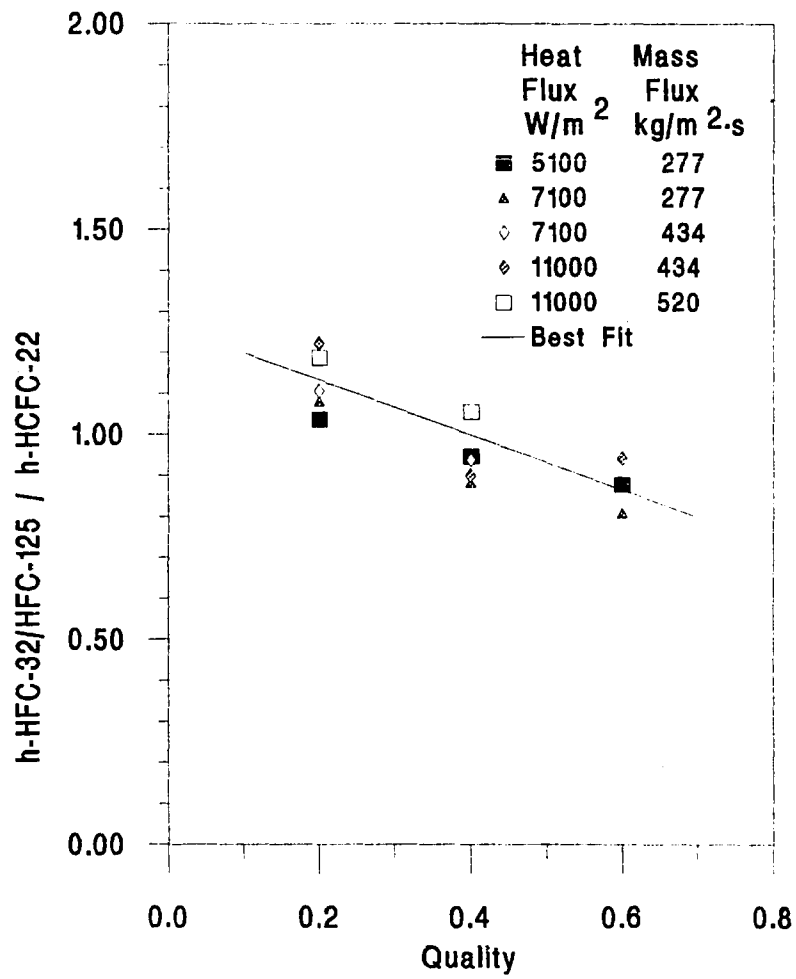


Figure 8.1 The Ratio of HFC-32/HFC-125 and HCFC-22 Two-phase Heat Transfer Coefficients.

The overall effect was that HCFC-22 was a better fluid based upon the heat transfer properties than HFC-32/HFC-125 in a smooth tube and for qualities of 40 and 60 percent. A best fit line was found in the form of Equation 8.4.

$$\frac{h_{\text{HFC-32/HFC-125}}}{h_{\text{HCFC-22}}} = \frac{-2}{3} \cdot \text{Quality} + 1.27 \quad (8.4)$$

The pressure drop in the tube for a HFC-32/HFC-125 mixture was lower than that of HCFC-22. In Figure 8.2, The ratio of pressure drop of HFC-32/HFC-125 to that of HCFC-22 was shown with quality for the common heat and mass flux combinations.

These pressure drop ratios were less than 0.5 for all of the cases shown. The viscosity of HFC-32/HFC-125 was less than that of HCFC-22 and therefore the pressure drop was lower. The use of HFC-32/HFC-125 in air-conditioners might be comparable to HCFC-22 because of this lower pressure drop. The designer might be able to use surfaces that promote heat transfer better and still keep pressure drop in line with that when using HCFC-22. The major trend here was a slightly increasing ratio of pressure drop as quality increased. A simple best fit equation was determined from the pressure drop ratio data and takes the form shown in Equation 8.5.

$$\frac{\Delta P_{\text{HFC-32/HFC-125}}}{\Delta P_{\text{HCFC-22}}} = \frac{1}{4} \cdot \text{Quality} + 0.305 \quad (8.5)$$

The T-s or temperature entropy diagram was shown in Figure 8.3. A near ideal vapor compression cycle for both HCFC-22 and a HFC-32/HFC-125 mixture is superimposed onto the T-s saturated region. This cycle consists of isentropic vapor compression, constant pressure condensation, a constant enthalpy expansion to a quality of 20 percent and finally a constant temperature evaporation. The saturation regions were significantly different in size and shape but the two cycles were similar when operating over the same temperature.

The pressure enthalpy diagram shown in Figure 8.4 reveals the differences with the two refrigerants even though the same cycle is as shown. The pressure - enthalpy data for the entire saturation region for the HFC-32/HFC-125 mixture was unavailable. However, the portion near the critical point was not relevant to the air-conditioning vapor compression cycle.

The HFC-32/HFC-125 mixture operates over much higher pressures than HCFC-22. In a practical sense this means that the air-conditioner coils and compressor will need to be made structurally stronger.

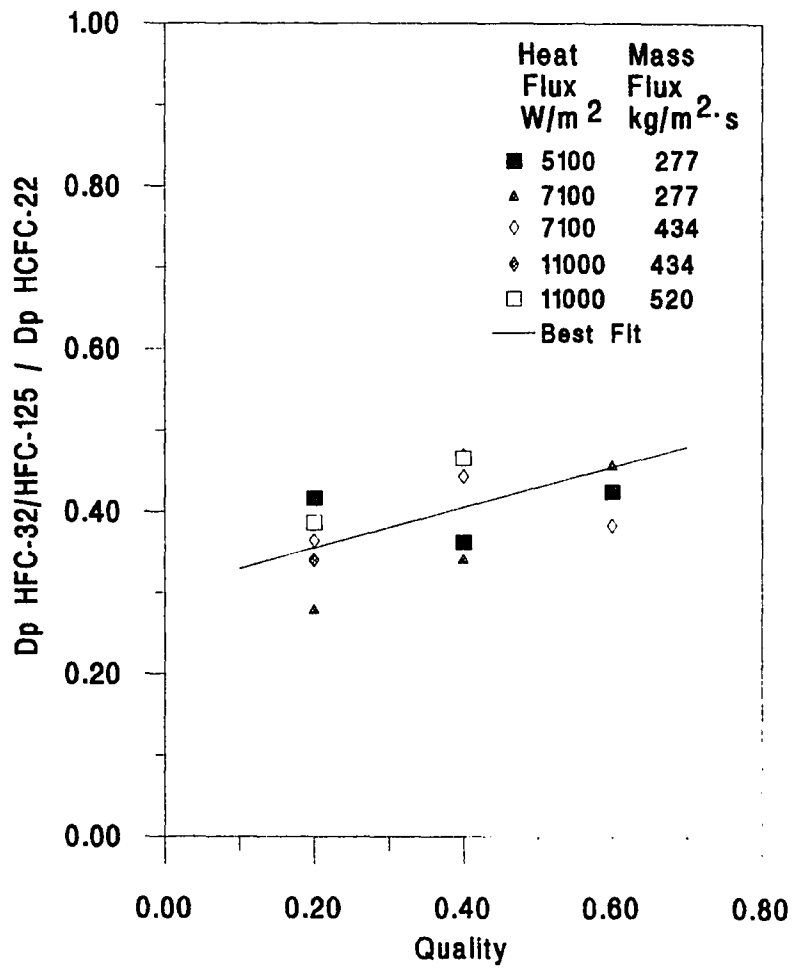


Figure 8.2 The Ratio of HFC-32/HFC-125 and HCFC-22 Two-phase Pressure Drops.



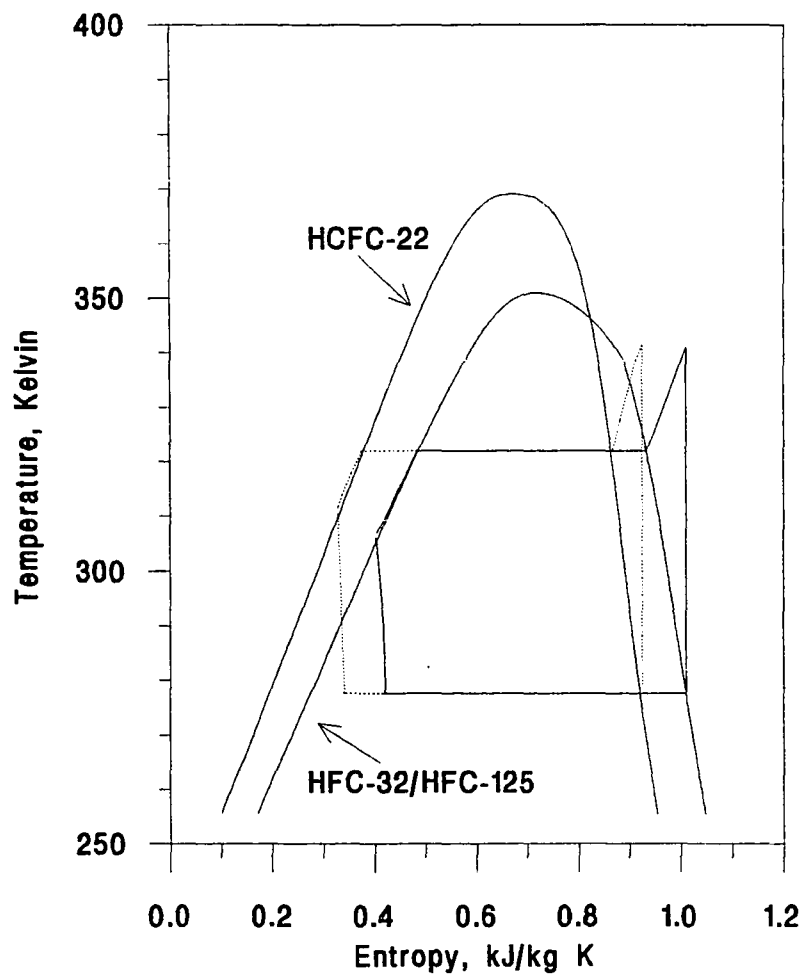


Figure 8.3 T-s Diagram of a Vapor Compression Cycle for HCFC-22 and HFC-32/HFC-125.

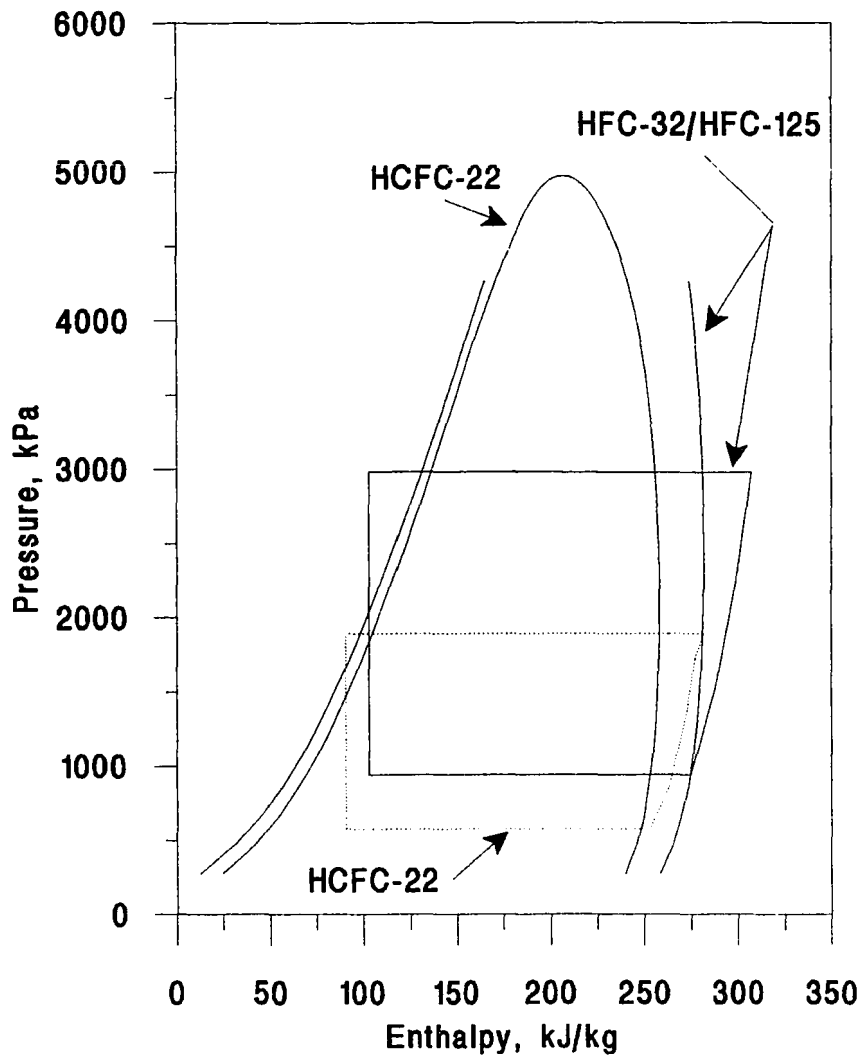


Figure 8.4 Pressure-Enthalpy Diagram of a Vapor Compression Cycle for HCFC-22 and HFC-32/HFC-125.

## CHAPTER IX

### CONCLUSIONS AND RECOMMENDATIONS

The heat transfer and flow characteristics of HCFC-22 and a potential replacement, a 50% / 50% mixture on a mass basis of HFC-32/HFC-125 were examined. The refrigerants were studied at mass fluxes of 277, 434 and 520  $\text{kg/m}^2\text{s}$  (57, 88 and 106  $\text{lb}_m/\text{ft}^2\text{s}$ ) and the mixture was additionally studied at 700  $\text{kg/m}^2\text{s}$  (143  $\text{lb}_m/\text{ft}^2\text{s}$ ). Heat fluxes of 5100, 7100 and 11000  $\text{W/m}^2$  (1617, 2251 and 3488  $\text{Btu/hr}\cdot\text{ft}^2$ ) were used in the experiments to represent a low, medium and high heat flux. Qualities of 10 to 60 percent were examined in this study. The pressure drop and heat transfer coefficient were determined for each of these tests. From these data, a pressure drop correlation and heat transfer correlation for HFC-32/HFC-125 were developed for use with smooth tubes. Oil was added to the HFC-32/HFC-125 mixture in a batch process in concentrations of 2.6 and 5.4 percent. The heat transfer coefficients and pressure drops were once again recorded. The conclusions drawn from this study and recommendations for future work are presented in this chapter.

HCFC-22 and HFC-32/HFC-125 flowed through a copper tube 2.7 meter long and 8.0 mm in diameter. The tube was wrapped with heating tape. The wall temperature of the tube and the inlet and exit pressures were recorded. HCFC-22 results were recorded at qualities of 20 to 60 percent.

#### CONCLUSIONS

The HCFC-22 heat transfer coefficients increase corresponded to increases in mass flux, heat flux and quality. This type of performance was consistent with a convective dominated heat transfer process. A comparison with flow pattern maps suggested that HCFC-22 was in the annular flow pattern for these experiments and a convective mechanism would dominate heat transfer.

HFC-32/HFC-125 was also compared to the flow pattern maps and slug flow was predicted at low qualities and annular flow at higher qualities. The heat transfer coefficient often declined at low qualities and increased at higher qualities. The decline in heat transfer coefficient was associated with the suppression of nucleate boiling and the transition to convective heat transfer. The slug flow pattern was associated with a nucleate boiling process and the annular flow pattern was associated with a convective flow pattern. This information indicated that the nucleate boiling process affected the overall heat transfer at low qualities for a HFC-32/HFC-125 mixture. The HFC-32/HFC-125 mixture had a higher thermal conductivity, lower surface tension and lower viscosity than HCFC-22. All three variables would promote increased nucleate boiling.

A polyol ester oil was added to the HFC-32/HFC-125 mixture in mass concentrations of 2.6 percent and 5.4 percent. The addition of oil increased the surface tension and viscosity of the mixture. The heat transfer coefficient did not decline at low qualities as it did in the pure case. The addition of oil was thought to suppress the nucleation. The heat transfer coefficient was generally higher for a mixture containing the higher concentrations of oil when the refrigerant flowed at a low mass flux. The heat transfer coefficient increased with quality at low mass fluxes. At high mass fluxes, the heat transfer coefficient declined as quality increased. The governing theory stated that annular flow patterns existed when there were high mass fluxes. A thin liquid film developed along the wall in annular flow patterns. As the refrigerant evaporates the quality increases and the oil and liquid refrigerant remain in the liquid film at the wall. This leads to high oil concentrations in the liquid next to the tube wall.

The heat transfer coefficient of HFC-32/HFC-125 was up to 20 percent higher than the heat transfer coefficient of HCFC-22 at a quality of 20 percent. The heat transfer coefficients were approximately the same at a quality of 40 percent. The heat transfer coefficients of HFC-32/HFC-125 were up to 25 percent lower than HCFC-22 at a quality of 60 percent. The heat transfer coefficients of the HFC-32/HFC-125 mixture would be

lower than those of HCFC-22 in an air-conditioner as the quality entering the evaporator is usually about 20 percent.

The heat transfer coefficient of HFC-32/HFC-125 was compared to four prediction correlations of Shah [1982], Gungor and Winterton [1982], Kandlikar [1990] and Chen [1966]. These correlations under predicted the nucleate boiling contribution at low qualities. An asymptotic model was developed and used to predict the heat transfer coefficient within a mean deviation of 8.7 percent. The asymptotic model used a corrected convective term and a corrected nucleate boiling term. The convective term consisted of the product of the Dittus Boelter liquid single phase equation and the enhancement factor suggested by Chen [1966]. The nucleate boiling term consisted of the product of a suppression factor and the nucleate boiling value predicted by Cooper [1982]. The suppression factor was developed by modifying the suppression factor suggested by Collier [1982] and Chen [1966]. This correlation provided a better fit of the HFC-32/HFC-125 data.

The pressure drop of the HFC-32/HFC-125 mixture and HCFC-22 in the test section was recorded for all of the experiments. The pressure drop increased nearly linearly with quality for any given mass flux or heat flux. The heat flux had almost no effect upon the pressure drop.

By plotting the experimental pressure drop divided by the single-phase pressure drop calculated from the Blasius equation, a linear relationship between quality and the ratio of two-phase and single-phase pressure drops was recognized. The pressure drop was compared to a homogeneous model and two separate flow models. The separate flow models were the Martinelli model and the Friedel model. The proposed relationship fit the data much better.

Oil viscosity was 55 percent higher than the refrigerant. The addition of oil increased the viscosity of the total mixture. The increased viscosity of the total mixture

increased the pressure drop. The pressure drop with oil ranges from 20 percent to 80 percent higher than the pure case.

The HFC-32/HFC-125 mixture had a lower viscosity, a lower surface tension and a lower ratio of vapor to liquid density than HCFC-22. The pressure drop recorded for HFC-32/HFC-125 was 60 percent lower than the pressure drop of HCFC-22 flowing at the same conditions. The difference in physical properties was the primary reason that the pressure drop was lower for HFC-32/HFC-125.

The anticipated contributions of this investigation are as follows: (1) generation of experimental heat transfer and pressure drop data for a wide range of conditions for HCFC-22 and a HFC-32/HFC-125 mixture (2) characterization of the effects of oil upon heat transfer and pressure drop upon HFC-32/HFC-125, (3) a better prediction model for determining the heat transfer coefficient of HFC-32/HFC-125, (4) a prediction equation for determining the pressure loss in a smooth tube of two-phase HFC-32/HFC-125, and (5) a direct comparison between HCFC-22 and HFC-32/HFC-125 that could be used by air conditioner designers if adapting HFC-32/HFC-125 to residential use.

## RECOMMENDATIONS

In the present study, convective heat transfer coefficient and pressure drop were recorded for a range of qualities, heat fluxes and mass fluxes using a smooth tube and HFC-32/HFC-125 with and without oil. The test conditions chosen represent values found in residential air conditioners. The obvious continuation of this work would include expanding the range of input parameters in this study. The following would be a guideline for a range of operating parameter (1) heat fluxes  $5000 \text{ W/m}^2$  to  $30000 \text{ W/m}^2$ , (2) mass fluxes  $200 \text{ kg/m}^2\text{s}$  to  $1000 \text{ kg/m}^2\text{s}$ , (3) qualities from 10 to 100 percent, (4) temperatures of  $7^\circ\text{C}$ ,  $23^\circ\text{C}$  and  $43^\circ\text{C}$ , and (5) tube diameters of five, eight and 16 millimeters. Internally grooved tubes are often used in air-conditioning equipment and should be incorporated in future generations of experiments. These changes would further allow comparison of data to heat pump systems and light industrial applications.

It is further recommended that since the proposed correlations are functions of the single-phase heat transfer coefficient and pressure drop, that single-phase experimental work is carried out to verify the accuracy of single-phase correlations. These correlations were developed for pure substances and may not accurately predict the single-phase pressure drop and heat transfer coefficient.

## REFERENCES

- Anderson, M. K. 1987. CFCs Is the sky falling. *ASHRAE Journal* Nov. pp. 21-28.
- Anderson, S.W., D. G. Rich, and D. F. Geary. 1966. Evaporation of refrigerant 22 in a horizontal 3/4 in. OD tube. *ASHRAE Transactions* Vol. 72, Part 1, pp. 28-41.
- ASHRAE. 1984. *ANSI/ASHRAE Standard 41.4-1984, Standard method for measurement of proportion of oil in liquid refrigerant* Atlanta: American Society of Heating, Refrigerating, and Air-Conditioning Engineers, Inc.
- ASHRAE. 1986. *ASHRAE Handbook-1986 refrigeration*. Atlanta: American Society of Heating, Refrigerating, and Air-Conditioning Engineers, Inc.
- Baker, O. 1954. Simultaneous flow of oil and gas. *Oil and Gas Journal*. Vol. 53, p. 185.
- Beardsley, M. 1990. Seeking safe ways to save the ozone. *Dallas Morning News*. pp. 6D, June 25, 1990.
- Bjorge, R.W., G. R. Hall, and W. M. Rehsenow. 1982. Correlation of forced convective boiling heat transfer data. *Int J Heat Mass Transfer* Vol. 25, No. 6, pp. 753-757.
- Braswell, A. 1988. Impact of CFC regulations on the air conditioning and refrigeration industry. *Progress in the Design and Construction of Refrigeration Systems*. Purdue, Indiana, July 18-21.
- Bryan, W.L. and G. W. Quint. 1955. Heat Transfer Coefficients in Horizontal Tube Evaporators. *Refrigerating Engineering* Vol. 63, No. 5, May, pp. 36-45.
- Carey, V.B. 1992. *Liquid-vapor phase-change phenomena* New York: Hemisphere Publishing Corporation.
- Chaddock, J. B. 1986. Influence of oil on in tube refrigerant evaporator performance. *Heat Transfer in Air Conditioning and Refrigeration equipment* HTD-Vol 65., New York, ASME, pp. 33-46.
- Chaddock, J.B. and A. Mathur. 1980. Heat transfer to oil-refrigerant mixtures evaporating in tubes. *Proceedings of the Multi-phase Flow and Heat Transfer Symposium-Workshop* Miami Beach, Florida, Vol. 2, pp. 861-884.



Chaddock, J.B., and Noerager, J. A. 1966. Evaporation of R-12 in a horizontal tube with constant heat flux. *ASHRAE Transactions* Vol. 72, Part I, pp. 99-103.

Chen, J.C. 1966. A correlation for boiling heat transfer to saturated fluids in convective flow. *Industrial and Engineering Chemistry, Process Design and Development* Vol (3): 322-329.

Chisholm, D. 1967. A theoretical basis for the Lockhart-Martinelli correlation for two-phase flow. *Int J Heat Mass Transfer* Vol. 10, pp1767-1778.

Coleman, Hugh W. and W. Glenn Steele, Jr. 1989. *Experimentation and Uncertainty Analysis for Engineers*, John Wiley & Sons, New York.

Collier, J.G. 1982. *Convective Boiling and Condensation*, 2nd Edition, McGraw-Hill, New York.

Cooper, M.G. 1984. Saturated pool boiling-A simple correlation. *International Chemical Engineering Symposium Series* 86 : 785-792.

Dengler, C. E., and Addoms, J. N. 1956. Heat transfer mechanisms for vaporization of water in a vertical tube. *Eng Prog Symp Series* Vol. 52, No. 18, pp. 95-103.

Dittus, F.W. and L.M.K. Boelter. 1930. University of California at Berkeley, *Publ. Eng.* 2, 443.

El-Sallak, M., S. M. Morcos and A. Mobarak. 1988. Experimental investigation of boiling flow characteristics of pure refrigerant in a horizontal tube. *Experimental Heat Transfer Fluid mechanics, and Thermodynamics* Elsevier Science Publishing Co., Inc., New York, pp. 1611-1617.

Forster, H.K. and N. Zuber. 1955. Dynamics of vapour bubbles and boiling heat transfer. *AIChE Journal* I: 531-535.

Freidel, L. 1979. Improved friction pressure drop correlations for horizontal and vertical two-phase flow. *European Two-phase Flow Group Meeting*. Ispra, Italy.

Guerrieri, S. A., and R.D. Talty. 1956. A study of heat transfer to organic liquids in a single tube, natural circulation, vertical tube boilers *Chem Eng Prog Sym Series* Vol. 56, No. 18, pp. 69-77.

Gungor, K. E., and R.H.S. Winterton. 1986. A general correlation for flow boiling in tubes and annul., *Int. J. Heat Mass Transfer* Vol. 29, No. 3, pp. 351-358.

- Hambraeus, K. 1991. Two-phase flow boiling of oil-HFC134a Mixture. *XVIII International Congress of Refrigeration* Montreal, August 10-17.
- Hearn, B. 1990. CFC Regulations on Refrigeration Compressors Used in Environmental Test Chambers. *Journal of the IES* Nov./Dec., pp. 27-32.
- Hsu, Y. Y., and R. W. Graham. 1976. *Transport Process in Boiling and Two-Phase Systems*. Hemisphere Publishing, New York.
- Jensen, M.K, and D.L. Jackman. 1984. Predictions of nucleate pool boiling heat transfer coefficients of refrigerant-oil mixtures. *Journal of Heat Transfer* Vol. 106, pp. 184-190.
- Kandlikar, S. G. 1988. A parametric study of saturated flow boiling heat transfer inside horizontal and vertical tubes. *Experimental Heat Transfer, Fluid mechanics, and Thermodynamics* Elsevier Science Publishing Co., Inc., New York, pp. 1618-1626.
- Kandlikar, S.G. 1990. A general correlation for saturated two-phase flow boiling heat transfer inside horizontal and vertical tubes. *ASME Journal of Heat Transfer* 112: 219-228.
- Kandlikar, S.G. 1991. Correlating flow boiling heat transfer data in binary systems. *Phase Change Heat Transfer* ASME HTD, 159: 163-170.
- Khanpara, J.C., M. B. Pate and A. E. Bergles. 1986. Local evaporation heat transfer in a smooth tube and a micro-fin tube using refrigerants 22 and 113. *ASHRAE Transactions* Vol. 92, Part 2, pp. 31-39.
- Kim, Y. 1993. Two-phase flow of HCFC-22 and HFC-134a through short tube orifices. Ph.D. Dissertation. Texas A&M University. College Station, Texas.
- Kohler, J.A. and R.L. Stine. 1988. Test loop for measuring in-tube enhancement of evaporating or condensing flow. *ASHRAE Journal* pp. 65-70.
- Kubanek, G.H. and D. L. Miletti. 1979. Evaporative Heat Transfer and Pressure Drop Performance of Internally-Finned Tubes with Refrigerant 22. *Journal of Heat Transfer* August, V 101, 447-452.
- Kultateladze, S.S. 1961. Boiling heat transfer. *International Journal of Heat and Mass Transfer* 4: 31-45.
- Lavin, G. J., and E. H. Young. 1965. Heat transfer to evaporating refrigerants in two-phase flow. *AIChE Journal* Vol. 11, No. 6, pp. 1124-1132.

- Likes, P. W. 1988. Impact of CFC regulations on commercial refrigeration equipment manufacturers. *Progress in the Design and Construction of Refrigeration Systems* Purdue, Indiana, July 18-21.
- Lockhart, R.W., and R. C. Martinelli. Proposed correlation of data for isothermal two-phase two-component flow in pipes. *Chem Eng Progress* 1949, Vol. 45, No. 1, pp.39-48.
- Martinelli, R.C. and D. B. Nelson. Prediction of pressure drop during forced circulation of boiling water. *Trans. ASME* 70, 695, (1948).
- Mathur, A. and J. Hashizome. 1983. Evaporation. *ASHRAE Journal* V 5, No. 2, Feb.
- McAdams, W.H. 1942. *Heat Transmission* 2d ed. New York: McGraw Hill.
- McLinden, Mark O. and D. A. Didion. 1987. Quest for Alternatives. *ASHRAE Journal* V 29, No. 12, Dec.
- Moffat, R.J., 1988. Describing the Uncertainties in Experimental Results. *Experimental Thermal and Fluid Science* 1: 3-17.
- Murata, Keiji and K. Hashizume. 1988. An investigation on forced convection boiling of nonazeotropic refrigerant mixtures. *Trans JSME*. 54 (506), pp. 2856-2863.
- Reid, R. S., M. B. Pate and A. E. Bergles. 1988. A comparison of augmentation techniques during in-tube evaporation of R-113. *ASHRAE Transactions* Vol. 2, pp21-30.
- Reitz, K. 1990. CFCs for Water Chillers. *Heating, Piping, Air Conditioning* April 1990, pp. 57-61.
- Riedle, K., and J.C. Purcupile. 1973. Experimental and analytical investigation boiling heat transfer in evaporator tubes horizontal flow. *ASHRAE Semi-annual meeting* Chicago, No. 2271, pp. 142-156, Jan. 1973.
- Ross, H., R. Radermacher, M. Di Marzo and D. Didion. 1987. Horizontal flow boiling of pure and mixed refrigerants. *International Journal of Heat and Mass Transfer* Vol. 30, No. 5, pp. 979-992.
- Schlager, L.M., A.E. Bergles and M.B. Pate. 1987. A survey of refrigerant heat transfer and pressure drop emphasizing oil effects and in-tube augmentation. *ASHRAE Transactions* Vol. 94, part 1, pp. 149-166.

- Shah, M. M. 1982. Chart correlation for saturated boiling heat transfer: equations and further study. *ASHRAE Transactions* Vol. 88, Part I, pp. 185-196.
- Taitel, Y and A. E. Dukler. 1976. A model for predicting flow regime transitions in horizontal and near horizontal gas-liquid flow. *AIChE J* 22, 47-55.
- Tichy, J. A., W.M.B. Duval and N.A. Macken. 1986. An experimental investigation of heat transfer in forced convection evaporation of oil refrigerant mixtures. *ASHRAE Transactions* Vol. 92, Part 2A, pp. 450-460.
- Wattelet, J.P., J.C. Chato, J.M.S. Jabardo, J.S. Panek and J.P. Renie. 1991. An experimental comparison of evaporation characteristics of HFC-134a and CFC-12. *XVIII International Congress of Refrigeration* Montreal, August 10-17, 1991.
- Wattelet, J.P., J.C. Chato, A.L. Souza and B.R. Christofferson. 1994. Evaporative Characteristics of R-12, R-134a, and MP-39 at low mass fluxes. *ASHRAE*.
- Whalley, P.B. 1987. *Boiling, Condensation and Gas-Liquid Flow* Oxford University Press, New York.
- Zuber, N. 1961. The dynamics of vapor bubbles in non-uniform temperature fields. *Int. J. Heat Mass Transfer* Vol. 2, pp. 82-93.

## APPENDIX A

### UNCERTAINTY ANALYSIS

Uncertainty analysis was performed to estimate the uncertainty in refrigerant mass flow rates, quality, pressure drop and heat transfer coefficient. Refrigerant mass flow rate was calculated from measured volumetric flow rate and refrigerant density. The density was determined from the measured refrigerant pressure and temperature. The quality was calculated from the electric heating load provided to the preheater, the flow rate, specific heat of the refrigerant, the enthalpy of vaporization of the refrigerant and the entering single phase temperature to the preheater. Pressure drop was calculated from the pressure measurement at the inlet and exit of the test section. Heat transfer coefficient is calculated from the outer test section wall temperature, the refrigerant temperature determined from the pressure, and the test section wall temperature. The equations used to calculate each value is shown in Equation A.1 through A.5.

$$\dot{m}_r = \rho \cdot \dot{V} \quad (\text{A.1})$$

$$\frac{\Delta P}{L} = \frac{P_2 - P_1}{L} \quad (\text{A.2})$$

$$q = h \cdot A \cdot (T_w - T_r) \quad (\text{A.3})$$

$$A = \pi \cdot D \cdot L \quad (\text{A.4})$$

$$x = \frac{q - \dot{m} \cdot c_{pL} \cdot (T_i - T_{sat}(P))}{i_g \cdot \dot{m}} \quad (\text{A.5})$$

Uncertainty analysis outlined by Coleman and Steele [1989] and Moffat [1988] identifies two types of errors. The residual fixed error is described by its bias limit,  $B_x$ . The bias error should not change of the course of an experiment and is often provided by the manufacturer of a sensor for a primary measurement. The random error is described by in precision index,  $Sx_i$ . The precision index accounts for uncertainty over the course of an experiment. The bias limits for measure variables are shown in Table A.1

Table A.1 Primary Variable Bias Limit

Primary Variable	Bias Limit
Temperature (T)	$\pm 0.1^\circ\text{C}$ ( $\pm 0.18^\circ\text{F}$ )
Pressure (P)	$\pm 3.0$ kPa ( $\pm 0.43$ psi)
Volumetric Flowrate ( $\dot{V}$ )	$\pm 0.461$ mL/s ( $\pm 0.0073$ GPM)
Power Input ( $Q_H$ )	$\pm 0.5\%$ of Rated Output

The technique outlined by Coleman and Steele [1989] states that for a variable " r " which is a function of one variable " X " , such as shown in Equation A.6, the bias limit may be calculated from Equation A.7. The bias limit in " r " is equal to the partial derivative of " r " with respect to " X " multiplied by the bias limit in " X ". The precision index is calculated using the same equation but substituting precision index

for bias limit. The uncertainties of intermediate variables dependent upon only one measured variable are shown in Table A.2.

$$r = f(X) \quad (\text{A.6})$$

$$B_r = \left[ \frac{\partial r}{\partial X} \cdot B_x \right] \quad (\text{A.7})$$

Table A.2 Bias Limit in Variables Dependent Upon a Single Measurement

Refrigerant	r	X	$\frac{\partial r}{\partial X}$	$B_x$	$B_r$
HCFC-22	$\rho$ kg/m <sup>3</sup>	T Celsius	3.50	0.1 Celsius	0.35 kg/m <sup>3</sup>
	$i_{fg}$ kJ/kg	T Celsius	0.75	0.1 Celsius	0.075 kJ/kg
	$c_{pL}$ kJ/kg·°C	T Celsius	0.004	0.1 Celsius	0.0004 kJ/kg·°C
	$T_{sat}$ Celsius	P kPa	0.056	3.0 kPa	0.17 Celsius
HFC-32 / HFC-125	$\rho$ kg/m <sup>3</sup>	T Celsius	6.07	0.1 Celsius	0.607 kg/m <sup>3</sup>
	$i_{fg}$ kJ/kg	T Celsius	1.05	0.1 Celsius	0.105 kJ/kg
	$c_{pL}$ kJ/kg·°C	T Celsius	0.0015	0.1 Celsius	0.00015 kJ/kg·°C
	$T_{sat}$ Celsius	P kPa	0.035	3.0 kPa	0.12 Celsius

Coleman and Steele [1989] provide for the calculation of uncertainty for values dependent upon multiple variables. Given a variable " r " that is a function of the variables " X<sub>1</sub> " through " X<sub>J</sub> ", such as shown in Equation A.8, the bias limit may be calculated from Equation A.9. The bias limit in " r " is equal to the partial derivative of

"  $r$  " with respect to "  $X_i$  " multiplied by the bias limit in "  $X_i$  " summed over all variables.

$$r = r(X_1, X_2, \dots, X_n) \quad (\text{A.8})$$

The precision index is calculated in the same manner as the bias limit in equation A.9. The precision index is calculated using A.10. The uncertainty of a variable is calculated by combining the bias limit and precision index and the Student t multiplier. The Student t multiplier is equal to two for sample sizes over 30 and the 95% confidence interval.

$$B_r = \left[ \sum_{i=1}^J \left( \frac{\partial r}{\partial X_i} \right)^2 B_{X_i}^2 \right]^{(0.5)} \quad (\text{A.9})$$

$$S_r = \left[ \sum_{i=1}^J \left( \frac{\partial r}{\partial X_i} \right)^2 S_{X_i}^2 \right]^{(0.5)} \quad (\text{A.10})$$

$$U_r = \left\{ \left( B_r \right)^2 + \left( t S_r \right)^2 \right\}^{0.5} \quad (\text{A.11})$$



The bias limit for pressure drop per unit length and area are calculated in Equations A.10 and A.11. The values for the bias limit for pressure drop per unit length and area are shown in Table A.3.

$$\left(\frac{B_A}{A}\right)^2 = \left(\frac{B_D}{D}\right)^2 + \left(\frac{B_L}{L}\right)^2 \quad (\text{A.12})$$

$$\left[\frac{\frac{B_{\Delta P}}{L}}{\Delta P}\right]^2 = 2 \cdot \left(\frac{B_P}{\Delta P}\right)^2 + \left(\frac{B_L}{L}\right)^2 \quad (\text{A.13})$$

Table A.3 Uncertainties in Pressure and Area

	Bias Limit
Pressure Drop Per Unit Length	2.0 %
Area	0.0011 m <sup>2</sup>

Because the mass flow rate was calculated from the volumetric flow rate, the bias limit is calculated from Equation A.12 and shown in Table A.4.

$$B_m = \dot{m} \left( \left( \frac{B_\rho}{\rho} \right)^2 + \left( \frac{B_V}{V} \right)^2 \right)^{0.5} \quad (\text{A.14})$$

Table A.4 Bias Limit in Mass Flow Rate

Refrigerant	$\dot{m}$ kg/s	$V$ m <sup>3</sup> /s	$B_{\dot{m}}$ %
HCFC-22	0.038	2.98 E-5	1.55
	0.072	5.65 E-5	0.82
	0.097	7.61 E-5	0.62
HFC-32/HFC-125	0.038	3.23 E-5	1.44
	0.072	6.10 E-5	0.78
	0.097	8.24 E-5	0.60

The bias limit for heat transfer coefficient is calculated with Equation A.13 and the values are shown in Table A.5.

$$\left[ \frac{B_h}{h} \right]^2 = \left[ \frac{B_q}{q} \right]^2 + \left[ \frac{B_A}{A} \right]^2 + \left[ \frac{B_{T_R}}{T_w - T_r} \right]^2 + \left[ \frac{B_{T_w}}{T_w - T_r} \right]^2 \quad (\text{A.15})$$

Table A.5 Bias Limit in Heat Transfer Coefficient

Refrigerant	q (W)	A (m <sup>2</sup> )	T <sub>r</sub> (°C)	T <sub>w</sub> (°C)	B <sub>h</sub> (W/m <sup>2</sup> )
HCFC-22	357	0.070	3.5	4.8	470
	497	0.070	3.5	4.9	510
	770	0.070	3.5	5.3	367
HFC-32 / HFC-125	q (W)	A (m <sup>2</sup> )	T <sub>r</sub> (°C)	T <sub>w</sub> (°C)	B <sub>h</sub> (W/m <sup>2</sup> )
	357	0.070	4.5	5.8	373
	497	0.070	4.5	5.9	403
	770	0.070	4.5	6.3	294

The bias limit for quality is given by Equation A.14. The calculation requires certain values of input and these are listed in Table A.6. The values of bias limit for quality are given in Table A.7.

$$\begin{aligned}
 B_x^2 = & \left( \frac{U q}{i fg \cdot m} \right)^2 + \left( \frac{q}{i fg \cdot m} \cdot \frac{1}{2} \cdot B \dot{m} \right)^2 + \left( \frac{(T_i - T_{sat}(P))}{i fg} \cdot B cp_L \right)^2 \\
 & + \left( \frac{cp_L}{i fg} \cdot B T_i \right)^2 + \left( \frac{cp_L}{i fg} \cdot B T_{sat}(P) \right)^2 + \\
 & \left( \frac{q - \dot{m} \cdot cp_L \cdot (T_i - T_{sat}(P))}{i fg^2 \cdot m} \cdot B i fg \right)^2
 \end{aligned}$$

(A.16)

Table A.6 Input Values for Quality Bias Limit Calculations

Refrigerant	$i_{fr}$ kJ/kg	$c_{pL}$ kJ/kg $^{\circ}$ C	$T_i$ $^{\circ}$ C	$T_{sat}$ $^{\circ}$ C
HCFC-22	199	1.21	0.5	3.5
HFC-32 / HFC-125	214	1.29	1.5	4.5

Table A.7 Bias Limit in Quality

Refrigerant	$\dot{m}$ kg/s	$q$ Watt	$B_x$ %
HCFC-22	0.038	357	1.4
	0.097	497	1.3
	0.072	770	1.5
HFC-32/HFC-125	0.038	357	1.4
	0.097	497	1.3
	0.072	770	1.5

The standard deviation is used as the precision index of a measure value. The standard deviation of measured values are shown in Table A.8.

Table A.8 Primary Variable Standard Deviation

Primary Variable	S
Temperature (T)	$\pm 0.12^{\circ}\text{C}$ ( $\pm 0.22^{\circ}\text{F}$ )
Pressure (P)	$\pm 2.8$ kPa ( $\pm 0.41$ psi)
Volumetric Flowrate ( $\dot{V}$ )	$\pm 2.25\%$ of Output
Power Input ( $Q_H$ )	$\pm 2.8\%$ of Rated Output

The precision index of variables dependent upon a single measurement are calculated using equation A.7 and replacing the bias limit with the precision index. The precision index for values of variables dependent upon a single measurement are shown in Table A.9.

Table A.9 Precision Index of Variables Dependent Upon a Single Measurement

Refrigerant	$r$	$X$	$\frac{\partial r}{\partial X}$	$S_X$	$S_r$
HCFC-22	$\rho$ kg/m <sup>3</sup>	T Celsius	3.50	0.12 Celsius	0.42 kg/m <sup>3</sup>
	$i_{fg}$ kJ/kg	T Celsius	0.75	0.12 Celsius	0.09 kJ/kg
	$cp_L$ kJ/kg·°C	T Celsius	0.004	0.12 Celsius	0.0005 kJ/kg·°C
	$T_{sat}$ Celsius	P kPa	0.056	2.8 kPa	0.16 Celsius
HFC-32 / HFC-125	$\rho$ kg/m <sup>3</sup>	T Celsius	6.07	0.12 Celsius	0.73 kg/m <sup>3</sup>
	$i_{fg}$ kJ/kg	T Celsius	1.05	0.12 Celsius	0.13 kJ/kg
	$cp_L$ kJ/kg·°C	T Celsius	0.0015	0.12 Celsius	0.00018 kJ/kg·°C
	$T_{sat}$ Celsius	P kPa	0.035	2.8 kPa	0.10 Celsius

The precision index for variables dependent upon multiple variables is calculated using Equation A.10. The precision index for pressure drop per unit length, mass flow rate, heat transfer coefficient and quality are shown in Tables A.10, A.11, A.12 and A.14, respectively. Input values required for the calculation of the quality precision index are given in Table A.13.

Table A.10 Precision Index of Pressure Drop Per Unit Length

	$S_{\frac{\Delta P}{L}}$
Pressure Drop Per Unit Length	0.62 %

Table A.11 Precision Index of Mass Flow Rate

Refrigerant	m kg/s	V m <sup>3</sup> /s	S <sub>m</sub> %
HCFC-22	0.038	2.98 E-5	2.25
	.072	5.65 E-5	
	0.097	7.61 E-5	
HFC-32/HFC-125	0.038	3.23 E-5	2.25
	0.072	6.10 E-5	
	0.097	8.24 E-5	

Table A.12 Precision Index of Heat Transfer Coefficients

Refrigerant	q (W)	A (m <sup>2</sup> )	T <sub>r</sub> (°C)	T <sub>w</sub> (°C)	S <sub>h</sub> (W/m <sup>2</sup> )
HCFC-22	357	0.070	3.5	4.8	476
	497	0.070	3.5	4.9	513
	770	0.070	3.5	5.3	374
HFC-32 / HFC-125	q (W)	A (m <sup>2</sup> )	T <sub>r</sub> (°C)	T <sub>w</sub> (°C)	S <sub>h</sub> (W/m <sup>2</sup> )
	357	0.070	4.5	5.8	373
	497	0.070	4.5	5.9	434
	770	0.070	4.5	6.3	294

Table A.13 Input Values for Quality Precision Index Calculations

Refrigerant	$i_{fr}$ kJ/kg	$c_{pL}$ kJ/kg $^{\circ}$ C	$T_i$ $^{\circ}$ C	$T_{sat}$ $^{\circ}$ C
HCFC-22	199	1.21	0.5	3.5
HFC-32 / HFC-125	214	1.29	1.5	4.5

Table A.14 Precision Index of Quality

Refrigerant	$\dot{m}$ kg/s	$q$ Watt	$S_x$ %
HCFC-22	0.038	357	1.6
	0.097	497	1.4
	0.072	770	1.7
HFC-32/HFC-125	0.038	357	1.0
	0.097	497	1.0
	0.072	770	1.6

The uncertainty is calculated using Equation A.11. The uncertainty for measured variables, variables dependent upon a single measurement, mass flow, heat transfer coefficient and quality are shown in Tables A.15, A.16, A.17 and A.18, respectively.



Table A.15 Primary Variable Uncertainty

Primary Variable	Uncertainty
Temperature (T)	$\pm 0.26^{\circ}\text{C}$ ( $\pm 0.47^{\circ}\text{F}$ )
Pressure (P)	$\pm 6.4$ kPa ( $\pm 0.93$ psi)
Volumetric Flowrate ( $\dot{V}$ )	$\pm 1.031$ mL/s ( $\pm 0.0163$ GPM)
Power Input ( $Q_H$ )	$\pm 5.6\%$ of Rated Output

Table A.16 Uncertainty in Variables Dependent Upon a Single Measurement

Refrigerant	Variable	Uncertainty
HCFC-22	$\rho$ kg/m <sup>3</sup>	0.91
	$if_g$ kJ/kg	0.195
	$cp_L$ kJ/kg°C	0.0011
	$T_{sat}$ °C	0.36
	Area m <sup>2</sup>	0.0011
	$\Delta P/\Delta L$ % Output	2.3
HFC-32/HFC-125	$\rho$ kg/m <sup>3</sup>	1.58
	$if_g$ kJ/kg	0.028
	$cp_L$ kJ/kg°C	0.00039
	$T_{sat}$ °C	0.23
	Area m <sup>2</sup>	0.0011
	$\Delta P/\Delta L$ % Output	2.3

Table A.17 Uncertainty in Mass Flow Rate

Refrigerant	$\dot{m}$ kg/s	$V$ m <sup>3</sup> /s	$U_{\dot{m}}$ %
HCFC-22	0.038	2.98 E-5	4.76
	0.072	5.65 E-5	4.57
	0.097	7.61 E-5	4.54
HFC-32/HFC-125	0.038	3.23 E-5	4.72
	0.072	6.10 E-5	4.57
	0.097	8.24 E-5	4.54

Table A.18 Uncertainty in Heat Transfer Coefficient

Refrigerant	q (W)	A (m <sup>2</sup> )	T <sub>r</sub> (°C)	T <sub>w</sub> (°C)	U <sub>h</sub> (W/m <sup>2</sup> )
HCFC-22	357	0.070	3.5	4.8	1062
	497	0.070	3.5	4.9	1141
	770	0.070	3.5	5.3	823
HFC-32 / HFC-125	q (W)	A (m <sup>2</sup> )	T <sub>r</sub> (°C)	T <sub>w</sub> (°C)	U <sub>h</sub> (W/m <sup>2</sup> )
	357	0.070	4.5	5.8	834
	497	0.070	4.5	5.9	915
	770	0.070	4.5	6.3	657

Table A.19 Uncertainty of Quality

Refrigerant	m kg/s	q Watt	U <sub>x</sub> %
HCFC-22	0.038	357	3.5
	0.097	497	3.1
	0.072	770	3.7
HFC-32/HFC-125	0.038	357	2.4
	0.097	497	2.4
	0.072	770	3.5

**APPENDIX B**

**LETTER OF PERMISSION**

9210 Shadowcrest  
College Station, TX 77845  
May 18, 1993

Mr. John G. Collier  
Field House  
Longridge, Sheepscombe  
Nr. Stroud  
Gloucester GL6 7QY  
United Kingdom

Dear Mr. Collier:

I respectfully request permission to use a reproduction of Figure 4.16 on page 138 of your book, "Convective Boiling and Condensation" for descriptive purposes in my dissertation. I am a student at Texas A&M University and would like to use the diagram to explain in general terms what is happening in two-phase flow. I am currently writing my dissertation and your response is appreciated.

Thank you for your time. Feel free to mark your response on this letter and return in the enclosed envelope.

Sincerely,

*Bert A. McJimsey*  
Bert A. McJimsey

Enclosure

*Bert McJimsey*  
*You have my permission to*  
*reproduce Fig 4.16 of my*  
*book solely for the purposes*  
*stated above. + Sweet thanks!*  
*J. G. Collier*  
*22<sup>nd</sup> May 1993*

## VITA

Bert Ashford McJimsey was born on March 18, 1960 in Dallas, Texas. His parents are Dr. Bert A. McJimsey and Marilyn D. McJimsey. He graduated from Sherman High School in 1978 and entered Texas A&M University in September of that same year. He graduated from Texas A&M University with a Bachelor of Science degree in Petroleum Engineering in May of 1982. In August of 1982, he married the lovely Karen Ann Fleming. Bert stayed in school and finished his Master of Science degree in Petroleum Engineering in December of 1985. He started his own oil and gas production company in Longview, Texas and continued that venture through 1988. He enrolled in the Doctoral Program in 1989 at Texas A&M to study Mechanical Engineering. Bert has two sons, Trey and Mason.

Bert Ashford McJimsey's permanent address is: 4043 Shady Hill, Dallas, Texas 77259.